

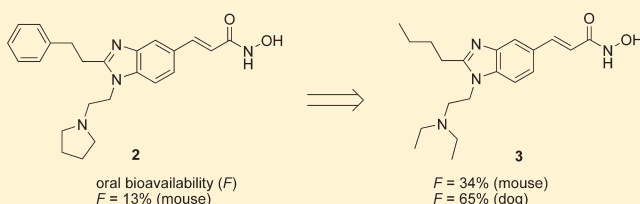
# Discovery of (2*E*)-3-{2-Butyl-1-[2-(diethylamino)ethyl]-1*H*-benzimidazol-5-yl}-*N*-hydroxyacrylamide (SB939), an Orally Active Histone Deacetylase Inhibitor with a Superior Preclinical Profile

Haishan Wang,<sup>\*,†</sup> Niefang Yu,<sup>†</sup> Dizhong Chen,<sup>†</sup> Ken Chi Lik Lee,<sup>†</sup> Pek Ling Lye,<sup>†</sup> Joyce Wei Wei Chang,<sup>†</sup> Weiping Deng,<sup>†</sup> Melvin Chi Yeh Ng,<sup>†</sup> Ting Lu,<sup>†</sup> Mui Ling Khoo,<sup>†</sup> Anders Poulsen,<sup>†</sup> Kanda Sangthongpitag,<sup>‡</sup> Xiaofeng Wu,<sup>‡</sup> Changyong Hu,<sup>‡</sup> Kee Chuan Goh,<sup>‡</sup> Xukun Wang,<sup>‡</sup> Lijuan Fang,<sup>‡</sup> Kay Lin Goh,<sup>‡</sup> Hwee Hoon Khng,<sup>‡</sup> Siok Kun Goh,<sup>‡</sup> Pauline Yeo,<sup>§</sup> Xin Liu,<sup>§</sup> Zahid Bonday,<sup>‡</sup> Jeanette M. Wood,<sup>‡</sup> Brian W. Dymock,<sup>†</sup> Kantharaj Ethirajulu,<sup>§</sup> and Eric T. Sun<sup>†</sup>

<sup>†</sup>Chemistry Discovery, <sup>‡</sup>Biology Discovery, and <sup>§</sup>Pre-Clinical Development, S\**BIO* Pte Ltd., 1 Science Park Road, No. 05-09 The Capricorn, Singapore Science Park II, Singapore 117528, Singapore

## S Supporting Information

**ABSTRACT:** A series of 3-(1,2-disubstituted-1*H*-benzimidazol-5-yl)-*N*-hydroxyacrylamides (**1**) were designed and synthesized as HDAC inhibitors. Extensive SARs have been established for in vitro potency (HDAC1 enzyme and COLO 205 cellular IC<sub>50</sub>), liver microsomal stability (*t*<sub>1/2</sub>), cytochrome P450 inhibitory (3A4 IC<sub>50</sub>), and clogP, among others. These parameters were fine-tuned by carefully adjusting the substituents at positions 1 and 2 of the benzimidazole ring. After comprehensive in vitro and in vivo profiling of the selected compounds, SB939 (**3**) was identified as a preclinical development candidate. **3** is a potent pan-HDAC inhibitor with excellent druglike properties, is highly efficacious in in vivo tumor models (HCT-116, PC-3, A2780, MV4-11, Ramos), and has high and dose-proportional oral exposures and very good ADME, safety, and pharmaceutical properties. When orally dosed to tumor-bearing mice, **3** is enriched in tumor tissue which may contribute to its potent antitumor activity and prolonged duration of action. **3** is currently being tested in phase I and phase II clinical trials.



## INTRODUCTION

Genomic DNA is packaged with histone to form chromatin, which is further condensed to chromosomes.<sup>1</sup> The histone proteins play an important role in the control of gene expression via modification through chemical reactions such as acetylation, phosphorylation, and methylation. The amino termini of histones extend from the nucleosomal core and are modified by histone acetyltransferases and histone deacetylases (HDACs) during the cell cycle.<sup>2</sup> In most cases, histone acetylation enhances transcription while histone deacetylation represses transcription.<sup>3,4</sup> Inhibition of HDACs leads to the accumulation of acetylated histones, resulting in a variety of cell type dependent responses such as apoptosis, necrosis, differentiation, cell survival, inhibition of proliferation, and cytostasis. HDAC enzymes are divided into four different classes:<sup>5,6</sup> class I (HDACs 1–3, 8), class IIa (HDACs 4, 5, 7, 9), class IIb (HDACs 6, 10), class III (SIRT1–7), and class IV (HDAC 11). Classes I, II, and IV are zinc dependent enzymes. Class III HDACs, the sirtuins, employ NAD<sup>+</sup> as a cofactor for their catalytic activity instead of zinc and are generally not inhibited by class I and class II inhibitors. Regulation of chromatin structure via modulation of histone acetylation is generally regarded as the primary mechanism of action of the class I HDACs. Subsequent effects on cell proliferation and apoptosis single out these nuclear proteins as key targets for an anticancer HDAC inhibitor.<sup>7</sup> HDACs 1, 2, 3, and 8 have been associated with uncontrolled tumor growth. For example,

selective knockdown studies on HDACs suggest that the class I HDACs, particularly HDACs 1 and 3, are essential to the proliferation and survival of mammalian carcinoma cells.<sup>8,9</sup> Class I HDACs, especially HDACs 1, 2, and 3, are considered as the most relevant targets for cancer therapy because inhibitors of these enzymes usually show strong antiproliferative and apoptosis-inducing activity.<sup>9,10</sup> Class II HDACs are more specifically involved in regulating cell migration and angiogenesis. Non-histone proteins are deacetylated by classes II and IV HDACs located predominantly in the cytoplasm<sup>7</sup> as well as by class I HDACs. For example, HDAC6 deacetylates tubulin and HSP90, and both HDAC1 and SIRT1 deacetylate p53.<sup>11</sup> Class III HDACs (sirtuins) may also play an important role in regulating tumor onset and/or progression. At present it remains unclear exactly what role sirtuins may play in oncogenesis and if their dominant role may be as tumor suppressors or oncogenes.<sup>7</sup>

HDAC inhibitors have been studied for their therapeutic effects on cancer cells.<sup>12</sup> Suberoylanilide hydroxamic acid (SAHA, vorinostat) is the first HDAC inhibitor approved by the FDA in 2006 for the treatment of cutaneous T-cell lymphoma (CTCL).<sup>13</sup> In November 2009, FDA also approved romidepsin (FK228) for treatment of CTCL in patients who have received at least one prior

Received: March 28, 2011

Published: June 02, 2011

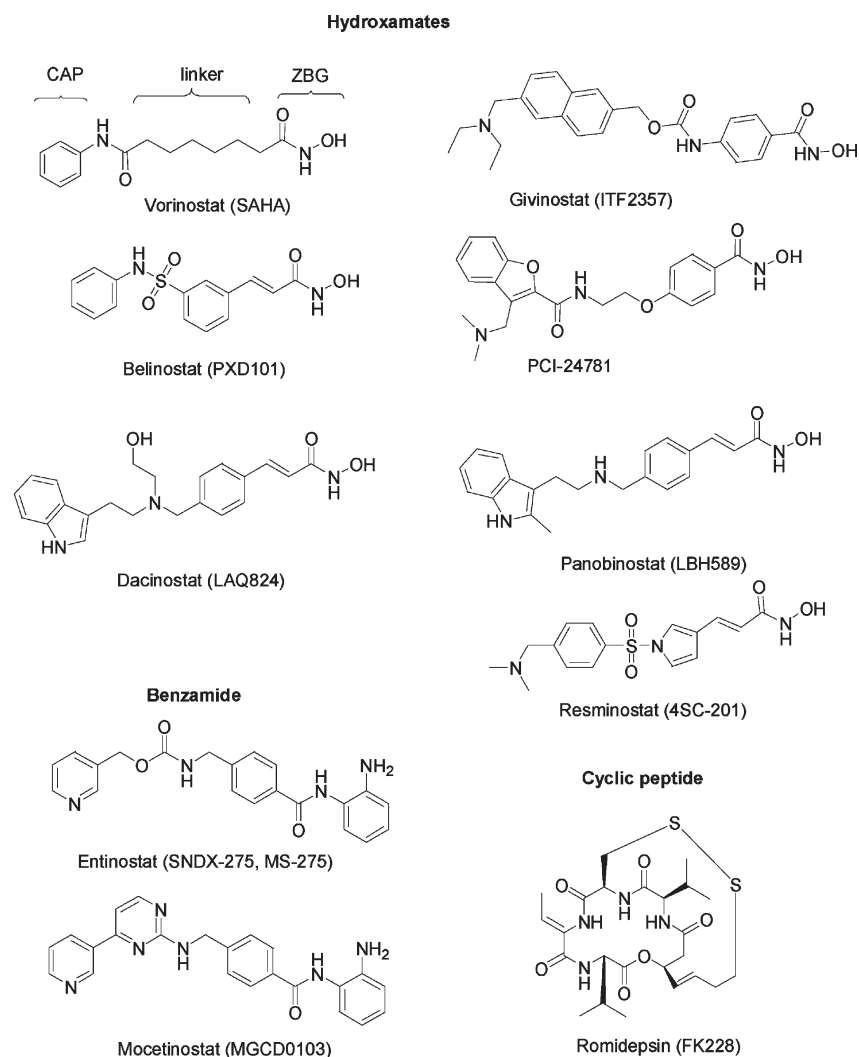


**Figure 1.** Clinically tested HDAC inhibitors.

systemic therapy.<sup>14</sup> These two approved drugs have validated the therapeutic use of HDAC inhibitors in cancer therapy.

There are a number of HDAC inhibitors that are currently undergoing clinical trials either as a single agent therapy or in combination with standards of care (SOC) or other targeted therapies for the treatment of solid and hematologic malignancies (Figure 1). Most of the compounds are pan-inhibitors, but there are also isoform selective or class selective HDAC inhibitors in development.<sup>15,16</sup> The morphology of the HDAC inhibitor pharmacophore, as exemplified by vorinostat (Figure 1), is characterized by three portions: a metal- or zinc-binding group (ZBG), a hydrophobic group (CAP) for protein surface recognition or interaction, and a linker to connect both ZBG and CAP. The common linkers are aliphatic chain (e.g., six-carbon chain in vorinostat), aromatic ring (e.g., 1,4-phenylene in entinostat), and vinyl-aromatic (e.g., styryl in belinostat). The most common ZBGs are hydroxamic acid and benzamide. The disulfide bond of romidepsin can be reduced *in vivo* by glutathione (GSH) to form Zn-binding free thiols and conjugates with GSH. There are other types of ZBGs such as ketone, thiol,  $\alpha$ -acetylmercapto ketone, and so on,<sup>15</sup> but hydroxamic acid remains the most potent ZBG reported for inhibition of class I HDACs.

As part of our ongoing effort to discover novel anticancer agents, we have designed and synthesized a number of chemical

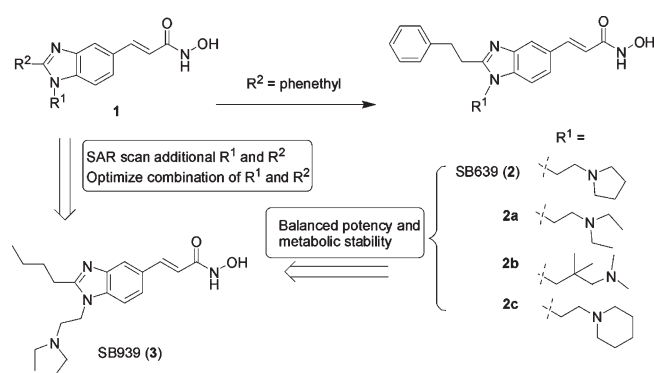


**Figure 2.** Benzimidazole based hydroxamic acid **1** and structures of **2**, **2a–c**, and **3**.

series of hydroxamates.<sup>17</sup> We recently reported *N*-hydroxy-1,2-disubstituted-1*H*-benzimidazol-5-ylacrylamides (**1**) (Figure 2) as novel HDAC inhibitors, and SB639 (**2**),<sup>18</sup> one of the representative compounds, showed promising pharmacological and pharmacokinetic properties. In general, compounds with good *in vitro* potency from the initial series **1** (e.g., **2**, **2a–c**, Figure 2) are

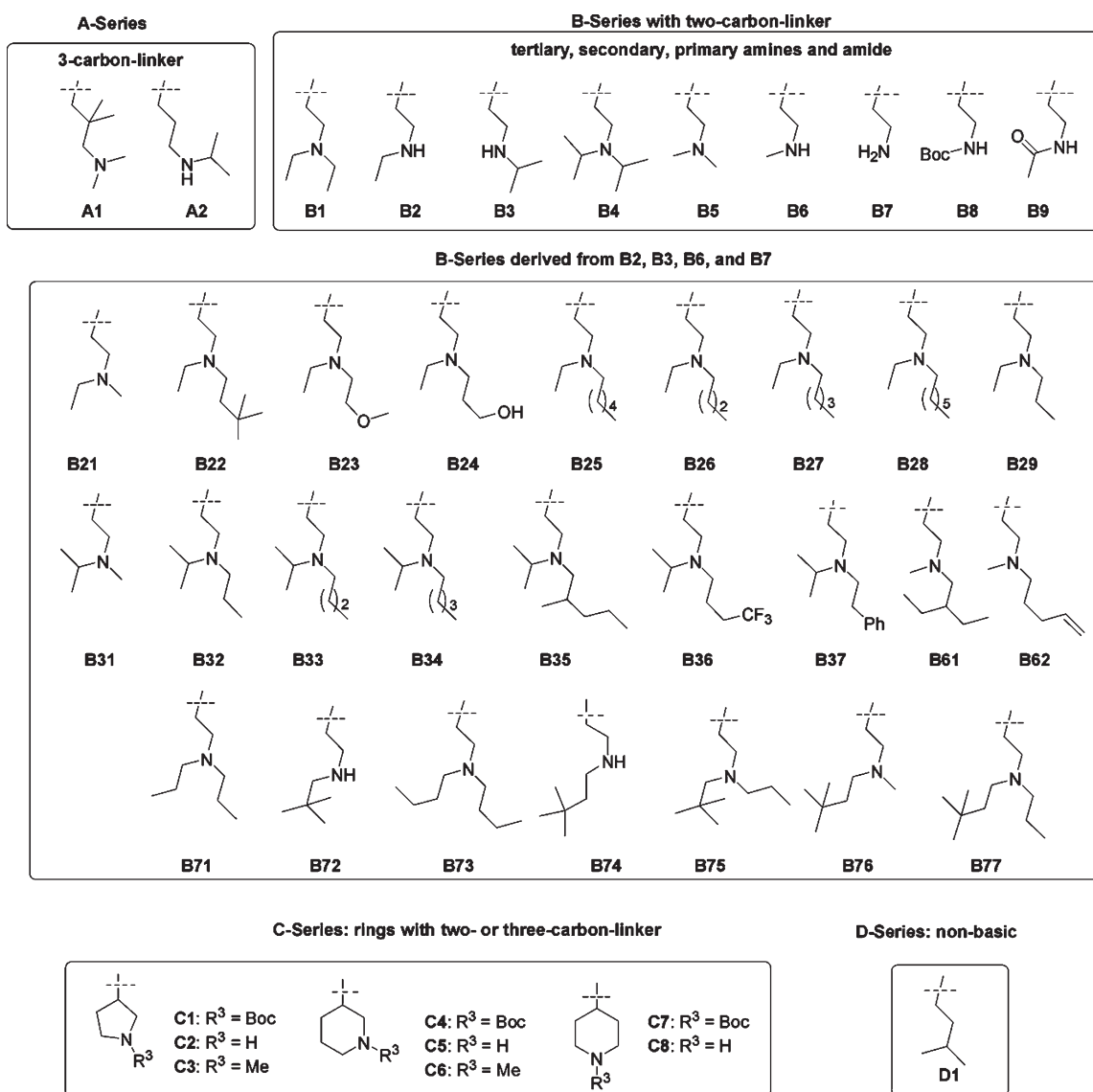


**Figure 3.** Representative R<sup>1</sup> side chains for optimization of benzimidazole based hydroxamic acid **1**. B8, C1, C4, and C7 are Boc protected R<sup>1</sup> groups and used for syntheses of intermediates for **1**.

metabolically unstable in human liver microsomal assays, with the exception of **2**.<sup>18</sup> A preliminary metabolism study using rat liver hepatocytes revealed that **2** was metabolized by oxidation of the R<sup>1</sup> group (pyrrolidinylethyl) and reduction of hydroxamic acid (CONHOH) to amide (CONH<sub>2</sub>) which is no longer a potent ZBG. The formation of the amide metabolite was also observed after 1 h of incubation of **2** with human hepatocytes. Thus, metabolic stability was identified as a major issue for this series of compounds. From a medicinal chemistry perspective, the primary focus was then to synthesize compounds metabolically stable in both human assay systems and preclinical species. Herein, we describe the further optimization and development of series **1** that led to the discovery of SB939 (**3**) (Figure 2),<sup>15,16,19</sup> currently in multiple phase I and phase II clinical trials.<sup>20,21</sup>

## RESULTS AND DISCUSSION

**Chemistry.** An efficient synthesis of a wide range of benzimidazole based hydroxamic acids **1** (Figure 2) was developed and

reported earlier<sup>18</sup> and extended herein to introduce more complex R<sup>1</sup> and R<sup>2</sup> groups. Representative R<sup>1</sup> side chains are listed in Figure 3, and R<sup>2</sup> side chains are listed in Figure 4. Four types of R<sup>1</sup> were selected. Type A series have linkers of three carbons between N<sup>1</sup> of the benzimidazole ring and the basic nitrogen in the R<sup>1</sup> group. Type B series have two-carbon linkers. C series have a rigid ring system with a two-carbon or three-carbon equivalent linker, and type D series R<sup>1</sup> groups are neutral. R<sup>1</sup> side chains with a free basic NH were further derivatized via reductive amination, alkylation with alkyl halides, or acylation. For example (Figure 3), B21–29, B31–37, B61–62, and B71–77 are derived from B2, B3, B6, and B7, respectively. Three types of R<sup>2</sup> were selected: Type a series are  $\alpha$ -branched either cyclic or acyclic. Type b series are  $\alpha$ -unsubstituted with either a methylene linker, hydrogen, methyl or trifluoromethyl, and type C series are basic.

Chemical synthesis and characterization of key compounds which were used for SAR determination and in vivo evaluations are described in the Experimental Section, and those compounds used for general supportive SAR establishment are described in

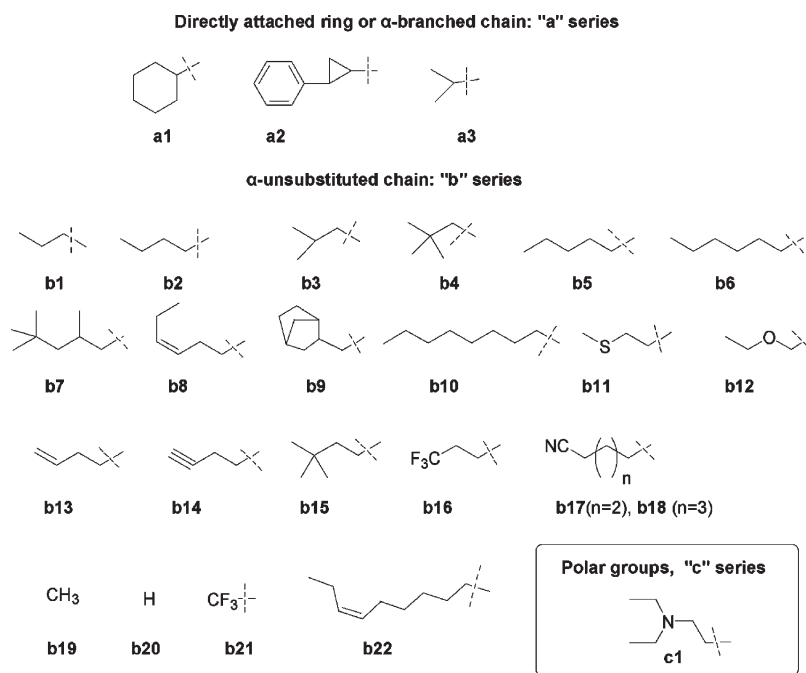
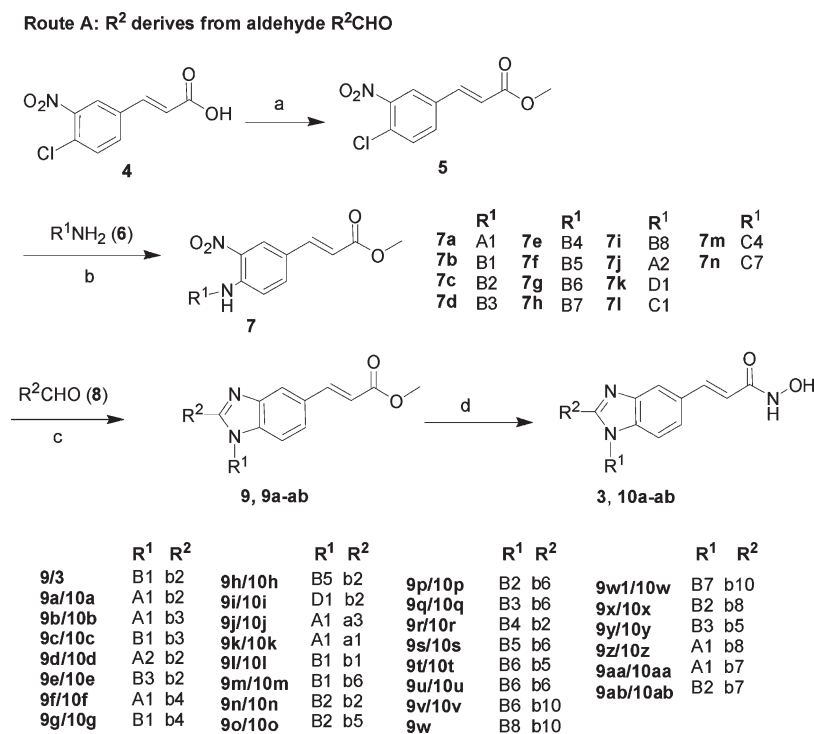


**Figure 4.** Representative  $R^2$  side chains for optimization of benzimidazole based hydroxamic acid **1**.

### Scheme 1<sup>a</sup>

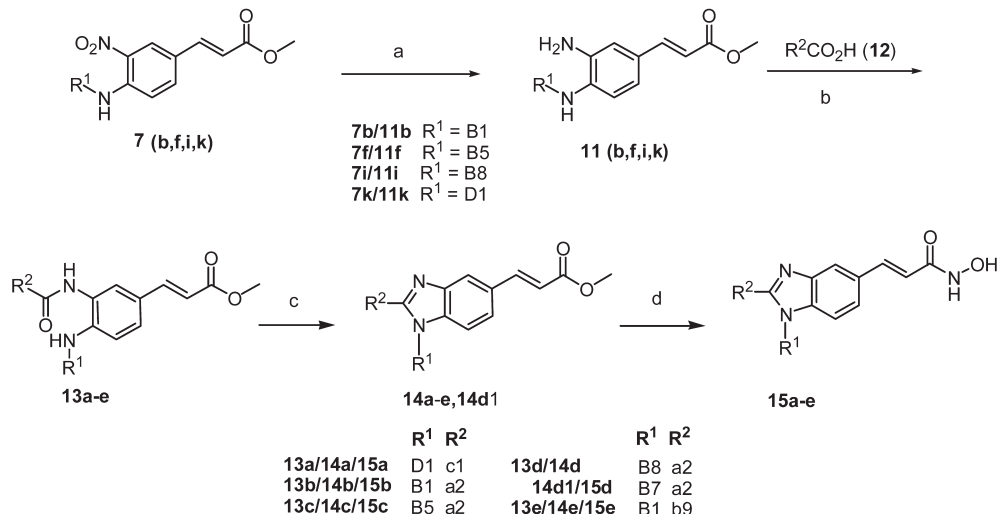


<sup>a</sup> Reagents and conditions: (a) MeOH,  $\text{H}_2\text{SO}_4$ , reflux, 95%; (b)  $\text{Et}_3\text{N}$ , dioxane, 80–100 °C, 53–98%; (c)  $\text{SnCl}_2 \cdot 2\text{H}_2\text{O}$  (5 equiv), AcOH–MeOH (1:9), 40 °C, 15–65%; (d)  $\text{NH}_2\text{OH} \cdot \text{HCl}$  (10 equiv)/NaOMe (20 equiv)/MeOH, 0 °C to room temp, 10–90%; (e) conc HCl, HOAc, 70 °C, de-Boc of **9w** to afford **9w1**. Codes for  $R^1$  and  $R^2$  groups are defined in Figures 3 and 4, respectively.

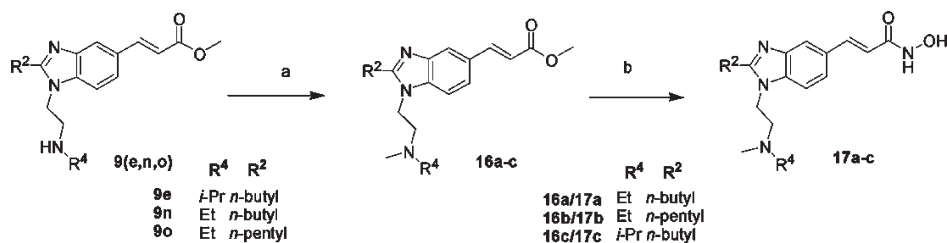
the Supporting Information (see Table S1 for a full list of the target compounds synthesized for this report).

Scheme 1 (route A) illustrates the procedure used for preparing compounds of formula **10** (and **3**), starting with commercially

available *trans*-3-nitro-4-chlorocinnamic acid (**4**) which was esterified in acidic methanol to give the methyl ester (**5**) in almost quantitative yield. Then the chloride ortho to the activating electron-withdrawing nitro group was displaced by the appropriate amine

Scheme 2<sup>a</sup>Route B: R<sup>2</sup> derives from acid R<sup>2</sup>CO<sub>2</sub>H

<sup>a</sup> Reagents and conditions: (a) SnCl<sub>2</sub>·2H<sub>2</sub>O (5 equiv), AcOH–MeOH (1:9), 40 °C; (b) coupling reagent (EDCI/HOBt), DIEA, DCM; (c) HOAc, 90–100 °C; (d) NH<sub>2</sub>OH·HCl (10 equiv)/NaOMe (20 equiv)/MeOH, 0 °C to room temp; (e) HCl, 70 °C, de-Boc of **14d** to give **14d1**. Codes for R<sup>1</sup> and R<sup>2</sup> groups are defined in Figures 3 and 4, respectively.

Scheme 3<sup>a</sup>

<sup>a</sup> Reagents and conditions: (a) HCHO, MeOH, NaBH(OAc)<sub>3</sub>, room temp; (b) NH<sub>2</sub>OH·HCl (10 equiv)/NaOMe (20 equiv)/MeOH, 0 °C to room temp.

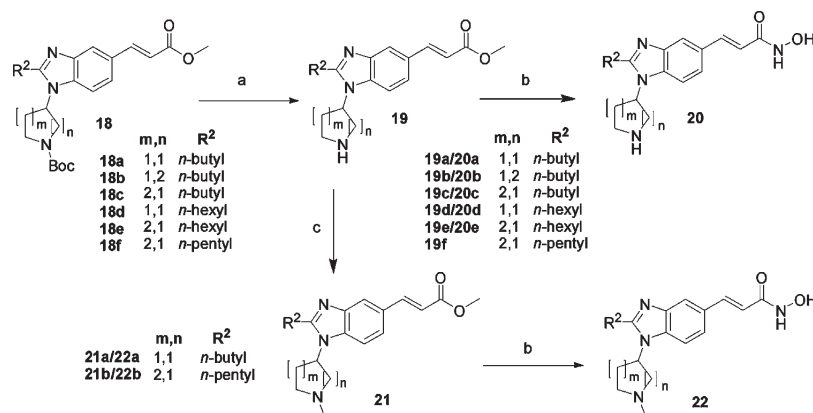
component R<sup>1</sup>NH<sub>2</sub> (**6**) in the presence of a base (e.g., triethylamine) to give a substituted aniline (**7**) in 53–98% yield. The key one-pot reductive cyclization with aldehyde R<sup>2</sup>CHO (**8**) forms the benzimidazole ring.<sup>22</sup> In this reaction the nitro group of **7** was reduced by a reducing agent such as tin(II) chloride in acetic acid, and in the presence of the appropriate aldehyde component **8**, cyclization was achieved to give benzimidazoles (**9**) in 15–65% yield. Methyl esters **9/9a–ab** were treated with hydroxylamine (hydroxylamine hydrochloride + excessive sodium methoxide in methanol) and converted to the target hydroxamates **3/10a–ab** in 10–90% yield. For most of the compounds, the reaction mixture of **3/10a–ab** was quenched with trifluoroacetic acid (TFA) or HCl and purified by preparative reverse phase HPLC, affording the final products **3/10a–ab** as TFA salts. Alternatively, the pH of the reaction mixture of **3/10a–ab** was adjusted to around 8, and the freebase of **3/10a–ab** was isolated by filtration. The pure base was further converted to the hydrochloride salt, and the stoichiometry of the salt was determined by elemental analysis. Compounds used for in vivo evaluations were all hydrochloride salts. Chemical structures were confirmed by 1D and 2D NMR, LC–MS, and elemental analysis.

When aldehyde **8** was not commercially available, a second synthetic route (route B, Scheme 2) was used. Nitro compound **7**

was reduced to aniline **11**. Then **11** was subsequently reacted with acid R<sup>2</sup>CO<sub>2</sub>H (**12**) to form amide(s) **13** under routine coupling conditions. Normally, **13** was not isolated or purified but used directly for the next step of cyclization forming benzimidazole **14** when heated in acetic acid. This method is applicable to most acids (**12**) including acetic acid and TFA. Compound **14d1** was made by removal of the Boc protecting group of **14d**. Methyl esters **14a–c**, **14d1**, and **14e** were converted to hydroxamic acids **15a–e** as described for synthesis of **3/10a–ab**.

R<sup>1</sup> side chains of benzimidazoles **9** could be further derivatized before converting to hydroxamate. Scheme 3 describes the derivatization of R<sup>1</sup> side chains bearing a secondary amine. Benzimidazole methyl ester amines **9e**, **9n**, and **9o** were alkylated by reductive amination. The alkylation products **16a–c** were subsequently converted to hydroxamates **17a–c**.

The above-described methods were also applied to benzimidazole methyl ester **18**, which has a Boc protected cyclic amine at the R<sup>1</sup> position (Scheme 4). **18a–f** were made from **7l**, **7m**, and **7n** (Scheme 1) by using methods described for **9** and **9a–ab**. Cleavage of the Boc group from **18a–f** was achieved under acidic conditions (HCl, MeOH, reflux) to afford secondary amines **19a–f**, of which **19a–e** were converted to hydroxamates **20a–e**.

Scheme 4<sup>a</sup>

<sup>a</sup> Reagents and conditions: (a) MeOH, 1.25 M HCl, reflux; (b) NH<sub>2</sub>OH·HCl (10 equiv)/NaOMe (20 equiv)/MeOH, 0 °C to room temp; (c) HCHO, NaBH(OAc)<sub>3</sub>, MeOH, room temp, 1 h.

Secondary amines **19a** (R<sup>2</sup> = *n*-butyl) and **19f** (R<sup>2</sup> = *n*-pentyl) were alkylated by reductive amination to afford the tertiary amines **21a,b** which were subsequently converted to hydroxamates **22a,b** after reaction with hydroxylamine.

The above representative synthetic methods and strategies were used to prepare the majority of target compounds. Additional synthetic methods and details not mentioned in the Experimental Section may be found in the Supporting Information.

**In Vitro Biological Evaluation and SAR.** HDAC isozyme HDAC1 and human colon cancer cell line COLO 205 were used as routine enzymatic and cellular antiproliferation screening tests, respectively. Vorinostat was used as positive control in all experiments. After the primary tests, compounds passed the selection criteria (i.e., IC<sub>50</sub>(HDAC1) ≤ 50 nM and IC<sub>50</sub>(COLO 205) ≤ 0.050 μM) and those picked for better understanding of an individual profile (e.g., **3**, **10c**, **10n**, and **10z**) were tested against additional cancer cell lines.

Preliminary SAR established in early work<sup>18</sup> suggested that there was a preferred distance between the basic nitrogen of the R<sup>1</sup> side chain and the N<sup>1</sup> of the benzimidazole ring for benzimidazole hydroxamates **1** (R<sup>2</sup> = PhCH<sub>2</sub>CH<sub>2</sub>-). Extension of this SAR to new hydroxamates **3**, **10a–ab**, **15a–e**, **17a–c**, **20a–e**, and **22a,b**, is described in Schemes 1–4, respectively, and biological data are listed in Table 1. With the same R<sup>2</sup> group, compounds having R<sup>1</sup> with two-carbon linkers are generally on the more potent side than those of three-carbon linkers, for example, **3** versus **10a**, **10c** versus **10b**, **10e** versus **10d**. Of the 60 R<sup>1</sup> compounds in this series, there were 18 with three-carbon linkers (Table S2, Supporting Information) and 42 with two-carbon linkers (Table S3, Supporting Information); they all followed the general trend of two-carbon linker being preferred. However, with a bulkier R<sup>2</sup> (i.e., *tert*-butylmethyl) this trend was reversed; for example, **10g** is less potent than **10f**. **10f** appears to be an outlier, with unexpectedly good enzyme and cellular potency.

A basic center is important in the R<sup>1</sup> group, as evident by comparing **10h** with **10i** (Table 1). **10i** lost over an order of magnitude of its enzymatic and cellular activity, and the binding efficiency index (BEI)<sup>23</sup> is significantly reduced from 21.3 to 17.0 after replacing the R<sup>1</sup> basic nitrogen of **10h** with a carbon. By addition of a basic center to the R<sup>2</sup> group, such as in **15a**, the enzymatic potency can be improved compared to nonbasic **10i**, but the BEI is still very low, and both the enzymatic and cellular

potency is still weak compared to those with basic centers at R<sup>1</sup> (**3**, **10a–h**). Thus, a basic center in the R<sup>1</sup> group is crucial for optimal biological activity of this series.

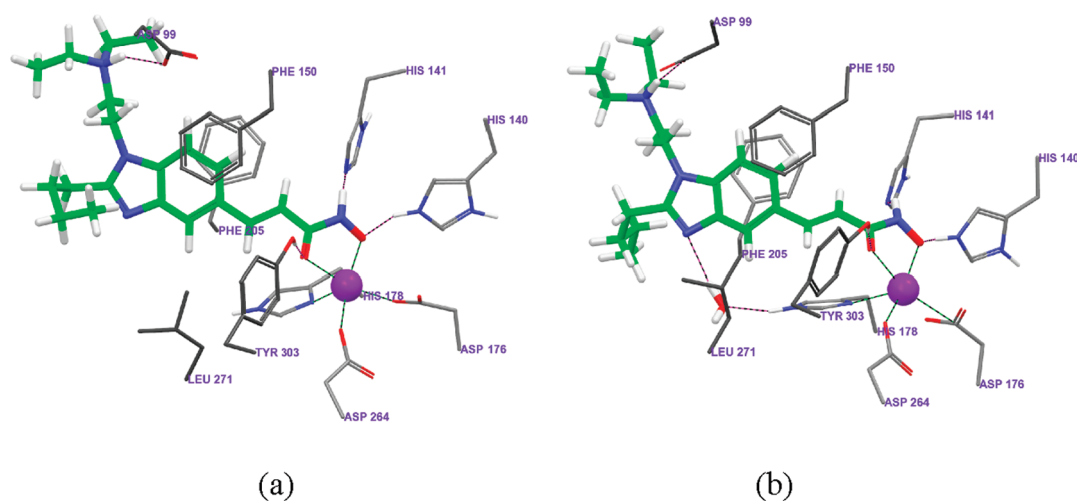
The above SAR can be satisfactorily explained by docking studies of compounds into a homology model of the enzyme active site. Docking compound **3** into the HDAC1 homology model<sup>24</sup> revealed a key electrostatic interaction between the R<sup>1</sup> basic center and Asp99 (Figure 5). There may be an additional hydrogen bonding interaction between benzimidazole N<sup>3</sup> and His178 via a water molecule (Figure 5b); thus, both basic centers contribute to the binding of the most potent compounds. For compounds with longer three-carbon linkers, due to their increased distance between the R<sup>1</sup> basic center and the benzimidazole, the side chain is more floppy and the conformational entropy increases. In addition, to make similar interactions with Asp99 the R<sup>1</sup> side chain is forced into a higher energy conformation; hence, the potency is reduced compared to the more optimal two-carbon linkers. However, **10f** has a bulky *gem*-dimethyl group in the R<sup>1</sup> side chain and a bulky *tert*-butylmethyl group at R<sup>2</sup> which may force it to adopt a more favorable conformation for effective interaction with Asp99. The increased bulk of the R<sup>1</sup> side chain increases lipophilic interactions with the protein. When **10f** is docked into the HDAC1 homology model, the R<sup>1</sup> side chain has double the number of atom–atom van der Waals contacts with the protein compared to the R<sup>1</sup> side chain of **3**. These factors may contribute to the better potency of **10f** among the three-carbon linker series.

Hydroxamates with directly attached cyclic R<sup>1</sup> groups (**20a–e** and **22a,b**, Table 2) have linkers of two to four carbons between the basic nitrogen in the side chain and the core benzimidazole nitrogen N<sup>1</sup>. They may be considered as rigid close comparators to the flexible acyclic R<sup>1</sup> compounds discussed from Table 1. With R<sup>2</sup> fixed as *n*-butyl, cyclic secondary amines **20a–c** exhibited comparable HDAC1 inhibitions (e.g., IC<sub>50</sub> and BEI) to their more flexible cousins, but the cellular activities of some compounds were poor possibly because of the strongly basic nature of some secondary amines which would have made them less permeable to cells. However, the data are more complex: there appears to be a correlation between the number of carbons (related to lipophilicity (log *P*)) and the cellular potency. For example, when R<sup>2</sup> in **20a** was changed to *n*-hexyl, giving **20d**, the clog*P* increased by 0.88 unit, leading to significant improvement

Table 1. R<sup>1</sup> SARs: Linker between R<sup>1</sup> basic Nitrogen and Benzimidazole N<sup>1</sup> and the Role of the Basic Center (Nitrogen)

| Compd | R <sup>1</sup> | R <sup>2</sup>    | MW  | clogP | HDAC1 <sup>a</sup><br>IC <sub>50</sub> (nM) | COLO 205 <sup>b</sup><br>IC <sub>50</sub> (μM) | HDAC1<br>BEI <sup>c</sup> |
|-------|----------------|-------------------|-----|-------|---|--|---------------------------|
| 3     |                | <i>n</i> -butyl   | 358 | 3.61  | 77 ± 14                                     | 0.56 ± 0.08                                    | 19.8                      |
| 10a   |                | <i>n</i> -butyl   | 372 | 4.12  | 150 ± 14                                    | 2.23 ± 0.33                                    | 18.3                      |
| 10b   |                | <i>iso</i> -butyl | 372 | 4.04  | 175 ± 7                                     | 2.69 ± 0.68                                    | 18.1                      |
| 10c   |                | <i>iso</i> -butyl | 358 | 3.52  | 92 ± 7                                      | 0.81 ± 0.34                                    | 19.6                      |
| 10d   |                | <i>n</i> -butyl   | 358 | 3.90  | 165 ± 6                                     | 2.89 ± 0.13                                    | 18.9                      |
| 10e   |                | <i>n</i> -butyl   | 344 | 3.46  | 42 ± 7                                      | 0.47 ± 0.06                                    | 21.4                      |
| 10f   |                |                   | 386 | 4.44  | 46 ± 7                                      | 0.57 ± 0.16                                    | 19.0                      |
| 10g   |                |                   | 372 | 3.92  | 135 ± 21                                    | 1.19 ± 0.32                                    | 18.4                      |
| 10h   |                | <i>n</i> -butyl   | 330 | 2.93  | 90 ± 1                                      | 0.65 ± 0.02                                    | 21.3                      |
| 10i   |                | <i>n</i> -butyl   | 329 | 4.80  | 2,490 ± 370                                 | 6.02 ± 0.94                                    | 17.0                      |
| 15a   |                |                   | 372 | 3.96  | 575 ± 34                                    | 6.81 ± 0.17                                    | 16.8                      |

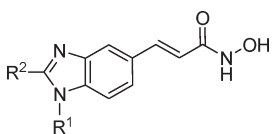
<sup>a</sup> Values are expressed as the mean ± standard deviation (SD) of at least two independent duplicate experiments. <sup>b</sup> Values are expressed as the mean ± SD of at least two independent triplicate experiments. <sup>c</sup> Binding efficiency index BEI =  $pIC_{50}/[MW \text{ (kDa)}] = -1000 \log[IC_{50} \text{ (M)}]/MW$ ; see ref 23.

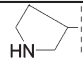
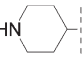
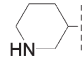
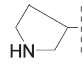
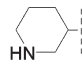
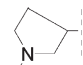
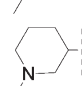


**Figure 5.** Compound 3 docked into two different homology models (built based on the HDLP X-ray structure 1C3R (a) or human HDAC2 X-ray structure 3MAX (b)). The basic center of the R<sup>1</sup> side chain attached to benzimidazole nitrogen N<sup>1</sup> has an electrostatic interaction with Asp99, and the benzimidazole nitrogen N<sup>3</sup> can also form a hydrogen bond with His178 via a water molecule (b). Key interactions between these basic centers with Asp99 and His178 contribute to the potency.

in cellular potency. A similar trend can be seen with 20c and 20e: 20e enjoyed a 3.6-fold improvement in cellular activity compared

to 20c. The trend of additional lipophilicity enhancing cellular potency continues when the secondary amine is methylated. The

Table 2. R<sup>1</sup> SARs: Directly Attached Cyclic Ammine as R<sup>1</sup>


| Compd | R <sup>1</sup>  | R <sup>2</sup>   | MW  | clogP | HDAC1 <sup>a</sup><br>IC <sub>50</sub> (nM) | COLO 205 <sup>b</sup><br>IC <sub>50</sub> (μM) | HDAC1<br>BEI <sup>c</sup> |
|-------|---|------------------|-----|-------|---|--|---------------------------|
| 20a   |  | <i>n</i> -butyl  | 328 | 2.87  | 110 ± 14                                    | 16.4 ± 6.6                                     | 21.2                      |
| 20b   |  | <i>n</i> -butyl  | 342 | 3.31  | 68 ± 1                                      | 7.00 ± 2.02                                    | 20.9                      |
| 20c   |  | <i>n</i> -butyl  | 342 | 3.31  | 190 ± 14                                    | 4.87 ± 2.77                                    | 19.6                      |
| 20d   |  | <i>n</i> -hexyl  | 356 | 3.75  | 41 ± 3                                      | 1.46 ± 0.63                                    | 20.7                      |
| 20e   |  | <i>n</i> -hexyl  | 370 | 4.19  | 105 ± 7                                     | 1.34 ± 0.71                                    | 18.8                      |
| 22a   |  | <i>n</i> -butyl  | 342 | 3.14  | 125 ± 21                                    | 1.09 ± 0.61                                    | 20.2                      |
| 22b   |  | <i>n</i> -pentyl | 370 | 4.02  | 158 ± 6                                     | 2.10 ± 0.42                                    | 18.4                      |

<sup>a</sup> Values are expressed as the mean ± standard deviation (SD) of at least two independent duplicate experiments. <sup>b</sup> Values are expressed as the mean ± SD of at least two independent triplicate experiments. <sup>c</sup> Binding efficiency index BEI =  $\text{pIC}_{50}/[\text{MW (kDa)}] = -1000 \log[\text{IC}_{50} (\text{M})]/\text{MW}$ ; see ref 23.

resulting tertiary amine's cellular potencies are significantly improved: there was 15-fold cellular potency enhancement for **22a** versus **20a** and 2.3-fold for **22b** versus **20c**. N-Methylation does not appear to affect the interaction between the basic center and HDAC1 Asp99 but does seem to improve cell permeability which in turn leads to better cellular activity. However, **20a–e** and **22a,b** are not as potent as their acyclic analogues with similar molecular weights (e.g., **3**, **10e**, **10h**, Table 1). Moreover, the acyclic compounds were achiral and more readily available for further synthetic and biological studies; thus, further optimization of the benzimidazole series focused on acyclic two-carbon-linker R<sup>1</sup> groups.

SARs of three representative benzimidazole hydroxamates **1** with  $\alpha$ -substituted R<sup>2</sup> side chains together with R<sup>1</sup> = 3-hydroxypropyl have been reported previously.<sup>18</sup> SAR studies were herein extended to R<sup>1</sup> groups with basic centers (Table 3). Both enzymatic and cellular potencies were improved for compounds **10j** and **10k** compared to their counterparts bearing R<sup>1</sup> = 3-hydroxypropyl. There are differences between compounds bearing linear R<sup>2</sup> groups, such as **10a** compared to those having  $\alpha$ -substituted R<sup>2</sup> chains (e.g., **10j** and **10k**) in terms of HDAC1 inhibition, but differences in cellular potency were negligible. A bulky cyclohexyl group at R<sup>2</sup> (**10k**) significantly lowers BEI compared to  $\alpha$ -unsubstituted or less bulky  $\alpha$ -substituted R<sup>2</sup> counterparts (i.e., **10a** and **10j**). By introduction of a cyclopropyl to replace the simple ethylene linker of **2a** (Table 3),<sup>18</sup> both enzymatic and cellular potencies of the resulting **15b** were reduced about 3- to 4-fold compared to **2a**. The rigidity and bulkiness of the R<sup>2</sup>  $\alpha$ -substituted side chain might prevent it from effective interaction with the HDAC binding pocket. Once the basic R<sup>1</sup> was changed to the less bulky dimethylamino, the

resultant **15c** had no change in activity. Further reducing the size of R<sup>1</sup> to a simple primary amine such as **15d** led to recovery of HDAC1 potency, but the cellular potency dropped significantly probably because of lower permeability of the primary amine and globally lower lipophilicity of the molecule. Thus, **2a** remains the best of these four compounds. If the phenethyl chain of **2a** was replaced by a simple *n*-butyl, the resultant **3** is not quite as potent as **2a** in cells, but it is significantly better than **15d** which is of similar molecular weight. This SAR suggests that a simple alkyl (linear or non- $\alpha$ -substituted) R<sup>2</sup> chain provides sufficient potency with better binding efficiency (i.e., BEI of 19.8 for **3**, 21.4 for **10e**, and 19.0 for **10f**, the higher the better) compared to complex or aromatic ring containing R<sup>2</sup> chains (i.e., BEI of 18.6 for **2**, 17.9 for **2a**, 17.5 for **2b**, and 18.2 for **2c**).

After establishment of the above-mentioned SAR on R<sup>1</sup> and R<sup>2</sup>, the additive or synergistic effect of R<sup>1</sup> and R<sup>2</sup> was then explored (Table 4). With a fixed R<sup>1</sup> group, both the enzymatic and cellular potency increased along with an increase of length of the R<sup>2</sup> chain or clogP. For example, with R<sup>1</sup> group fixed as diethylaminoethyl, the calculated clogP values for compounds **10l** (R<sup>2</sup> = *n*-propyl), **10c** (R<sup>2</sup> = isopropyl, Table 1), **3** (R<sup>2</sup> = *n*-butyl), and **10m** (R<sup>2</sup> = *n*-hexyl) are 3.17, 3.52, 3.61 and 4.49, respectively. Both their enzymatic potency (HDAC1, IC<sub>50</sub> of 155, 92, 77, and 45 nM, respectively) and cellular potency (COLO 205, IC<sub>50</sub> of 0.98, 0.81, 0.56, and 0.42 μM, respectively) are increased along with clogP. If one of the ethyl groups was removed from the R<sup>1</sup> side chain of **3**, the resultant compound **10n** still maintained good HDAC1 potency, but cellular potency against COLO 205 dropped slightly probably because of a decrease in lipophilicity. By increase of the length of the R<sup>2</sup> side chain of **10n**, more potent compounds **10o** and **10p** were obtained. This trend also held true



Table 3. R<sup>2</sup> SARs:  $\alpha$ -Substituted R<sup>2</sup> Side Chain

| Compd | R <sup>1</sup> | R <sup>2</sup>  | MW  | clogP | HDAC1 <sup>a</sup><br>IC <sub>50</sub> (nM) | COLO 205 <sup>b</sup><br>IC <sub>50</sub> ( $\mu$ M) | HDAC1<br>BEI <sup>c</sup> |
|-------|----------------|-----------------|-----|-------|---|--|---------------------------|
| 10a   |                | <i>n</i> -butyl | 372 | 4.12  | 150 $\pm$ 14                                | 2.23 $\pm$ 0.33                                      | 18.3                      |
| 10j   |                |                 | 358 | 3.61  | 308 $\pm$ 68                                | 1.73 $\pm$ 0.58                                      | 18.2                      |
| 10k   |                |                 | 398 | 4.44  | 421 $\pm$ 29                                | 2.45 $\pm$ 0.53                                      | 16.0                      |
| 15b   |                |                 | 418 | 3.89  | 169 $\pm$ 6                                 | 0.63 $\pm$ 0.08                                      | 16.2                      |
| 15c   |                |                 | 390 | 3.21  | 175 $\pm$ 6                                 | 0.69 $\pm$ 0.21                                      | 17.3                      |
| 15d   |                |                 | 362 | 2.42  | 84 $\pm$ 1                                  | 4.53 $\pm$ 1.15                                      | 19.5                      |
| 2a    |                |                 | 406 | 3.12  | 52 $\pm$ 25                                 | 0.22 $\pm$ 0.12                                      | 17.9                      |
| 3     |                | <i>n</i> -butyl | 358 | 3.61  | 77 $\pm$ 14                                 | 0.56 $\pm$ 0.08                                      | 19.8                      |

<sup>a</sup> Values are expressed as the mean  $\pm$  standard deviation (SD) of at least two independent duplicate experiments. <sup>b</sup> Values are expressed as the mean  $\pm$  SD of at least two independent triplicate experiments. <sup>c</sup> Binding efficiency index BEI =  $\text{pIC}_{50}/[\text{MW (kDa)}] = -1000 \log[\text{IC}_{50} (\text{M})]/\text{MW}$ ; see ref 23.

for both **10e** and **10q**, which had a secondary amine (isopropylamino) R<sup>1</sup> group: both were more potent than their diethylamino counterparts **3** and **10m**. When the diisopropylamino was introduced as the R<sup>1</sup> group of **10r**, its steric bulk hindered the interaction between the R<sup>1</sup> basic center and HDAC1 Asp99 (Figure 5). Compound **10r** was also less potent in cells than either **10e** or **10q**. Removing one methylene group from each of the diethylamino groups of **3** to give the smallest possible tertiary amino R<sup>1</sup>, **10h**, still provided good potency. Returning these two carbons back to the R<sup>2</sup> side chain of **3** gave *n*-hexyl **10s** which was more potent than **3** in both enzymatic and cellular assays. Similarly, transferring a methyl group from R<sup>1</sup> to R<sup>2</sup> of **10h** gave **10t** with the smallest secondary amine at R<sup>1</sup> but the same molecular weight as **10h** and showed enhanced HDAC1 potency but reduced cellular potency perhaps because of lower permeability of the more polar secondary amine. This reduced cellular potency can be reversed by raising clogP through addition of one more carbon to the R<sup>2</sup> group of **10t**, giving for example **10u** having regained submicromolar cellular potency. Adding a further two carbons to give **10v** with a high clogP of 4.43 resulted in the most potent compound (HDAC1 IC<sub>50</sub> = 15  $\pm$  2 nM) in this series. Although in vitro potency can be achieved in this way, metabolic consequences cannot be ignored with long alkyl chains. Fortunately there are choices within this series of R<sup>1</sup>/R<sup>2</sup> variations that permit study of the pharmacokinetic and metabolic profiles of very closely related compounds, all of which possess potentially acceptable enzyme and cellular potency. For example, the isomeric compounds of MW 358 present an excellent opportunity for such a comparison: compound **10p** is most potent among the isomeric series **3**, **10c**, **10s**, and **10w**. Further studies were done (see below), but any of these compounds are worthy of further study. Clearly in vitro potency can be adjusted or tuned by judicious placement of carbons between R<sup>1</sup> and R<sup>2</sup> side chains as long as the total number of carbons shared between R<sup>1</sup> and R<sup>2</sup> falls in the range of 7–10.

**Broad Antiproliferative Activity.** Selected compounds were tested against a range of tumor cell lines (Table 5) and compared with vorinostat, panobinostat, and belinostat. The selected compounds showed broad antiproliferative activity against representative tumor cells from ovarian (A2780), colon (HCT-116), and prostate (PC-3), similar to belinostat and more potent than vorinostat. Panobinostat is clearly a very potent antiproliferative agent, but as will be discussed later, absolute potency is not the only consideration when selecting the preferred compound for progression into patients.

**QSAR of Enzymatic and Cellular Potency.** With a significant body of in vitro enzymatic and cellular data available, QSAR studies were possible to carry out in order to focus on the most critical parameters for further lead optimization. Parameters included were enzyme and cellular IC<sub>50</sub> and 18 compounds having R<sup>1</sup> = A series (three-carbon linker, Figure 3, Table S2) and 42 compounds with R<sup>1</sup> = B series (two-carbon linker, Figure 3, excluding B4 subseries, Table S3). Earlier it was established that the chain length and total number of carbons in the R<sup>1</sup> and R<sup>2</sup> side chains affect the in vitro potency as discussed above; hence, the correlation between IC<sub>50</sub> and clogP was investigated. The results (Figure 6) showed that lipophilicity does play a role for in vitro potency for this class of compounds: both enzymatic potency pIC<sub>50</sub>(HDAC1) and cellular potency pIC<sub>50</sub>(COLO 205) have weak positive correlations with clogP for both A and B series (excluding B4 series). Regression lines for the B series are above those for the A series, for compounds with similar clogP. The B series compounds are more potent than A series in both HDAC1 and COLO 205 assays. Figure 6 clearly shows that the B series are generally more potent than the A series. When both series are combined ( $n = 60$ ) for linear regression/correlation, the cellular potency pIC<sub>50</sub>(COLO 205) still correlates with clogP ( $p = 0.0056$ ) (Figure 6b), while the correlation between enzymatic potency pIC<sub>50</sub>(HDAC1) is not significant ( $p = 0.0907$ ).

Table 4. SARs of R<sup>2</sup> Length, Lipophilicity (R<sup>1</sup> + R<sup>2</sup>), and in Vitro Potencies

| Compd <sup>a</sup> | R <sup>1</sup> | R <sup>2</sup>   | MW  | clogP | HDAC1 <sup>a</sup><br>IC <sub>50</sub> (nM) | COLO 205 <sup>b</sup><br>IC <sub>50</sub> (μM) | HDAC1<br>BEI <sup>c</sup> |
|--------------------|----------------|------------------|-----|-------|---|--|---------------------------|
| 3                  |                | <i>n</i> -butyl  | 358 | 3.61  | 77 ± 14                                     | 0.56 ± 0.08                                    | 19.8                      |
| 10m                |                | <i>n</i> -hexyl  | 386 | 4.49  | 45 ± 6                                      | 0.42 ± 0.12                                    | 19.0                      |
| 10l                |                | <i>n</i> -propyl | 344 | 3.17  | 155 ± 21                                    | 0.98 ± 0.19                                    | 19.8                      |
| 10n                |                | <i>n</i> -butyl  | 330 | 3.00  | 77 ± 18                                     | 0.88 ± 0.37                                    | 21.5                      |
| 17a                |                | <i>n</i> -butyl  | 344 | 3.27  | 109 ± 3                                     | 1.65 ± 0.78                                    | 20.2                      |
| 10o                |                | <i>n</i> -pentyl | 344 | 3.44  | 27 ± 2                                      | 0.42 ± 0.03                                    | 22.0                      |
| 17b                |                | <i>n</i> -pentyl | 358 | 3.71  | 41 ± 1                                      | 0.45 ± 0.02                                    | 20.6                      |
| 10p                |                | <i>n</i> -hexyl  | 358 | 3.88  | 20 ± 7                                      | 0.19 ± 0.04                                    | 21.5                      |
| 10e                |                | <i>n</i> -butyl  | 344 | 3.46  | 42 ± 7                                      | 0.47 ± 0.06                                    | 21.4                      |
| 17c                |                | <i>n</i> -butyl  | 358 | 3.73  | 45 ± 1                                      | 0.54 ± 0.01                                    | 20.5                      |
| 10q                |                | <i>n</i> -hexyl  | 372 | 4.34  | 36 ± 7                                      | 0.17 ± 0.03                                    | 20.0                      |
| 10r                |                | <i>n</i> -butyl  | 386 | 4.53  | 335 ± 64                                    | 1.87 ± 0.09                                    | 16.8                      |
| 10h                |                | <i>n</i> -butyl  | 330 | 2.93  | 90 ± 1                                      | 0.65 ± 0.02                                    | 21.3                      |
| 10s                |                | <i>n</i> -hexyl  | 358 | 3.81  | 28 ± 6                                      | 0.33 ± 0.14                                    | 21.1                      |
| 10t                |                | <i>n</i> -pentyl | 330 | 3.10  | 41 ± 1                                      | 0.95 ± 0.05                                    | 22.4                      |
| 10u                |                | <i>n</i> -hexyl  | 344 | 3.54  | 29 ± 2                                      | 0.55 ± 0.01                                    | 21.9                      |
| 10v                |                | <i>n</i> -octyl  | 372 | 4.43  | 15 ± 2                                      | 0.23 ± 0.04                                    | 21.0                      |
| 10w                |                | <i>n</i> -octyl  | 358 | 3.90  | 22 ± 6                                      | 0.54 ± 0.03                                    | 21.4                      |

<sup>a</sup> Values are expressed as the mean ± standard deviation (SD) of at least two independent duplicate experiments. <sup>b</sup> Values are expressed as the mean ± SD of at least two independent triplicate experiments. <sup>c</sup> Binding efficiency index BEI =  $\text{pIC}_{50}/[\text{MW (kDa)}] = -1000 \log[\text{IC}_{50} (\text{M})]/\text{MW}$ ; see ref 23.

Relationships between enzymatic potency  $\text{pIC}_{50}(\text{HDAC1})$  and cellular potency  $\text{pIC}_{50}(\text{COLO 205})$  were also examined (Figure 7).  $\text{pIC}_{50}(\text{HDAC1})$  positively correlates with  $\text{pIC}_{50}(\text{COLO 205})$  for the A series ( $p < 0.0001$ ,  $n = 18$ ), B series ( $p < 0.0001$ ,  $n = 42$ ), and the combined A and B series ( $p < 0.0001$ ,  $n = 72$ ). Correlation with HDAC1 is also true for other tumor cell lines: 14 compounds were tested in all four cell lines (Table 5 and Figure S1, Supporting Information), and they all showed significant correlations for COLO 205 ( $p = 0.0009$ ), HCT-116 ( $p = 0.0019$ ), A2780 ( $p < 0.0001$ ), and PC-3 ( $p = 0.0033$ ). These studies confirm that HDAC1 plays an important role in cell

proliferation and that inhibitors of class I HDACs, especially HDACs 1, 2, and 3, usually show strong antiproliferative and apoptosis-inducing activity.<sup>7–10</sup> In summary, both enzymatic and cellular potencies may be tuned by judicious choice of the combination of R<sup>1</sup> and R<sup>2</sup> groups. The resultant potencies are in general predictable; thus, with this series there is a considerable freedom to optimize physicochemical and pharmacokinetic parameters without adversely affecting target potency.

**In Vitro Pharmacodynamic Biomarker: Quantification of Inhibition of HDAC in Cells.** A hallmark of HDAC inhibition is the increase in the acetylation level of histones. Acetylation of

Table 5. IC<sub>50</sub> of Selected Compounds

| compd        | HDAC1 IC <sub>50</sub> (nM) <sup>a</sup> | cellular IC <sub>50</sub> (μM) <sup>b</sup> |               |               |               |
|--------------|--|---|---------------|---------------|---------------|
|              |  | A2780                                       | COLO 205      | HCT-116       | PC-3          |
| 2            | 29 ± 10                                  | 0.19 ± 0.14                                 | 0.13 ± 0.05   | 0.19 ± 0.11   | 0.15 ± 0.08   |
| 2b           | 42 ± 21                                  | 0.11 ± 0.01                                 | 0.11 ± 0.07   | 0.16 ± 0.10   | 0.18 ± 0.08   |
| 2c           | 23 ± 13                                  | 0.031 ± 0.001                               | 0.087 ± 0.063 | 0.10 ± 0.03   | 0.12 ± 0.04   |
| 3            | 77 ± 15                                  | 0.48 ± 0.21                                 | 0.56 ± 0.08   | 0.48 ± 0.27   | 0.34 ± 0.06   |
| 10e          | 42 ± 7                                   | 0.38 ± 0.01                                 | 0.47 ± 0.06   | 0.34 ± 0.06   | 0.23 ± 0.05   |
| 10f          | 46 ± 7                                   | 0.44 ± 0.04                                 | 0.57 ± 0.16   | 0.80 ± 0.30   | 0.50 ± 0.15   |
| 10c          | 92 ± 7                                   | 1.24 ± 0.15                                 | 0.81 ± 0.34   | 1.30 ± 0.35   | 0.95 ± 0.24   |
| 10n          | 77 ± 18                                  | 0.76 ± 0.34                                 | 0.88 ± 0.37   | 1.11 ± 0.27   | 0.38 ± 0.20   |
| 10p          | 20 ± 7                                   | 0.24 ± 0.06                                 | 0.19 ± 0.04   | 0.23 ± 0.12   | 0.21 ± 0.06   |
| 10q          | 36 ± 7                                   | 0.20 ± 0.04                                 | 0.17 ± 0.03   | 0.21 ± 0.07   | 0.17 ± 0.06   |
| 10s          | 28 ± 6                                   | 0.23 ± 0.01                                 | 0.33 ± 0.14   | 0.33 ± 0.02   | 0.25 ± 0.15   |
| 10x          | 21 ± 4                                   | 0.20 ± 0.02                                 | 0.31 ± 0.09   | 0.66 ± 0.16   | 0.16 ± 0.01   |
| 10y          | 30 ± 9                                   | 0.23 ± 0.01                                 | 0.28 ± 0.10   | 0.26 ± 0.12   | 0.12 ± 0.08   |
| 10z          | 53 ± 1                                   | 0.37 ± 0.02                                 | 0.62 ± 0.16   | 0.92 ± 0.31   | 0.38 ± 0.04   |
| 10aa         | 37 ± 1                                   | 0.23 ± 0.02                                 | 0.15 ± 0.01   | 0.41 ± 0.06   | 0.31 ± 0.04   |
| 10ab         | 23 ± 2                                   | 0.14 ± 0.01                                 | 0.14 ± 0.04   | 0.27 ± 0.05   | 0.10 ± 0.01   |
| 15e          | 32 ± 13                                  | 0.21 ± 0.03                                 | 0.39 ± 0.04   | 0.33 ± 0.00   | 0.53 ± 0.18   |
| vorinostat   | 119 ± 37                                 | 1.62 ± 0.47                                 | 2.12 ± 0.64   | 2.85 ± 1.61   | 1.21 ± 0.85   |
| belinostat   | 63 ± 27                                  | 0.67 ± 0.41                                 | 0.70 ± 0.39   | 0.60 ± 0.21   | 0.45 ± 0.19   |
| panobinostat | 6.8 ± 4.4                                | 0.035 ± 0.011                               | 0.018 ± 0.006 | 0.048 ± 0.028 | 0.024 ± 0.020 |

<sup>a</sup> Values are expressed as the mean ± standard deviation (SD) of at least two independent duplicate experiments. <sup>b</sup> Values are expressed as the mean ± SD of at least two independent triplicate experiments.

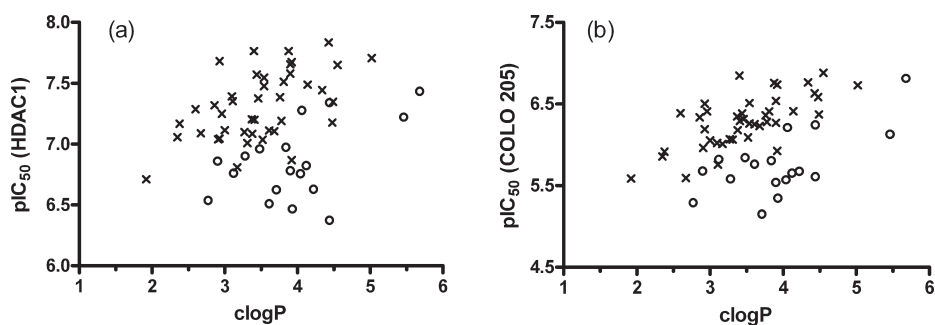


**Figure 6.** Both enzymatic and cellular potencies (pIC<sub>50</sub>) correlate with lipophilicity clogP. pIC<sub>50</sub> = -log[IC<sub>50</sub> (M)]. (a) pIC<sub>50</sub> (HDAC1) correlate with clogP: A series (○, *n* = 18, Pearson *r* = 0.5121, *p* = 0.0298); B series (×, *n* = 42, Pearson *r* = 0.5347, *p* = 0.0003). (b) pIC<sub>50</sub> (COLO 205) correlate with clogP: A series (○, *n* = 18, Pearson *r* = 0.6595, *p* = 0.0029), linear regression equation pIC<sub>50</sub>(COLO 205) = 0.3389 clogP + 4.426, *R*<sup>2</sup> = 0.4350; B series (×, *n* = 42, Pearson, *r* = 0.6947, *p* < 0.0001), linear regression equation pIC<sub>50</sub>(COLO 205) = 0.3379 clogP + 5.112, *R*<sup>2</sup> = 0.4827.

histones H3, H4, and H2A can be detected by Western immunoblotting. To increase the throughput of the analysis, an enzyme linked immunosorbent assay (ELISA) was developed to detect and quantify acetylated histone 3 (AcH3) in the protein lysates obtained from cancer cell lines treated with the HDAC inhibitors. Key compounds reported herein were tested for their ability to increase AcH3 level in an in vitro assay in COLO 205 cells at 10 μM. The level of AcH3 was benchmarked to that of vorinostat, which was also tested at 10 μM. Twenty-nine compounds generated a range of 0.8- to 2.5-fold of AcH3 compared to that of vorinostat (Table S4, Supporting Information). The AcH3 level was found to correlate with both enzymatic potency pIC<sub>50</sub>(HDAC1) (*p* = 0.0141) and cellular potency pIC<sub>50</sub>(COLO 205) (*p* = 0.0266) (Figure 8). The AcH3 level in COLO 205 cells may be modulated by different doses of HDAC inhibitors. For a small number of

compounds, the effective dose to induce a 50% increase of AcH3 (EC<sub>50</sub>) in COLO 205 cells was also determined. The cellular potency pIC<sub>50</sub>(COLO 205) also positively correlates with pEC<sub>50</sub> (Figure S2 and Table S5, Supporting Information). These results confirmed that these benzimidazole hydroxamates are targeting histone deacetylases in cells with equal or greater efficiency than vorinostat in inducing hyperacetylation of H3. A compound's inhibitory potency against HDAC targets in cells can be assessed with measurement of the AcH3 level it induces.

**Inhibition of HDAC Isoenzymes.** Only HDAC1 was used for enzymatic primary screening assays. For selected compounds, profiling against the isozymes was also performed (Table 6). BIOMOL substrate (KI-104) was used for profiling HDACs 1–11. Compounds 3 and 10f were confirmed as substrate competitive inhibitors of HDAC1 (data not shown); therefore,

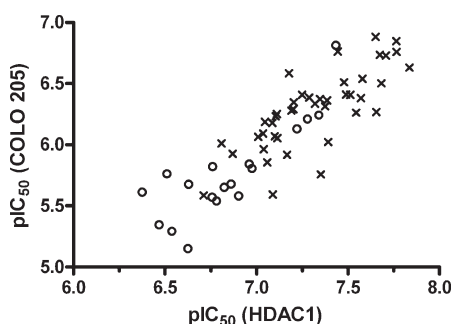


**Figure 7.** Cellular activity  $pIC_{50}(\text{COLO 205})$  correlates with enzymatic activity  $pIC_{50}(\text{HDAC1})$ . A series alone ( $\circ$ ,  $n = 18$ ,  $p < 0.0001$ ): linear regression equation  $pIC_{50}(\text{COLO 205}) = 1.065 pIC_{50}(\text{HDAC1}) - 1.529$ ,  $R^2 = 0.7104$ . B series alone ( $\times$ ,  $n = 42$ ,  $p < 0.0001$ ): linear regression equation  $pIC_{50}(\text{COLO 205}) = 0.8775 pIC_{50}(\text{HDAC1}) - 0.1304$ ,  $R^2 = 0.5963$ . For combined A and B series ( $n = 60$ ,  $p < 0.0001$ ): linear regression equation  $pIC_{50}(\text{COLO 205}) = 1.007 pIC_{50}(\text{HDAC1}) - 1.093$ ,  $R^2 = 0.7530$ . Linear regression equation with both  $pIC_{50}(\text{HDAC1})$  and  $\log P$ :  $pIC_{50}(\text{COLO 205}) = 0.9639 pIC_{50}(\text{HDAC1}) + 0.0991 \log P - 1.1436$ .  $R^2 = 0.7877$  for combined A and B series ( $n = 60$ ).

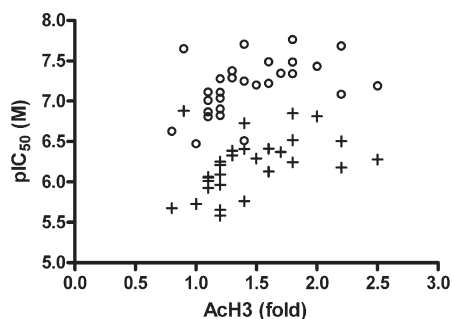


**Figure 8.** Level of acetylated histone 3 (ACh3) correlates both enzymatic potency  $pIC_{50}(\text{HDAC1})$  ( $\circ$ ,  $n = 29$ , Pearson  $r = 0.4636$ ,  $p = 0.0113$ ) and cellular potency  $pIC_{50}(\text{COLO 205})$  ( $+$ ,  $n = 29$ , Pearson  $r = 0.4356$ ,  $p = 0.0182$ ). "ACh3 (fold)" is the fold of protein concentration compared with that of vorinostat.

all the hydroxamates in Table 6 were assumed as competitive inhibitors for all the isozymes and  $K_i$  values were calculated using the Cheng–Prusoff equation (Table 6). The results showed that these compounds are pan-HDAC inhibitors, broadly similar to vorinostat, belinostat, panobinostat, and the **2** series (**2**, **2b**, and **2c**), with the exception of HDAC6 in most cases. Compound **10x** is an exception among the compounds tested in Table 6, since it did show good activity against HDAC6. It contains a cis double bond in the  $R^2$  side chain which may be crucial to the HDAC6 inhibition. Vorinostat, panobinostat, and belinostat are more potent against HDAC6 than the majority of other isozymes. All of them have aromatic rings as the CAP group, so an aromatic ring or a cis double bond in the CAP group might be important for HDAC6 inhibition. Indeed, benzimidazole HDAC inhibitors with phenethyl  $R^2$  groups (e.g., **2**, **2b**, and **2c**) do show good HDAC6 inhibitory potency compared to those with alkyl  $R^2$  groups (Table 6).

Our selectivity profiling results for hydroxamates such as vorinostat, belinostat, and panobinostat are generally in line with those published and tested with generic acetyllysine derived substrate(s).<sup>25–27</sup> Lahm et al. described that class IIa HDACs possess a weak but measurable intrinsic capability of hydrolyzing

acetyllysine-based substrates (including BIMOL KI-104) and concluded that most of the enzymatic activity associated with class IIa HDACs ectopically expressed in mammalian cells is due to endogenous class I HDACs present in the class IIa protein complex.<sup>28</sup> They also identified Boc-Lys-( $\epsilon$ -trifluoroacetyl)-MCA as an active and selective substrate for class IIa HDACs.<sup>28</sup> When trifluoroacetyllysine based substrates were used in the class IIa HDAC assays, hydroxamates such as vorinostat, belinostat, and panobinostat showed much reduced potency,<sup>27,29–31</sup> becoming HDACs 1–3 and 6 selective inhibitors.<sup>31</sup>

We profiled the compounds in Table 6 in 2005. Unfortunately no inhibitory data were generated for class IIa HDACs using trifluoroacetyllysine as substrate. However, it is reasonable to assume that these benzimidazoles behave like the hydroxamates that have been tested with the trifluoroacetyllysine substrate(s) and hence are weak class IIa inhibitors in vitro under the reported assay conditions (i.e., protein preparation and substrate). Recent results from studies on class IIa inhibitors and substrates suggest that inhibition of the catalytic activity of HDAC4 by small molecules is not a viable approach for cancer therapy,<sup>32</sup> and class IIa HDACs may function as receptors rather than enzymes (deacetylases) of acetyllysine in a protein sequence.<sup>31</sup> From analysis of our data it appears that whether these benzimidazole hydroxamates are potent or weak class IIa HDAC inhibitors in vitro is not relevant to the in vitro antiproliferative activity. Correlation analysis of the 11 benzimidazoles in Table 6 shows that the cellular potency ( $pIC_{50}$ ) positively correlates with the inhibitory constant  $pK_i$  of HDAC3 (Figure S3, Supporting Information,  $p = 0.0455$ ,  $0.0070$ ,  $0.0351$ , and  $0.0142$  for A2780, COLO 205, HCT-116, and PC-3, respectively) and has a similar trend with  $pK_i$  (HDAC1).  $pK_i$  (HDAC3) also significantly ( $p = 0.0151$ ) correlates with  $pK_i$  (HDAC1). PC-3 cellular potency ( $pIC_{50}$ ) correlates with both  $pK_i$  (HDAC3) ( $p = 0.0142$ , Figure S3d) and  $pK_i$  (HDAC1) ( $p = 0.0113$ ). These results suggest that these benzimidazole-based HDAC inhibitors are mainly targeting class I HDACs, particularly HDAC3 and HDAC1, to achieve antiproliferative activity in tumor cells, in line with early reports.<sup>11–13</sup> Wilson et al. reported that protein expression of HDAC3 was significantly up-regulated in a panel of human colon tumors (Caco-2, COLO 205, HCT-116, HT-29, etc.) and in small intestinal adenomas derived from Apc1638<sup>N/+</sup> mice, and a significant up-regulation of HDAC1 and HDAC2 protein expression in colon tumors was observed. Their findings demonstrate aberrant expression of HDAC3 and other class I HDACs in colon cancer.<sup>33</sup> HDAC3 not only functions primarily in histone deacetylation but also plays a role in biological processes beyond transcriptional repression.<sup>34</sup> This evidence supports the correlations between HDAC1 (or HDAC3) inhibitory potency and cellular antiproliferative potency established for benzimidazole HDAC inhibitors.

**In Vitro ADME Profiling and SAR.** One of our major goals was to improve upon the metabolic stability of HDAC inhibitors for optimal oral dosing in patient, in particular the phase 1 metabolic liability often suffered by hydroxamic acids as demonstrated by their short half-lives ( $t_{1/2}$ ) in liver microsomal assays. Indeed, the **2** series (**2** and **2a–c**) in general had poor microsomal stability, a clear liability for oral administration.<sup>18</sup> In our screening cascade only compounds that passed predefined potency criteria were evaluated in human liver microsomal stability assays (HLM). A total of 38 compounds (Table S6, Supporting Information) were identified with HLM  $t_{1/2}$  data in a wide range, applicable for a QSAR analysis. In general, only those compounds with HLM  $t_{1/2} \geq 30$  min were tested in mouse liver microsomal assays (MLM), which generally turned these compounds over faster. We strongly suspected that

Table 6. Inhibition of HDAC Isozymes by Selected Compounds

| compd        | dissociation constant $K_i$ (nM) (mean $\pm$ SD) for HDAC Isozymes <sup>a</sup> |               |               |               |               |               |               |              |               |             |               |
|--------------|---|---------------|---------------|---------------|---------------|---------------|---------------|--------------|---------------|-------------|---------------|
|              | 1   | 2             | 3             | 4             | 5             | 6             | 7             | 8            | 9             | 10          | 11            |
| 2            | 11 $\pm$ 2  | 36 $\pm$ 4    | 12 $\pm$ 1    | 8.5 $\pm$ 1.6 | 17 $\pm$ 2    | 20 $\pm$ 1    | NT            | 95 $\pm$ 27  | 19 $\pm$ 1    | 19 $\pm$ 1  | 13 $\pm$ 3    |
| 2b           | 15 $\pm$ 1  | 39 $\pm$ 7    | 11 $\pm$ 2    | 10 $\pm$ 2    | 16 $\pm$ 1    | 23 $\pm$ 4    | NT            | NT           | 21 $\pm$ 6    | 23 $\pm$ 4  | 16 $\pm$ 7    |
| 2c           | 12 $\pm$ 2  | 39 $\pm$ 2    | 11 $\pm$ 1    | 8.7 $\pm$ 1.8 | 18 $\pm$ 2    | 27 $\pm$ 1    | NT            | NT           | 24 $\pm$ 3    | 23 $\pm$ 1  | 14 $\pm$ 3    |
| 3            | 28 $\pm$ 1  | 27 $\pm$ 1    | 19 $\pm$ 1    | 16 $\pm$ 1    | 21 $\pm$ 1    | 247 $\pm$ 10  | 104 $\pm$ 1   | 48 $\pm$ 1   | 24 $\pm$ 1    | 23 $\pm$ 6  | 24 $\pm$ 1    |
| 10e          | 26 $\pm$ 5  | 33 $\pm$ 1    | 27 $\pm$ 2    | 11 $\pm$ 1    | 11 $\pm$ 1    | 225 $\pm$ 61  | 77 $\pm$ 5    | 78 $\pm$ 9   | 30 $\pm$ 1    | 34 $\pm$ 2  | 18 $\pm$ 1    |
| 10f          | 24 $\pm$ 1  | 26 $\pm$ 4    | 20 $\pm$ 1    | 7.9 $\pm$ 1.4 | 11 $\pm$ 1    | 94 $\pm$ 5    | 89 $\pm$ 4    | 65 $\pm$ 3   | 11 $\pm$ 2    | 34 $\pm$ 4  | 14 $\pm$ 2    |
| 10p          | 11 $\pm$ 4  | 18 $\pm$ 3    | 13 $\pm$ 1    | 6.2 $\pm$ 0.6 | 6.8 $\pm$ 0.5 | 282 $\pm$ 52  | 35 $\pm$ 1    | 54 $\pm$ 10  | 14 $\pm$ 1    | 28 $\pm$ 1  | 13 $\pm$ 3    |
| 10q          | 20 $\pm$ 4  | 18 $\pm$ 2    | 15 $\pm$ 1    | 6.6 $\pm$ 0.3 | 6.6 $\pm$ 0.5 | 348 $\pm$ 94  | 41 $\pm$ 3    | 57 $\pm$ 8   | 16 $\pm$ 1    | 29 $\pm$ 1  | 14 $\pm$ 2    |
| 10s          | 19 $\pm$ 2  | 21 $\pm$ 5    | 20 $\pm$ 2    | 5.3 $\pm$ 1.0 | 9.2 $\pm$ 0.3 | 300 $\pm$ 5   | 70 $\pm$ 5    | 136 $\pm$ 7  | 11 $\pm$ 2    | 13 $\pm$ 2  | 11 $\pm$ 1    |
| 10x          | 7.7 $\pm$ 0.4   | 8.6 $\pm$ 0.4 | 16 $\pm$ 1    | 2.4 $\pm$ 0.1 | 3.1 $\pm$ 0.1 | 4.0 $\pm$ 2.5 | 12 $\pm$ 1    | 55 $\pm$ 7   | 5.7 $\pm$ 0.4 | 18 $\pm$ 1  | 8.8 $\pm$ 1.5 |
| 10y          | 10 $\pm$ 1  | 14 $\pm$ 2    | 10 $\pm$ 3    | 3.6 $\pm$ 0.6 | 5.6 $\pm$ 0.3 | 227 $\pm$ 1   | 42 $\pm$ 2    | 94 $\pm$ 8   | 4.4 $\pm$ 0.1 | 19 $\pm$ 2  | 4.2 $\pm$ 0.2 |
| vorinostat   | 60 $\pm$ 7  | 42 $\pm$ 3    | 36 $\pm$ 3    | 20 $\pm$ 6    | 36 $\pm$ 10   | 29 $\pm$ 13   | 129 $\pm$ 44  | 173 $\pm$ 49 | 49 $\pm$ 23   | 60 $\pm$ 16 | 31 $\pm$ 6    |
| panobinostat | 2.5 $\pm$ 0.2   | 1.9 $\pm$ 0.1 | 2.3 $\pm$ 0.3 | 0.6 $\pm$ 0.1 | 0.7 $\pm$ 0.1 | 0.7 $\pm$ 0.4 | 2.3 $\pm$ 0.1 | 22 $\pm$ 0.5 | 1.2 $\pm$ 0.1 | 31 $\pm$ 1  | 3.5 $\pm$ 0.2 |
| belinostat   | 26 $\pm$ 2  | 22 $\pm$ 2    | 19 $\pm$ 2    | 15 $\pm$ 1    | 25 $\pm$ 1    | 10 $\pm$ 2    | 51 $\pm$ 1    | 22 $\pm$ 8   | 24 $\pm$ 1    | 59 $\pm$ 2  | 27 $\pm$ 1    |

<sup>a</sup> The  $K_i$  was calculated using the Cheng–Prusoff equation:  $K_i = IC_{50} / \{1 + ([\text{substrate}]/K_m)\}$ .  $IC_{50}$  values of HDACs 1–11 for  $K_i$  calculation were measured using Fluor de Lys substrate (KI-104, BIOMOL International, L.P) at pH 7.5, room temp. NT: not tested.

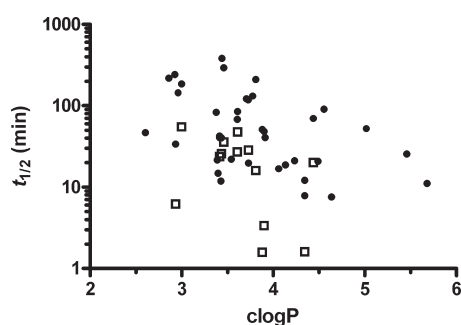


**Figure 9.** Relationship between liver microsomal half-life ( $t_{1/2}$ ) and  $\text{clogP}$ . The  $\log[t_{1/2}$  (HLM)] correlates with  $\text{clogP}$  negatively ( $\bullet$ ,  $n = 38$ , Pearson  $r = -0.4601$ ,  $p = 0.0037$ ). Linear regression equation is  $\log[t_{1/2}$  (HLM, min)] =  $-0.3079 \text{ clogP} + 2.848$ ,  $R^2 = 0.2117$ , but  $\log[t_{1/2}$  (MLM)] has no significant correlation with  $\text{clogP}$  ( $\square$ ,  $n = 13$ , Pearson  $r = -0.4358$ ,  $p = 0.1366$ ).

liver microsomal turnover increased with lipophilicity, and after analysis of the data from 38 compounds, the liver microsomal stability data ( $\log t_{1/2}$ ) was found to be negatively correlated with  $\text{clogP}$  ( $p = 0.0037$ ) (Figure 9). Because of the limited data for MLM (Table S6, Supporting Information), there was no significant correlation between  $\log t_{1/2}$  (MLM) and  $\text{clogP}$  ( $p = 0.1366$ ,  $n = 13$ ), but a trend was evident. The MLM  $t_{1/2}$  was generally lower than that of HLM for the same compound or for compounds with the same  $\text{clogP}$  (Figure 9), but no significant correlation ( $p = 0.0633$ ,  $n = 13$ ) was observed between  $\log t_{1/2}$  (HLM) and  $\log t_{1/2}$  (MLM) data. According to the QSAR equation established (Figure 9), for  $t_{1/2}$  (HLM)  $\geq 30$ , 60, and 90 min,  $\text{clogP}$  should be no more than 4.5, 3.5, and 2.9, respectively. These  $\text{clogP}$  values are for  $t_{1/2}$  (MLM) of 5, 17, and 35 min, respectively. These numbers were used as guidelines for target compound design.

Compounds selected for in vivo evaluations were also tested in rat and dog liver microsomal assays (Table 7). In general the benzimidazoles are relatively stable in human and dog microsomes but variable in rodent species. Studies on in vitro metabolism of **3** in mouse, rat, dog, and human liver microsomes revealed that the

major metabolites were products of mono-N-deethylation and bis-N-deethylation of the diethylamino group of **3**. The amide metabolite formed via reduction of hydroxamic acid was also observed, but it was in trace amounts. The details of these studies will be published elsewhere.<sup>35</sup>

Physicochemical properties were also evaluated: high throughput kinetic solubility at pH 7 revealed that these compounds are very soluble and present no concerns for oral or iv dosing for in vivo studies (Table 7). The  $\log D$  values were also measured on selected compounds and were found to be within the desired range of around 2.0, higher than the more polar vorinostat. Both the  $N^3$  of benzimidazole ring (HCl salt  $pK_a \approx 4.1$ ) and basic center in the  $R^1$  side chain ( $pK_a \approx 7.4$ ) are able to be protonated at acidic pH (i.e.,  $\text{pH} < 5-6$  for protonation of basic nitrogen at  $R^1$  side chain, and  $\text{pH} < 2-3$  for protonation of both basic centers); thus, the resultant salts are very soluble. For example, the dihydrochloride salt of **3** is very soluble in pure water ( $>100$  mg/mL, pH 2.2), in saline (0.9% NaCl) ( $>50$  mg/mL), in phosphate buffer ( $>50$  mg/mL, pH 4.5), and in 1% methylcellulose/0.1% Tween 80 ( $>25$  mg/mL) for oral dosage formulation.

Permeability and efflux of **3**, **10f**, **10p** and **10s** were assessed in Caco-2 cells. The rates of transport apparent permeability  $P_{app}$  (A $\rightarrow$ B) of **10f**, **3**, and **10s** were  $19.4 \times 10^{-6}$ ,  $7.04 \times 10^{-6}$ , and  $9.59 \times 10^{-6}$  cm/s, respectively. These rates are higher than that reported for vorinostat ( $1.70 \times 10^{-6}$  cm/s).<sup>13</sup> However, **10p** showed lower permeability ( $0.97 \times 10^{-6}$  cm/s) and had significant efflux,  $P_{app}$ (A $\rightarrow$ B)/ $P_{app}$ (B $\rightarrow$ A) ratio or efflux ratio of 10.8, probably due to the secondary amine. Compound **2** is permeable but also has significant efflux (efflux ratio of 9.2). Compounds **3**, **10e**, **10f**, and **10s** are highly permeable and have no significant efflux, an important improvement over the **2** series.

Fluorescence assays against recombinant P450 isoforms such as 3A4 and 2D6 were used to assess potential for drug–drug interactions. Potential candidate compounds were further tested in human liver microsomes with P450 isozyme selective substrates. To our knowledge, the  $IC_{50}$  obtained in the fluorescence assays using recombinant CYP proteins was about an order of magnitude more potent than that obtained from the microsomal assay system. These

Table 7. Profiling Data of Selected Compounds for in Vivo Studies

| compd      | liver microsomal stability ( $t_{1/2}$ , min) |       |     |     | solubility ( $\mu\text{M}$ ) <sup>a</sup> | log <i>D</i> at pH 7.4 <sup>b,f</sup> | clogP <sup>c</sup> | Caco-2 permeability ( $10^{-6}$ cm/s) <sup>d,f</sup><br>$P_{\text{app}}(\text{A} \rightarrow \text{B})/P_{\text{app}}(\text{B} \rightarrow \text{A})$ |
|------------|---|-------|-----|-----|---|---------------------------------------|--------------------|---|
|            | human   | mouse | rat | dog |   |                                       |                    |   |
| 2          | 60  | 5     | 4.3 | 18  | >200                                      | 2.1                                   | 2.97               | 3.01/27.7   |
| 3          | >60   | 27    | 7.8 | >60 | >200                                      | 2.07                                  | 3.61               | 7.04/19.4   |
| 10e        | >60   | 36    | 3.3 | >60 | >200                                      | NT                                    | 3.46               | NT  |
| 10f        | >60   | 20    | 41  | >60 | >200                                      | 2.41                                  | 4.44               | 19.4/14.9   |
| 10p        | 51  | 1.6   | 1.1 | 48  | >200                                      | NT                                    | 3.88               | 0.97/10.5   |
| 10s        | >60   | 16    | 10  | 10  | >200                                      | NT                                    | 3.81               | 9.59/26.0   |
| vorinostat | >60   | >60   | >60 | >60 | >200                                      | 1.04                                  | 1.84               | 1.70 <sup>e</sup> /—  |

<sup>a</sup> Kinetic solubility at pH 7 with 2.5% of DMSO. <sup>b</sup> Determined in 1-octanol/sodium phosphate buffer (pH 7.4). <sup>c</sup> clogP (octanol/water) values were calculated using MOE 2008.10, Chemical Computing Group. <sup>d</sup> Significant efflux: efflux  $P_{\text{app}}(\text{A} \rightarrow \text{B})/P_{\text{app}}(\text{B} \rightarrow \text{A}) > 3.0$  and  $P_{\text{app}}(\text{B} \rightarrow \text{A}) > 1.0 \times 10^{-6}$  cm/s. <sup>e</sup> See ref 13. <sup>f</sup> NT: not tested.

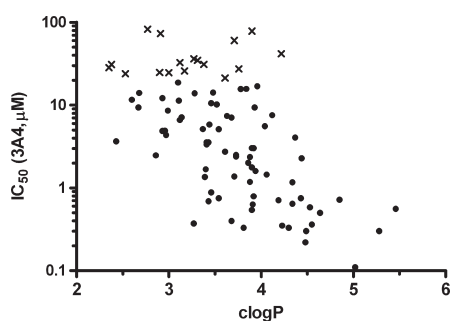


**Figure 10.** Relationship between CYP3A4 inhibitory potency  $\text{IC}_{50}$  and clogP. There are a total of 89 compounds in the figure, 72 of them with  $\text{IC}_{50} < 20 \mu\text{M}$  (●) and 17 of them with  $\text{IC}_{50} \geq 20 \mu\text{M}$  (×). The inhibitory potency  $\text{IC}_{50}$  correlates with clogP very significantly (●,  $n = 72$ ,  $p < 0.0001$ ), linear regression equation  $\log[\text{IC}_{50}(\text{3A4}, \mu\text{M})] = -0.5779 \text{ clogP} + 2.519$ ,  $R^2 = 0.3965$ .

benzimidazole hydroxamates inhibited mainly recombinant CYP3A4 in the fluorescence assay. The relation between  $\text{IC}_{50}(\text{3A4})$  and clogP is clear (Figure 10): There were 72 compounds with  $\text{IC}_{50}(\text{3A4}) \leq 20 \mu\text{M}$  and 17 compounds with  $\text{IC}_{50}(\text{3A4}) > 20 \mu\text{M}$  (Tables S7 and S8, Supporting Information). The logarithm  $\text{IC}_{50}(\text{3A4})$  was correlated with clogP significantly,  $p < 0.0001$ . According to the QSAR equation established in Figure 10, clogP should be no more than 4.36 and higher than 2.63 for  $\text{IC}_{50}(\text{3A4})$  between 1 and  $10 \mu\text{M}$ . Considering that the  $\text{IC}_{50}$  obtained in the microsomal system is about an order of magnitude lower than the recombinant system, it is sufficient to ensure that the clogP is below 4.36 to achieve an  $\text{IC}_{50}(\text{3A4})$  above  $10 \mu\text{M}$  in the physiologically more relevant microsomal assay. Actually, 87% (77/89) of the compounds has clogP < 4.36, and 84% (64/77) of these 77 compounds has  $\text{IC}_{50}(\text{3A4}) \geq 1 \mu\text{M}$ . Compounds generally have no significant CYP liabilities; results from both the fluorescence assay and microsomal probe substrate assay for three representative compounds (3, 10f, 10u) are shown in Table 8. Compound 3 has  $\text{IC}_{50} = 5.78 \mu\text{M}$  for CYP2C19, and the plasma concentration achieved in human is much lower than this value, indicating no potential to cause any drug–drug interaction.

**Pharmacokinetics (PK) in Preclinical Species.** PK studies were first performed in Wistar rats, but the bioavailabilities ( $F$ ) were poor for 10f (4.0%), 10e (9.0%), 10p (1.4%), and 3 (3.1%), probably related to the poor metabolic stabilities for 3, 10p, and 10e in rat liver microsomes (Table 7). Reference compounds

also showed poor bioavailability in rats, for example, 4.3% (S\*BIO in-house data) for belinostat and 8.0% (S\*BIO in-house data) or 10.9%<sup>13</sup> for vorinostat. Rat was hence felt to be an unsuitable species for pharmacokinetic evaluation of these hydroxamates. In nude mice, 10f and 3 were sufficiently bioavailable: 51% for 10f (Table S9, Supporting Information) and 34% for 3 (Table 9). In contrast, vorinostat, belinostat, and panobinostat showed  $F = 8.3\%$ ,  $6.7\%$ , and  $4.6\%$ , respectively.<sup>36</sup> Both 3 and 10f were also tested in Beagle dogs and demonstrated good bioavailability of  $65 \pm 16\%$  and  $110 \pm 54\%$ , respectively. Consistent with the increasing microsomal half-life from rat to mouse to dog (Table 7),  $F$  also increased as did intravenous terminal half-life  $t_{1/2}$  (rat 0.89 h, mouse 2.26 h, dog 3.90 h) for compound 3 (Table 9). Orally administered 3 was rapidly absorbed with  $t_{\text{max}} = 0.24$ , 0.17, and 0.75 h for rat, mouse, and dog at doses of 10, 50, and 10 mg/kg, respectively. 3 exhibits an overall better PK profile and oral bioavailability in non-rodent (dog) compared to rodent (mouse and rat) and was predicted by allometry to have an acceptable human oral PK profile.<sup>37</sup> Mouse and dog were hence selected as suitable preclinical species for further safety evaluation of benzimidazole hydroxamates such as 3 and 10f.

**In Vivo Antitumor Efficacy.** Compounds 3, 10f, 10e, 10s, and 10p were selected for in vivo antitumor evaluation in subcutaneous xenograft mouse models (Table 10). All these compounds were stable in HLM assays (Table 7). 3 and 10f also demonstrated good PK in mice. 10s is potent and relatively stable in the MLM assay. Compound 10p is potent, but its MLM stability and permeability are poor compared to the other four, but it was included for assessing which in vitro parameter is more important for antitumor efficacy: high in vitro enzymatic and cellular potency, a good in vitro ADME profile, or more likely, a combination of both.

The HCT-116 xenograft model was chosen for primary efficacy screening, as this model had been successfully used for HDAC inhibitors such as belinostat<sup>38</sup> and dacinostat (LAQ824)<sup>39</sup> in the literature. Vorinostat was used as positive control for most of the experiments. Compounds were dissolved in a mixture of 0.5% or 1% methylcellulose and 0.1% Tween 80 in water and administered orally to the tumor-bearing mice. Compounds were dosed up to the maximum tolerated dose (MTD), which was defined by <20% loss in mean body weight per treatment group and no more than one treatment-related death among 7–10 treated animals. Antitumor response was assessed by determination of tumor growth inhibition (TGI) in treated groups compared to the control (vehicle) group.

Table 8. Inhibition of CYP Isozymes

| compd | IC <sub>50</sub> (μM)             |             |   |      |      |      |     |
|-------|-----------------------------------|-------------|---|------|------|------|-----|
|       | recombinant isozymes <sup>a</sup> |             | pooled HLM with CYP isozyme probe substrate |      |      |      |     |
|       | 3A4                               | 2D6         | 1A  | 2C9  | 2C19 | 2D6  | 3A4 |
| 3     | 2.73 ± 0.84                       | >10         | >25   | >25  | 5.78 | >25  | >25 |
| 10f   | 2.28 ± 0.76                       | >10         | >25   | >25  | 8.10 | 13.9 | >25 |
| 10s   | 0.33 ± 0.07                       | 3.17 ± 0.29 | >25   | 10.4 | 10.3 | >25  | >25 |

<sup>a</sup> Values are expressed as the mean and standard deviation (SD) of at least two independent duplicates.

Table 9. Pharmacokinetic Parameters of 3 in Mouse, Rat, and Dog

| parameter                           | female nude mouse <sup>a</sup> |          | Wistar rat <sup>b</sup> |         | Beagle dog <sup>c</sup> |         |
|-------------------------------------|--------------------------------|----------|-------------------------|---------|-------------------------|---------|
|                                     | iv                             | po       | iv                      | po      | iv                      | po      |
| dose (mg/kg (nmol/kg)) <sup>d</sup> | 10 (23)                        | 50 (116) | 2 (4.6)                 | 10 (23) | 2 (4.6)                 | 10 (23) |
| C <sub>max</sub> (μM)               |                                | 6.10     |                         | 0.139   |                         | 3.56    |
| t <sub>max</sub> (h)                |                                | 0.17     |                         | 0.24    |                         | 0.75    |
| t <sub>1/2</sub> (h)                | 2.26                           | 2.44     | 0.89                    | 2.02    | 3.90                    | 4.12    |
| CL/F ((L/h)/kg)                     | 9.2                            | 27.2     | 4.45                    | 153     | 1.45                    | 2.29    |
| V <sub>SS</sub> (L/kg)              | 3.46                           |          | 1.66                    |         | 4.24                    |         |
| AUC <sub>0-∞</sub> (μM·h)           | 2.52                           | 4.27     | 1.15                    | 0.181   | 3.22                    | 10.49   |
| F (%)                               |                                | 34       |                         | 3.1     |                         | 65      |

<sup>a</sup> Three female BALB/c nude mice (ARC, West Australia), 16.5–19.4 g, 10–12 weeks of age, per time point per route. <sup>b</sup> Three male Wistar rats each for iv (230–250 g, 6–8 weeks of age) and po (330–370 g, 8 weeks of age). <sup>c</sup> Six male non-naive Beagle dogs, age 1–2 years, 12–16 kg for iv (*n* = 3) and po (*n* = 3). <sup>d</sup> Compound was tested as the dihydrochloride salt and was dissolved in saline for iv injection and in 0.5% methylcellulose/0.1% Tween 80 in water for oral administration.

The five compounds in Table 7 were assessed in three separate experiments with vorinostat as the positive control. In the first experiment (Table 10), the MTD for vorinostat was established as 300 mg/kg, but 200 mg/kg was shown to be the maximum absorbed or effective dose; MTD for 10e was 200 mg/kg. The MTD for 10p was above 200 mg/kg. Both 10f and 10e demonstrated significant antitumor activities at their respective MTDs and at half MTD dose levels with good tolerability for the entire 21-day treatment period. Compound 10p did not show significant antitumor activity until the high dose of 200 mg/kg and even then only 41% TGI. This compound is metabolically unstable and of low permeability, even though it is the most potent compound among the tested compounds. Its poor ADME most likely significantly reduced its exposure below effective levels in vivo. A higher dose of 10p may have been as effective as 10e. Both the MTD dose groups of 10f and 10e were significantly better (*p* < 0.001) than the vorinostat 200 mg/kg group, but there was no statistically significant difference between the latter and other treatment groups except for the 50 and 100 mg/kg groups of 10p. In the second experiment, 10s was tested together with vorinostat and belinostat, which also has a cinnamyl linker to a hydroxamic acid. However, the similarities with the compounds described herein appear limited: belinostat was weakly active up to 200 mg/kg which was the maximum absorbed dose in our hands. 10s showed significant toxicity at 200 mg/kg; hence this compound was only dosed qd × 7, showing TGI = 53% (*p* < 0.05) on day 22. 10s was also active at its daily dosing MTD (100 mg/kg) with TGI = 50% (*p* < 0.05) but not at 50 mg/kg. Vorinostat performed well in this model with 73% TGI, but it was not statically better than the 10s 100 mg/kg group. In a further experiment, 3 was tested together with vorinostat (Table 10). Compound 3 was clearly toxic at the highest

dose tested (200 mg/kg); however, at the MTD dose of 100 mg/kg and at 50 mg/kg, it demonstrated very significant antitumor effects on day 21 with TGI = 90% (*p* < 0.001) and 66% (*p* < 0.001), respectively, with acceptable body weight loss. Vorinostat was also active compared to the vehicle group with TGI = 41% (*p* < 0.05). The 100 mg/kg group of 3 was very significantly (*p* < 0.01) active compared to vorinostat when assessed by Dunnett's multiple comparison test using a vorinostat group as control. In a fourth experiment, both 3 and panobinostat were tested at their MTD doses, and they demonstrated significant efficacy compared to the vehicle group with TGI of 98% (*p* < 0.0001) and 61% (*p* < 0.01), respectively. The tumor growth inhibition of the 3 group was found to be significantly better than that of the panobinostat group (*p* < 0.001). In the above four experiments, compounds 3, 10f, and 10e demonstrated very significant (*p* < 0.001) antitumor activities at their respective MTD dose levels. At half MTD dose level, their respective mean tumor volumes were still significantly (*p* < 0.01) different from that of the vehicle (or nontreatment) group. Furthermore, the toxicity in terms of body weight loss is reversible. For example, the mean body weights of 3 of treated groups increased by 6.5% in the first 4 days after the last dose and fully recovered in 17 days for the MTD dose group. The major adverse effects observed for 3 in repeated oral dose toxicity studies in mice and dogs are dose-dependent mild myelosuppression and gastrointestinal effects that are consistent with effects reported for other HDAC inhibitors. However, in clinical trials 3 appears to be well tolerated with an overall favorable safety profile compared to other orally dosed HDAC inhibitors.<sup>21</sup>

3 and 10f emerged from this work as the top two candidates for further evaluations. 3 was selected as the preferred compound because of its attractive chemistry (e.g., chemical synthesis and

Table 10. Antitumor Activities of Selected Compounds in HCT-116 Xenograft Models

| entry      | compd <sup>a</sup> | dose (mg/kg) <sup>b</sup> | % TGI (day) <sup>c</sup> | statistical significance <sup>d</sup> | max body weight loss (%) (at day) | survivors on day 22 |
|------------|--------------------|---------------------------|--------------------------|---------------------------------------|-----------------------------------|---------------------|
| 1          | 10f                | 25                        | 30 (22)                  | ns                                    |                                   | 10/10               |
|            | 10f                | 50                        | 55 (22)                  | **                                    | 5.6 (5)                           | 10/10               |
|            | 10f                | 100                       | 85 (22)                  | ***                                   | 13.1 (22)                         | 10/10               |
|            | 10e                | 50                        | 19 (22)                  | ns                                    |                                   | 10/10               |
|            | 10e                | 100                       | 60 (22)                  | **                                    | 5 (8)                             | 10/10               |
|            | 10e                | 200                       | 90 (22)                  | ***                                   | 7.9 (19)                          | 9/10 <sup>e</sup>   |
|            | 10p                | 50                        | -9 (22)                  | ns                                    |                                   | 10/10               |
|            | 10p                | 100                       | -7 (22)                  | ns                                    |                                   | 10/10               |
|            | 10p                | 200                       | 41 (22)                  | ns                                    |                                   | 10/10               |
|            | vorinostat         | 200                       | 57 (22)                  | **                                    | 4.6 (19)                          | 10/10               |
| vorinostat | 300                | 54 (22)                   | *                        | 5.5 (19)                              | 8/10 <sup>f</sup>                 |                     |
| 2          | 10s                | 50                        | 17(22)                   | ns                                    | 1.9 (5)                           | 9/9                 |
|            | 10s                | 100                       | 50 (22)                  | **                                    | 4.9 (5)                           | 9/9                 |
|            | 10s                | 200                       | 53 (22)                  | **                                    | 18 (5)                            | 7/9 <sup>g</sup>    |
|            | vorinostat         | 200                       | 73 (22)                  | ***                                   | 8.9 (8)                           | 9/9                 |
|            | belinostat         | 50                        | 6 (22)                   | ns                                    |                                   | 9/9                 |
|            | belinostat         | 100                       | 26 (22)                  | ns                                    |                                   | 9/9                 |
| 3          | 3                  | 50                        | 66 (21)                  | ***                                   | 6.4 (17)                          | 9/9                 |
|            | 3                  | 100                       | 90 (21)                  | ***                                   | 14.6 (19)                         | 9/9                 |
|            | 3                  | 200                       | toxic(21)                |                                       | 25.5 (6)                          | 0/9 <sup>h</sup>    |
|            | vorinostat         | 200                       | 41 (21)                  | *                                     | 1.9 (19)                          | 9/9                 |
|            | panobinostat       | 50                        | 61 (18)                  | **                                    | 17.3 (12)                         | 10/10               |
| 4          | 3                  | 100                       | 98 (18)                  | ***                                   | 19.9 (20)                         | 10/10               |
|            | panobinostat       | 50                        | 61 (18)                  | **                                    | 17.3 (12)                         | 10/10               |

<sup>a</sup> Compounds **3**, **10e**, **10f**, **10p**, and **10s** were dosed as the dihydrochloride salt, and vorinostat was dosed as parent. Vehicle was 1% methylcellulose/0.1% Tween 80 in water for entries 1 and 2, and was 0.5% methylcellulose/0.1% Tween 80 in water for entries 3 and 4. <sup>b</sup> Dose schedule: po, qd  $\times$  21. Entry 1: female athymic nude mice (nu/nu, Harlan), 9 weeks of age. Entry 2: 6 weeks of age. Entries 3 and 4: female BALB/c nude mice (ARC, West Australia), 10–12 weeks of age. <sup>c</sup> The percent tumor growth inhibition (% TGI) =  $[(C_t - T_t)/(C_t - C_1)] \times 100$ .  $C_1$  and  $C_t$  are the mean tumor volumes for control group (vehicle) on day 1 and day  $t$ , respectively.  $T_t$  is the mean tumor volume for treatment group on day  $t$ . <sup>d</sup> One-way ANOVA followed by Dunnett's multiple comparison test was used to determine the statistical significance of (log transformed) tumor volume between a treatment group and the control (vehicle) group: ns = not significant, (\*)  $p < 0.05$ , (\*\*)  $p < 0.01$ , and (\*\*\*)  $p < 0.001$ . Entry 1: There were 2/10 very slow growing tumors in the vehicle group, which eliminated any statistical difference between this group and any of the treated groups; thus, the nontreated group was used as the control group. There was no significant difference in mean tumor volume between the nontreatment and vehicle group ( $p = 0.94$ , two-tailed unpaired Student's  $t$ -test). <sup>e</sup> One treatment-related death (TRD) occurred on day 3. <sup>f</sup> One TRD on day 13 and one non-treatment-related death due to accident on day 5. <sup>g</sup> One TRD on day 5 and another on day 8, only dosed qd  $\times$  7. <sup>h</sup> Four TRDs on day 6 and five TRDs on day 7.

stability), optimal balance of potency, in vitro ADME properties, good oral PK in mouse, dog and predicted human exposures, and strong efficacy in mouse xenograft models.

The goal for our HDAC inhibitor project was to develop a drug with a superior once daily oral dosage regimen; hence, compound **3** was compared to the leading clinical compounds available at the time, such as vorinostat, panobinostat, and belinostat in the same HCT-116 xenograft model experiment (Figure 11). Following continuous daily dosing the tumor volumes of the **3** group were very significantly different from the vehicle group on days 15 and 12 ( $p < 0.001$ ). Vorinostat reduced tumor growth moderately by days 15 and 12 ( $p < 0.05$ ); however, in this experiment, neither panobinostat nor belinostat showed significant differences from the vehicle group at their MTDs or maximum absorbed/efficacious dose levels. The mean tumor size of the **3** group was also significantly reduced compared to those of panobinostat, belinostat, and vorinostat groups on days 12 and 15. In an early report, belinostat was tested in the HCT-116 model with ip injection (40 mg/kg, qd  $\times$  7, in 10% DMSO),<sup>38</sup> and the TGI% was estimated to be 50% on day 10. Taken together, the low efficacy of orally administered belinostat

in mice was mainly due to its low bioavailability. Panobinostat (LBH589), an analogue of dacinostat, was administered to mice via either iv or ip injection in recent reports.<sup>40</sup> The 15 mg/kg iv group of panobinostat was much more efficacious than all the ip groups (15, 20, 30 mg/kg) in a NSCLC xenograft model. These data suggest that panobinostat has inadequate oral bioavailability in mice. In conclusion, the in vitro enzyme and cellular potency of **3** is improved over vorinostat, close to belinostat but inferior to panobinostat. We have demonstrated that **3** has a superior oral PK profile to the agents currently in clinical trials with a higher  $C_{max}$  and AUC than vorinostat, belinostat, and panobinostat at the same oral dose level,<sup>36</sup> leading to superior efficacy in the HCT-116 mouse xenograft model.

Compound **3** exhibited broad antiproliferative activity in tumor cell lines in vitro (Table 5), prompting us to explore its potential in other solid and hematological subcutaneous tumor models. Results from representative experiments for various xenograft models are summarized in Table 11. **3** has antiproliferative IC<sub>50</sub> values of 0.10, 0.14, 0.34, and 0.48  $\mu$ M for MV4-11 (acute monocytic leukemia), Ramos (lymphoma), PC-3 (prostate), and A2780 (ovarian) cancer cell lines, respectively. Consistent with its in



vitro potency against cell lines of these tumor types, **3** was more effective against hematopoietic cancers than solid tumors. The MV4-11 leukemia model was the most sensitive model tested, with significant antitumor activity observed at doses as low as 25 mg/kg (TGI = 61%,  $p < 0.001$ ) and 50 mg/kg (TGI = 111%,  $p < 0.001$ ). There were 6/10 complete tumor regressions (CR) and 2/10 partial tumor regressions (PR) of tumors observed at 50 mg/kg. After discontinuation of dosing on day 21, only 1/6 of the tumors had begun to regrow in the CR animals by day 28. The 50 mg/kg group was also very significantly more efficacious than the 25 mg/kg group ( $p < 0.01$ ). **3** was also tested in a Ramos xenograft model. After 14 days of daily oral dosing, the tumor volumes in the 50 mg/kg group were significantly different from the vehicle group with TGI = 75% ( $p < 0.05$ ). There were 3/10 CRs and 1/10 PRs in the **3** treated group. At the well-tolerated dose of 50 mg/kg, **3** was also tested in the PC-3 xenograft model together with the other HDAC inhibitors, and it demonstrated significant antitumor activity with

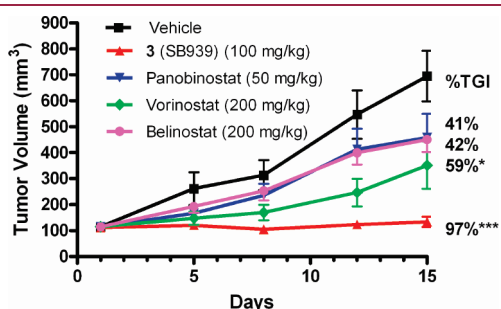


**Figure 11.** Antitumor activities of **3**, vorinostat, panobinostat, and belinostat in HCT-116 xenograft model. Tumor volume is expressed as the mean  $\pm$  standard error of the mean. **3** was dosed as the dihydrochloride salt. Vorinostat and belinostat were dosed as parent. Panobinostat was dosed as lactate, and vehicle is 0.5% methylcellulose/0.1% Tween 80 in water. Female BALB/c nude mice (ARC, West Australia), 10–12 weeks of age, seven mice per group, were dosed po, qd  $\times$  21. Tumor necrosis occurred among groups of vehicle, belinostat, and vorinostat after day 15; thus, only TGI on day 15 and before were used for efficacy assessment. See footnote of Table 10 for TGI calculation and statistical analysis.

TGI = 66% ( $p < 0.05$ ). In an ovarian cancer (A2780) xenograft model, the original dosing scheme was qd  $\times$  21. Unfortunately the tumor grew very quickly and multiple animals in the vehicle group reached their predefined end-point (tumor size of 1500 mm<sup>3</sup>); thus, mice were euthanized on day 8 (1/10), day 10 (6/10), and day 12 (1/10). Hence, only tumor volume data up to day 9 were used to assess efficacy (TGI). Tumor volumes of both 50 and 100 mg/kg groups were very significantly ( $p < 0.001$ ) different from that of the vehicle group with TGI of 44% and 63%, respectively. The vorinostat group was not significantly different from the vehicle group with TGI of 39%. Both the **3** groups were significantly different from the vorinostat group with  $p < 0.01$  and  $p < 0.001$  for 50 and 100 mg/kg groups, respectively.

In all these in vivo models, **3** demonstrated dose-dependent antitumor effects (statistically significant reductions in tumor growth compared with vehicle control) and was well tolerated (e.g., at 100 mg/kg, qd  $\times$  21). The toxicity in terms of body weight loss is reversible.

**Pharmacokinetic/Pharmacodynamic (PK/PD) Relationship of 3.** In a preliminary study, limited tissue distribution was assessed in nude mice bearing established HCT-116 tumors following a single oral administration of 50 and 100 mg/kg of **3**. As shown in Figure 12, **3** preferentially distributed to tumor tissues; the tumor concentration ( $\mu\text{mol/kg}$ )/plasma concentration ( $\mu\text{M}$ ) ratio reached 10 at about 5 h. The area under curve (AUC) of tumor tissue was 1.75- and 2.37-fold of that of plasma for 50 and 100 mg/kg dose, respectively (see Table S9, Supporting Information, for tissue distribution data). Clearly, **3** is enriched in tumor tissues.  $C_{\text{max}}$  concentrations were significantly higher than both HDAC1 and cell proliferation  $\text{IC}_{50}$  values. Tumor concentration levels of **3** were above the HDAC1  $\text{IC}_{50}$  level for the 50 and 100 mg/kg dose levels for 10 and 16 h, respectively, and the corresponding times above  $\text{IC}_{50}$  of HCT-116 cells were 5.1 and 7.1 h, respectively. Considering protein binding ( $91.8 \pm 0.3\%$  in human,  $83.5 \pm 1.8\%$  in dog,  $93.0 \pm 4.4\%$  in rat, and  $93.9 \pm 1.5\%$  in mouse plasmas as tested at 1000 ng/mL), the theoretical free drug concentration is still higher than the HDAC1  $\text{IC}_{50}$ . Perhaps a more meaningful measure of sufficient exposure is given by  $\text{AUC}/\text{IC}_{50}$  (equivalent

**Table 11.** Efficacy of Orally Administered **3** in Various Xenograft Models

| tumor  | compd <sup>a</sup> | schedule <sup>b</sup> | dose (mg/kg) | % TGI (day) <sup>c</sup> | statistical significance <sup>d</sup> | max body weight loss (day) (%) | survivors (day)         |
|--------|--------------------|-----------------------|--------------|--------------------------|---------------------------------------|--------------------------------|-------------------------|
| A2780  | vehicle            | qd $\times$ 21        |              |                          |                                       | 1.5 (5)                        | 9/10 (9) <sup>e</sup>   |
|        | vorinostat         | qd $\times$ 21        | 200          | 39 (9)                   | ns                                    | 9.3 (13)                       | 9/10 (9) <sup>f</sup>   |
|        | <b>3</b>           | qd $\times$ 21        | 100          | 63 (9)                   | ***                                   | 20.0 (20)                      | 10/10 (9) <sup>g</sup>  |
|        | <b>3</b>           | qd $\times$ 21        | 50           | 44 (9)                   | ***                                   | 8.9 (13)                       | 10/10 (9) <sup>h</sup>  |
| PC-3   | vehicle            | qd $\times$ 21        |              |                          |                                       | 0.5 (17)                       | 8/8 (22)                |
|        | <b>3</b>           | qd $\times$ 21        | 50           | 66 (22)                  | *                                     | 7.7 (17)                       | 8/8 (22)                |
| Ramos  | vehicle            | qd $\times$ 14        |              |                          |                                       | 0                              | 10/10 (15)              |
|        | <b>3</b>           | qd $\times$ 14        | 50           | 75 (15)                  | *                                     | 3.7 (12)                       | 10/10 (15) <sup>i</sup> |
| MV4-11 | vehicle            | qd $\times$ 21        |              |                          |                                       | 0                              | 10/10 (21)              |
|        | <b>3</b>           | qd $\times$ 21        | 50           | 114 (21)                 | ***                                   | 7.1 (19)                       | 10/10 (21) <sup>j</sup> |
|        | <b>3</b>           | qd $\times$ 21        | 25           | 61 (21)                  | ***                                   | 3.2 (10, 12)                   | 10/10 (21)              |

<sup>a</sup> Vehicle was 0.5% methylcellulose/0.1% Tween 80 in water. <sup>b</sup> Female BALB/c nude mice (ARC, West Australia), 10–12 weeks of age,  $5 \times 10^6$  cells (A2780, MV4-11), PC-3 (1 mm<sup>3</sup> fragment of PC-3 tumor), Ramos ( $7 \times 10^6$  cells). <sup>c</sup> The percent tumor growth inhibition (% TGI) =  $[(C_t - T_t)/(C_t - C_1)] \times 100$ .  $C_1$  and  $C_t$  are the mean tumor volumes for control group (vehicle) on day 1 and day  $t$ , respectively.  $T_t$  is the mean tumor volume for treatment group on day  $t$ . <sup>d</sup> One-way ANOVA followed by Dunnett's multiple comparison test was used to determine the statistical significance of (log transformed) tumor volume between a treatment group and the control (vehicle) group: ns = not significant, (\*)  $p < 0.05$ , (\*\*)  $p < 0.01$ , and (\*\*\*)  $p < 0.001$ . <sup>e</sup> One animal was euthanized because the tumor size reached the end-point on day 8, and 1/10 survived on day 21 because of spontaneous regression after day 13. <sup>f</sup> Vorinostat group, one non-treatment-related death on day 9, and 1/10 survived on day 21 because of CR (tumor disappeared after day 11). <sup>g</sup> 5/10 survived on day 21. <sup>h</sup> 2/10 survived on day 21. <sup>i</sup> Induced 3/10 CR and 1/10 PR. <sup>j</sup> Induced 6/10 CR and 2/10 PR.

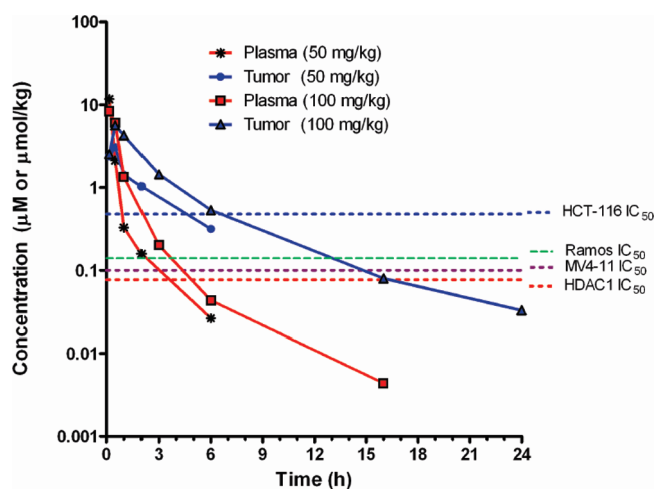


**Figure 12.** Plasma and tumor tissue distribution of **3** in HCT-116 tumor bearing mice. Female BALB/c nude mice, 10–12 weeks of age, were implanted subcutaneously in the right flank with  $5 \times 10^6$  cells of HCT-116 human colon carcinoma. When the tumor size reached approximately 100 mm<sup>3</sup>, these mice were orally administered with a single dose of **3** at 50 or 100 mg/kg. **3** was dissolved in 0.5% methylcellulose/0.1% Tween80 in water. There were seven time points (predose, 0.17, 0.5, 1, 2, 6, and 24 h) for 50 mg/kg group and eight time points (predose, 0.17, 0.5, 1, 3, 6, 16, and 24 h) for 100 mg/kg group. Two mice were sacrificed at each time point. Blood and tumor tissue samples were collected and analyzed for reach mouse. Only data points with concentrations (in  $\mu\text{M}$  for plasma or in  $\mu\text{mol}/\text{kg}$  for tumor tissue) above the quantification limit are shown.

exposure time at IC<sub>50</sub> level): HCT-116 cells have 14 and 31 h in tumor for 50 and 100 mg/kg dose levels, respectively, and 8.2 and 13 h in plasma, respectively. Concentrations in plasma are more easily measured compared to tumor tissue; thus, plasma AUC ( $\mu\text{M} \cdot \text{h}$ )/IC<sub>50</sub> ( $\mu\text{M}$ )  $\geq 8.2$  h can be used to predict the antitumor efficacy. For sensitive cell lines like MV4-11 (IC<sub>50</sub> = 0.10  $\mu\text{M}$ ), the exposure time at the IC<sub>50</sub> level for the 50 mg/kg dose group was 39 h, which is significantly longer than 8.2 h, hence explaining the excellent efficacy achieved at 50 mg/kg and even at 25 mg/kg dose levels in the MV4-11 xenograft model. With consideration of protein binding, the free drug exposures (about 1/10 of all drug exposure) are still high, especially with respect to the sensitivity of **3** toward MV4-11. HCT-116 cells are less sensitive, but **3** appears to reach sufficient levels over the first hours of exposure to significantly inhibit growth. This suggests that tumor growth can be sufficiently arrested if **3** can achieve IC<sub>50</sub> or above levels for about 8 h. Even when unbound drug levels are considered, plasma levels are still above IC<sub>50</sub> for 1 and 2 h at 50 and 100 mg/kg in mice, respectively. In summary, the antitumor efficacy of **3** in a variety of tumor models is explained by its excellent PK profile and preferred tissue distribution coupled with its enzymatic and cellular potency.

As expected for an HDAC inhibitor, **3** increased the level of both acylated histone **3** and  $\alpha$ -tubulin and up-regulated cyclin-dependent kinase inhibitor p21 protein expression in HCT-116 cells in a dose-dependent manner.<sup>19</sup> The relationship of PK (drug concentration) and PD (ACh3 level) was also studied in HCT-116 tumor bearing mice after a single oral dose of **3** (50, 100, or 125 mg/kg) or vorinostat (200 mg/kg). ACh3 was strongly induced in a dose dependent manner for **3** and the induction of ACh3 was more sustained (up to 16 h for **3** versus up to 8 h for vorinostat).<sup>19</sup> In conclusion, in vivo antitumor efficacy,

PK, and PD (ACh3) are closely related for **3**. These findings have translated successfully to the assessment of drug exposure and response in clinical trials.<sup>20,21</sup>

**Compound 3 Selected as Clinical Candidate.** On the basis of the above pharmacology and ADME data, **3** was selected for preclinical development. In vitro safety pharmacology was assessed by testing **3** against 26 different receptors and 33 different non-HDAC enzymes, which were selected based on their physiological function. At 10  $\mu\text{M}$ , **3** does not interfere with enzymes of other families including Zn<sup>2+</sup>-dependent enzymes and has no interactions with G-protein-coupled receptors, monoamine transporters, or ion channels. In particular, **3** did not inhibit <sup>3</sup>H-dofetilide binding to the hERG potassium channel or zinc-dependent enzymes such as MMP-3 and MMP-9 at concentrations up to 10  $\mu\text{M}$ . After toxicology studies in mice and dogs, the first dose in human was determined. **3** entered phase I trials in 2007 and is currently in multiple phase I and phase II clinical trials for treatment of patients with solid tumors and hematologic malignancies. The phase I data from treatment of patients with advanced solid malignancies showed that **3** had a manageable toxicity and favorable PK profile (dose-proportional PK).<sup>21</sup> The relative ACh3 values measured in PBMCs increased dose dependently from 10 to 60 mg and in proportion to **3** plasma levels.<sup>21</sup> The ongoing clinical phase II program is designed to take full advantage of the superior PK/PD properties of **3**.

## CONCLUSIONS

SARs for a series of 3-(1,2-disubstituted-1H-benzimidazol-5-yl)-N-hydroxyacrylamides have been established for the enzyme HDAC1, colon cancer cell line COLO 205, liver microsomal stability ( $t_{1/2}$ ), and CYP P450 (3A4) inhibition. These parameters were tuned by adjusting substituents at positions 1 and 2 of the benzimidazole ring (i.e., the R<sup>1</sup> and R<sup>2</sup> groups) to balance potency, ADME, and lipophilicity. In addition, stability due to phase 1 metabolism was significantly improved, together with improved permeability, resulting in a new generation of preclinical development candidates with demonstrably good PK profiles in both rodent (mouse) and non-rodent (dog) species and significant antitumor efficacies in a variety of tumor models. As an oral HDAC inhibitor, **3** demonstrates a superior preclinical profile compared to the leading clinical compounds available at the time, vorinostat, belinostat, and panobinostat in our profiling studies. **3** was selected as the preclinical development compound with the most favorable overall balance of in vitro and in vivo properties.

In summary, **3** is a potent pan-HDAC inhibitor with excellent druglike properties ( $\log D_{\text{pH}7.4} = 2.1$ , solubility at pH 5 of >10 mg/mL and of >100 mg/mL in water for the hydrochloride salt), is highly effective in in vivo tumor models, has high and dose-proportional oral bioavailability, and has very good ADME, safety, and pharmaceutical properties. **3** has a prolonged duration of action and is enriched in tumor tissue which may contribute to its potent antitumor activity. **3** is currently being tested in phase I and phase II clinical trials in both hematological and solid tumor patients, and preliminary data show that the superior preclinical profile is translated to the clinic.

## EXPERIMENTAL SECTION

Flash column chromatography was conducted using silica gel 60 (Merck KGaA, 0.040–0.063 mm, 230–400 mesh ASTM). Reverse-phase preparative high performance liquid chromatography (RPHPLC) was conducted on a Phenomenex column (Luna, 5  $\mu\text{m}$ , C18 100A, 150 mm  $\times$  21.2 mm) with adjustable solvent gradients, usually 5–95% of acetonitrile in

water + 0.1% TFA in 18 min at flow rate of 20 mL/min, and was used for routine purification. The preliminary purity and identity of all compounds were assessed after purification by tandem HPLC–mass spectrometry (LC–MS) experiments on a Waters Micromass ZQ mass spectrometer in electrospray ionization (ESI) positive mode after separation on a Waters 2795 separations module. The HPLC separations were performed on a Phenomenex column (Luna, 5  $\mu$ m, C18 100A, 50 mm  $\times$  2.00 mm) with a flow rate of 0.8 mL/min and a 4 min gradient of 5–95% or 30–95% of acetonitrile in water + 0.05% TFA, using a Waters 2996 photodiode array detector. Purity and identity were assessed on the integrated UV chromatograms (220–400 nm) and the mass spectra. The final purity was determined using a Waters 2695 separations module on a Waters Xterra RP18, 3.5  $\mu$ m, 4.6 mm  $\times$  20 mm IS column with a flow rate of 2.0 mL/min, gradient 5–95% of acetonitrile in water with 0.1% TFA over 5 min, and a Waters 2996 photodiode array detector. A longer column (Phenomenex Gemini, 5  $\mu$ m, C18, 110A, 4.6 mm  $\times$  150 mm) together with a flow rate of 1.0–1.2 mL/min and a 15 min gradient of 5–95% acetonitrile in water + 0.1% TFA was also used for purity check. Purity was >95% for all compounds reported for biological data except those indicated in their respective synthesis.

All the 1D and 2D NMR experiments for  $^1\text{H}$  (400.13 MHz),  $^{13}\text{C}$  (100.61 MHz),  $^{15}\text{N}$  (40.55 MHz), and  $^{19}\text{F}$  (376.47 MHz) nuclei were performed on a Bruker AVANCE-400 digital NMR spectrometer.  $^1\text{H}$ – $^1\text{H}$ ,  $^1\text{H}$ – $^{13}\text{C}$ , and  $^1\text{H}$ – $^{15}\text{N}$  2D experiments (COSY, HMQC, HSQC, and HMBC) were run with Z-gradient selection. NMR spectra are reported in ppm with reference to an internal tetramethylsilane standard (0.00 ppm for  $^1\text{H}$  and  $^{13}\text{C}$ ) or solvent peak(s) of  $\text{CDCl}_3$  (7.26 and 77.1 ppm) or  $\text{CD}_3\text{OD}$  (3.31 and 49.0 ppm), or  $\text{DMSO-}d_6$  (2.50 and 39.5 ppm). Other NMR solvents were used as needed. When peak multiplicities are reported, the following abbreviations are used: s = singlet, d = doublet, t = triplet, q = quartet, m = multiplet, br = broadened, dd = doublet of doublets, dt = doublet of triplets, bs = broadened singlet. Coupling constants, when given, are reported in hertz.

For TFA salts, the TFA content (w/w) and freebase content (w/w) of TFA salts were determined by  $^{19}\text{F}$  and  $^1\text{H}$  NMR using an internal reference standard (e.g., 2,2,2-trifluoroethylamine hydrochloride), and the molar ratio of TFA over freebase was also calculated. For those molecules containing a  $\text{CF}_3$  group, the  $\text{CF}_3$  group can also serve as an internal reference standard for TFA quantification, and the results of the TFA/freebase ratio obtained from this method are in line with the above method using a dedicated internal reference standard. Elemental analyses of CHN were performed on a Perkin-Elmer 2400 CHN/CHNS elemental analyzer. HRMS results were obtained from a Bruker micrOTOF-Q II instrument with direct injection.

**Preparation of *trans*-4-Chloro-3-nitrocinnamic Acid Methyl Ester (5).** To a suspension of *trans*-4-chloro-3-nitrocinnamic acid (4, 10.00 g, 43.94 mmol) in MeOH (200–250 mL) was added concentrated  $\text{H}_2\text{SO}_4$  (3 mL). The reaction mixture was allowed to stir at 80–85  $^\circ\text{C}$  for 4–6 h. The progress of the reaction was monitored by HPLC or LC–MS. When the acid (4) was completely converted to the corresponding ester (5), the reaction flask was cooled in an ice bath. The suspension was filtered, and the residue was washed with cold methanol several times and dried. Ester 5 was obtained as a yellowish solid (10.09 g, 95% yield). LC–MS  $m/z$  210 and 212 (very weak signal,  $[\text{M} + \text{H} - \text{MeOH}]^+$ ).  $^1\text{H}$  NMR ( $\text{CDCl}_3$ )  $\delta$  8.01 (d,  $J = 2.0$  Hz, 1H, H-2), 7.64 (dd,  $J = 8.5, 2.1$  Hz, 1H, H-6), 7.64 (d,  $J = 16.0$  Hz, 1H,  $-\text{CH}=\text{CH}-\text{CO}_2\text{Me}$ ), 7.58 (d,  $J = 8.4$  Hz, 1H, H-5), 6.50 (d,  $J = 16.1$  Hz, 1H,  $-\text{CH}=\text{CH}-\text{CO}_2\text{Me}$ ), 3.83 (s, 3H,  $\text{OCH}_3$ );  $^{13}\text{C}$  NMR ( $\text{CDCl}_3$ )  $\delta$  166.4 ( $\text{CO}_2\text{Me}$ ), 148.3 (C-3), 140.8 ( $-\text{CH}=\text{CH}-\text{CO}_2\text{Me}$ ), 134.5 (C-1), 132.5 (C-5), 131.8 (C-6), 128.3 (C-4), 124.5 (C-2), 121.4 ( $-\text{CH}=\text{CH}-\text{CO}_2\text{Me}$ ), 52.1 ( $\text{OCH}_3$ ).

**General Procedure A for Synthesis of Aniline Compound 7.** (E)-3-[4-(2-Dimethylamino-ethylamino)-3-nitrophenyl]acrylic Acid Methyl Ester (7f). A mixture of 5 (0.658 g, 2.72 mmol),  $N,N$ -dimethylethylenediamine (0.90 mL, 8.20 mmol), and triethylamine (1.2 mL, 8.6 mmol) in 1,4-dioxane (20 mL) was heated at 80  $^\circ\text{C}$  for 5 h.

The solution was evaporated, and to the residue were added dichloromethane (DCM) and aqueous  $\text{Na}_2\text{CO}_3$ . The DCM ( $\times 3$ ) extracts were concentrated, and to the residue was added EtOAc–hexanes. The resulting red solid was filtered to afford the title compound 7f (0.672 g, 84%). LC–MS  $m/z$  294.2 ( $[\text{M} + \text{H}]^+$ ).  $^1\text{H}$  NMR ( $\text{CDCl}_3 + \text{CD}_3\text{OD}$ )  $\delta$  8.21 (d,  $J = 2.1$  Hz, 1H), 7.56 (dd,  $J = 9.0, 2.1$  Hz, 1H), 7.48 (d,  $J = 16.0$  Hz, 1H), 6.81 (d,  $J = 9.0$  Hz, 1H), 6.20 (d,  $J = 15.9$  Hz, 1H), 3.70 (s, 3H), 3.34 (t,  $J = 6.5$  Hz, 2H), 2.56 (t,  $J = 6.4$  Hz, 2H), 2.23 (s, 6H);  $^{13}\text{C}$  NMR ( $\text{CDCl}_3 + \text{CD}_3\text{OD}$ )  $\delta$  167.3, 145.4, 142.6, 134.0, 131.1, 127.1, 121.3, 114.8, 114.0, 56.7, 51.1, 44.6, 40.1.

(E)-3-[4-(3-Dimethylamino-2,2-dimethylpropylamino)-3-nitrophenyl]acrylic Acid Methyl Ester (7a). 7a was prepared according to procedure A but using 3-dimethylamino-2,2-dimethylpropylamine as starting material and was obtained as a red solid (35 g, 95%). LC–MS  $m/z$  336.1 ( $[\text{M} + \text{H}]^+$ ).  $^1\text{H}$  NMR ( $\text{CDCl}_3$ )  $\delta$  9.73 (br s or t, 1H,  $-\text{NH}-$ ), 8.33 (d,  $J = 2.0$  Hz, 1H), 7.60 (dd,  $J = 8.9, 2.0$  Hz, 1H), 7.59 (d,  $J = 16.1$  Hz, 1H), 6.88 (d,  $J = 9.1$  Hz, 1H), 6.28 (d,  $J = 15.9$  Hz, 1H), 3.80 (s, 3H), 3.21 (d,  $J = 4.6$  Hz, 2H), 2.36 (s, 2H), 2.34 (s, 6H), 1.04 (s, 6H).

(E)-3-[4-(2-Diethylaminoethylamino)-3-nitrophenyl]acrylic Acid Methyl Ester (7b). 7b was prepared according to procedure A but using 2-diethylaminoethylamine as starting material and was obtained as a yellow solid (29 g, 82%). LC–MS  $m/z$  322.1 ( $[\text{M} + \text{H}]^+$ ).  $^1\text{H}$  NMR ( $\text{CDCl}_3$ )  $\delta$  8.72 (t-like,  $J = 4.2$  Hz, 1H,  $-\text{NH}-$ ), 8.32 (d,  $J = 2.1$  Hz, 1H), 7.61 (dd,  $J = 9.3, 2.1$  Hz, 1H), 7.58 (d,  $J = 15.9$  Hz, 1H), 6.85 (d,  $J = 9.0$  Hz, 1H), 6.29 (d,  $J = 15.9$  Hz, 1H), 3.79 (s, 3H), 3.35 (td,  $J = 5.4, 4.7$  Hz, 2H,  $-\text{NHCH}_2\text{CH}_2-$ ), 2.77 (t,  $J = 6.1$  Hz, 2H), 2.59 (q,  $J = 7.1$  Hz, 4H), 1.07 (t,  $J = 7.1$  Hz, 6H);  $^{13}\text{C}$  NMR ( $\text{CDCl}_3$ )  $\delta$  167.5, 146.1, 143.0, 134.3, 131.7, 127.7, 121.6, 115.3, 114.8, 51.6 ( $\text{OCH}_3$ ), 50.7 ( $-\text{NHCH}_2\text{CH}_2-$ ), 46.8 ( $-\text{NCH}_2\text{CH}_3$ ), 40.9 ( $-\text{NHCH}_2\text{CH}_2-$ ), 12.0 ( $-\text{NCH}_2\text{CH}_3$ ). HRMS (ESI)  $m/z$ :  $[\text{M} + \text{H}]^+$  calcd for  $\text{C}_{16}\text{H}_{24}\text{N}_3\text{O}_4$ , 322.1761; found 322.1767.

(E)-3-[4-(2-Ethylaminoethylamino)-3-nitrophenyl]acrylic Acid Methyl Ester (7c). 7c was prepared according to procedure A but using 2-ethylaminoethylamine as starting material and was obtained as a red solid (36 g, 56%). LC–MS  $m/z$  294.1 ( $[\text{M} + \text{H}]^+$ ).  $^1\text{H}$  NMR ( $\text{DMSO-}d_6$ )  $\delta$  8.49 (t,  $J = 6.1$  Hz, 1H,  $-\text{NH}-$ ), 8.35 (d,  $J = 2.0$  Hz, 1H), 7.96 (dd,  $J = 9.1, 1.9$  Hz, 1H), 7.62 (d,  $J = 16.0$  Hz, 1H), 7.20 (d,  $J = 9.1$  Hz, 1H), 6.52 (d,  $J = 16.0$  Hz, 1H), 3.75 (td,  $J = 6.5, 6.2$  Hz, 2H), 3.70 (s, 3H), 3.08 (t,  $J = 6.5$  Hz, 2H), 2.93 (q,  $J = 7.2$  Hz, 4H), 1.17 (t,  $J = 7.2$  Hz, 6H).

(E)-3-[4-(2-Isopropylaminoethylamino)-3-nitrophenyl]acrylic Acid Methyl Ester (7d). 7d was prepared according to procedure A but using 2-isopropylaminoethylamine as starting material and was obtained as a red solid (27 g, 57%). LC–MS  $m/z$  308.1 ( $[\text{M} + \text{H}]^+$ ).  $^1\text{H}$  NMR ( $\text{DMSO-}d_6$ )  $\delta$  8.58 (t,  $J = 5.6$  Hz, 1H, Ar– $\text{NH}-$ ), 8.33 (d,  $J = 2.0$  Hz, 1H), 7.94 (dd,  $J = 9.1, 1.9$  Hz, 1H), 7.60 (d,  $J = 16.0$  Hz, 1H), 7.14 (d,  $J = 9.2$  Hz, 1H), 6.49 (d,  $J = 16.0$  Hz, 1H), 3.70 (s, 3H), 3.56 (masked by water peak, identified by COSY, 2H), 3.01 (septet,  $J = 6.4$  Hz, 1H), 2.94 (t,  $J = 6.2$  Hz, 2H), 1.10 (d,  $J = 6.4$  Hz, 6H).

(E)-3-[4-(2-Diisopropylaminoethylamino)-3-nitrophenyl]acrylic Acid Methyl Ester (7e). 7e was prepared according to procedure A but using 2-diisopropylaminoethylamine as starting material and was obtained as a yellow solid (12 g, 79%). LC–MS  $m/z$  350 ( $[\text{M} + \text{H}]^+$ ).  $^1\text{H}$  NMR ( $\text{CDCl}_3$ )  $\delta$  8.76 (t-like,  $J = 4.3$  Hz, 1H), 8.32 (d,  $J = 2.0$  Hz, 1H), 7.61 (dd,  $J = 8.3, 2.7$  Hz, 1H), 7.58 (d,  $J = 15.8$  Hz, 1H), 6.85 (d,  $J = 9.0$  Hz, 1H), 6.29 (d,  $J = 15.9$  Hz, 1H), 3.79 (s, 3H), 3.31 (td,  $J = 5.3, 6.1$  Hz, 2H, Ar– $\text{NH}-$ ), 3.08 (septet,  $J = 6.6$  Hz, 2H,  $(\text{Me}_2\text{CH})_2\text{N}$ ), 2.84 (t,  $J = 6.2$  Hz, 2H), 1.07 (d,  $J = 6.6$  Hz, 12H).

(E)-3-[4-(2-Methylaminoethylamino)-3-nitrophenyl]acrylic Acid Methyl Ester (7g). 7g was prepared according to procedure A but using 2-methylaminoethylamine as starting material and was obtained as an orange solid (2.1 g, 100%). LC–MS  $m/z$  280 ( $[\text{M} + \text{H}]^+$ ).  $^1\text{H}$  NMR ( $\text{CDCl}_3$ )  $\delta$  8.54 (t-like,  $J = 4.2$  Hz, 1H), 8.33 (d,  $J = 2.1$  Hz, 1H), 7.63 (dd,  $J = 9.0, 2.2$  Hz, 1H), 7.59 (d,  $J = 16.0$  Hz, 1H), 6.90 (d,  $J = 9.0$  Hz, 1H),

6.31 (d,  $J = 15.9$  Hz, 1H), 3.80 (s, 3H), 3.45 (td,  $J = 5.8, 5.6$  Hz, 2H), 2.96 (t,  $J = 6.2$  Hz, 2H), 2.50 (s, 3H).

**(E)-3-[4-(2-Aminoethylamino)-3-nitrophenyl]acrylic Acid Methyl Ester (7h).** In method 1, **7h** was prepared according to procedure A but using 1,2-ethylenediamine as starting material and was obtained as an orange solid (2.8 g, 98%). LC–MS  $m/z$  266 ( $[M + H]^+$ ). In method 2, to a 150 mL flask were added **7i** (0.855 g, 2.34 mmol), MeOH (10 mL), and 6 N HCl (2 mL). The mixture was heated to reflux (65–70 °C) for 3 h (monitored by HPLC and LC–MS). The solution was evaporated to dryness. Then EtOAc/DCM was added and the solution was evaporated to dryness. **7h** was obtained as a red or orange solid (0.7069 g, 100% as the mono-HCl salt).

**(E)-3-[4-(2-tert-Butoxycarbonylaminoethylamino)-3-nitrophenyl]acrylic Acid Methyl Ester (7i).** **7i** was prepared according to procedure A but using *N*-Boc-ethylenediamine as starting material and was obtained as a bright yellow solid (0.193 g, 53%). LC–MS  $m/z$  366.1 ( $[M + H]^+$ ).  $^1\text{H NMR}$  ( $\text{CDCl}_3$ )  $\delta$  8.41 (br t like, 1H,  $-\text{NHAr}$ ), 8.31 (d,  $J = 1.8$  Hz, 1H), 7.63 (dd,  $J = 9.0, 1.7$  Hz, 1H), 7.57 (d,  $J = 16.0$  Hz, 1H), 6.98 (d,  $J = 8.9$  Hz, 1H), 6.30 (d,  $J = 15.9$  Hz, 1H), 4.91 (br t like, 1H, BocNH–), 3.80 (s, 3H), 3.52 (dt,  $J = 5.8, 5.5$  Hz, 2H), 3.45 (dt,  $J = 6.0, 5.9$  Hz, 2H), 1.45 (s, 9H);  $^{13}\text{C NMR}$  ( $\text{CDCl}_3$ )  $\delta$  166.9, 155.7, 145.8, 142.3, 134.1, 131.5, 127.1, 121.8, 115.4, 113.9, 79.5, 51.2, 42.7, 39.1, 27.9.

**General Procedures for Syntheses of Benzimidazoles 9 and 9a–ab. Procedure B. Preparation of (E)-3-[1-(2-Ethylaminoethyl)-2-hexyl-1H-benzimidazol-5-yl]acrylic Acid Methyl Ester (9p).** To a stirred solution of **7c** (8.174 g, 27.87 mmol) and heptaldehyde (4.85 g, 42.47 mmol) in AcOH and MeOH (1:9 v/v, 300 mL) was added  $\text{SnCl}_2 \cdot 2\text{H}_2\text{O}$  (31.45 g, 139.4 mmol) in portions. The resulting mixture was heated to 40 °C with stirring. The progress of the reaction was monitored by LC–MS. When the reaction was completed, solvent was removed under reduced pressure below 40 °C. The resultant residue was diluted with EtOAc (50 mL) and then basified (pH > 10) with saturated aqueous  $\text{Na}_2\text{CO}_3$  and extracted with DCM ( $\times 3$ ). The organic extracts were combined, dried ( $\text{Na}_2\text{SO}_4$ ), filtered, and evaporated to dryness. The resulting oily residue was purified by flash column chromatography (silica, 0–10% of MeOH in DCM). The title compound **9p** was obtained as a yellow solid (4.445 g, 44.6%). LC–MS  $m/z$  358.3 ( $[M + H]^+$ ).  $^1\text{H NMR}$  ( $\text{CDCl}_3$ )  $\delta$  7.88 (d,  $J = 1.2$  Hz, 1H), 7.83 (d,  $J = 16.0$  Hz, 1H), 7.43 (dd,  $J = 8.4, 1.4$  Hz, 1H), 7.33 (d,  $J = 8.4$  Hz, 1H), 6.43 (d,  $J = 15.9$  Hz, 1H), 4.22 (t,  $J = 6.6$  Hz, 1H), 3.80 (s, 3H), 3.01 (t,  $J = 6.6$  Hz, 2H), 2.89 (t,  $J = 7.9$  Hz, 2H), 2.65 (q,  $J = 7.1$  Hz, 2H), 1.91 (quintet,  $J = 7.8$  Hz, 2H), 1.46 (m, 2H), 1.40–1.30 (m, 4H), 1.07 (t,  $J = 7.1$  Hz, 3H), 0.90 (t,  $J = 7.0$  Hz, 3H);  $^{13}\text{C NMR}$  ( $\text{CDCl}_3$ )  $\delta$  167.3, 156.5, 145.5, 142.6, 136.3, 128.0, 121.7, 119.1, 115.1, 109.1, 51.0, 48.2, 43.7 (C  $\times 2$ ), 31.0, 28.7, 27.1 (C  $\times 2$ ), 22.0, 14.7, 13.5.

**(E)-3-[2-Butyl-1-(2-diethylaminoethyl)-1H-benzimidazol-5-yl]acrylic Acid Methyl Ester (9).** **9** was prepared and purified according to procedure B with yields of 38–73% as a yellow solid. LC–MS  $m/z$  358.2 ( $[M + H]^+$ ).  $^1\text{H NMR}$  ( $\text{CDCl}_3$ )  $\delta$  7.87 (d,  $J = 1.0$  Hz, 1H), 7.83 (d,  $J = 15.9$  Hz, 1H), 7.43 (dd,  $J = 8.4, 1.5$  Hz, 1H), 7.28 (d,  $J = 8.2$  Hz, 1H), 6.43 (d,  $J = 15.9$  Hz, 1H), 4.15 (t,  $J = 7.0$  Hz, 2H), 3.81 (s, 3H), 2.90 (t,  $J = 7.0$  Hz, 2H), 2.74 (t,  $J = 7.0$  Hz, 2H), 2.55 (q,  $J = 7.1$  Hz, 4H), 1.90 (quintet,  $J = 7.8$  Hz, 2H), 1.49 (sextet,  $J = 7.6$  Hz, 2H), 0.99 (t,  $J = 7.3$  Hz, 3H), 0.96 (t,  $J = 7.2$  Hz, 6H);  $^{13}\text{C NMR}$  ( $\text{CDCl}_3$ )  $\delta$  167.8, 157.0, 146.1 (CH), 143.1, 136.8, 128.4, 122.1 (CH), 119.6 (CH), 115.6 (CH), 109.5 (CH), 52.4, 51.5, 47.8, 43.2, 29.7, 27.3, 22.7, 13.8, 12.0. The nitrogens in ester **9** were also identified by  $^1\text{H}-^{15}\text{N}$  HMBC with  $\delta_{\text{N}}$  of 239.0 ppm for  $\text{N}^3$  of the benzimidazole ring, 151.8 ppm for  $\text{N}^1$ , and 42.6 ppm for the diethylamino group (reference to nitromethane  $\delta_{\text{N}} = 380.0$  ppm in  $\text{CDCl}_3$ ). HRMS (ESI)  $m/z$   $[M + H]^+$  calcd for  $\text{C}_{21}\text{H}_{32}\text{N}_3\text{O}_2$ , 358.2489; found, 358.2492.

**General Procedures for Synthesis of Hydroxamates 3, 10, 15, 17, 20, and 22. Procedure C for Small Scales (TFA Salt).** **(E)-3-[2-Butyl-1-(2-diethylaminoethyl)-1H-benzimidazol-5-yl]-N-hydroxyacrylamide (3).** Ester **9** (crude 0.177 g, made from

0.513 mmol of **7b** according to procedure B) was mixed with hydroxylamine hydrochloride (0.331 g, 4.76 mmol) and MeOH (3 mL) with stirring at room temperature. The reaction mixture was cooled over dry ice, followed by the addition of sodium methoxide (25% in MeOH, 2.4 mL, 10.5 mmol). The mixture was then allowed to warm slowly to room temperature. The reaction was monitored by LC–MS and was completed in  $\sim 30$  min. The reaction mixture was slowly acidified with 6 N hydrochloric acid to pH  $\approx 7$ , and water was added to achieve a clear solution, which was subsequently purified by RP-HPLC to afford compound **3** as the bis-TFA salt, light pinkish solid (0.061 g, 20% in two steps from **7b**). There was negative reaction in the silver nitrate test. LC–MS  $m/z$  359.2 ( $[M + H]^+$ ).  $^1\text{H NMR}$  ( $\text{CD}_3\text{OD}$ )  $\delta$  7.94 (d,  $J = 8.6$  Hz, 1H), 7.85 (s, 1H), 7.76 (d,  $J = 8.5$  Hz, 1H), 7.50 (d,  $J = 15.7$  Hz, 1H), 6.49 (d,  $J = 15.7$  Hz, 1H), 4.96 (overlapped with DHO, identified by COSY, 2H), 3.69 (t-like,  $J = 7.6$  Hz, 2H), 3.44 (q,  $J = 7.6$  Hz, 4H), 3.26 (t,  $J = 7.9$  Hz, 2H), 1.94 (quintet,  $J = 7.5$  Hz, 2H), 1.57 (sextet,  $J = 7.6$  Hz, 2H), 1.40 (t,  $J = 7.2$  Hz, 6H), 1.05 (t,  $J = 7.3$  Hz, 3H);  $^{13}\text{C NMR}$  ( $\text{CD}_3\text{OD}$ )  $\delta$  165.5, 157.7, 140.0, 134.8, 134.0, 133.8, 126.5, 119.9, 115.1, 113.6, 50.2, 48.7 (2C), 40.5, 29.4, 26.6, 23.3, 13.9, 8.9 (2C) (TFA peaks at 163.4, 163.0, 162.7, 162.3; 122.3, 119.5, 116.6).

**Procedure D for Freebase and Salt Formation. Preparation of (E)-3-[1-(2-Ethylaminoethyl)-2-hexyl-1H-benzimidazol-5-yl]-N-hydroxyacrylamide (10p).** To a solution of ester **9p** (4.428 g, 12.39 mmol) and  $\text{NH}_2\text{OH} \cdot \text{HCl}$  (8.66 g, 124.7 mmol) in dry MeOH (50 mL), which was stirred and cooled in a dry ice–acetone bath, was added NaOMe solution in MeOH (25%, 55 mL, 240 mmol). The reaction mixture was then stirred at room temperature. The progress of reaction was monitored by LC–MS (usually reaction completed within 30–90 min) and quenched by adding 6 N HCl (40 mL). To the mixture was added Milli-Q deionized water. The mixture was adjusted pH  $\approx 8$  with 1 N NaOH and was evaporated to remove the organic solvent. The resultant residue was washed with Milli-Q water ( $\times 3$ ) and redissolved in MeOH–DCM. The solution was filtered and diluted with Milli-Q water. The suspension was evaporated to remove the organic solvent, and the resultant residue was washed with Milli-Q water ( $\times 2$ ). The freebase of **10p** was obtained (HPLC purity at 254 nm, 98%). It was recrystallized from MeOH–ethyl acetate to afford a white or pale yellow solid. The freebase was dissolved in MeOH and excess 6 N HCl (final pH < 2), and the clear solution was evaporated to dryness and then diluted with MeOH and coevaporated with PhMe ( $\times 1$ ) and EtOAc ( $\times 2$ ). The solid was recrystallized from MeOH–EtOAc to give a white or pale yellow solid (3.298 g, 61.7%). HPLC purity at 254 nm: 98.4–99.6%. LC–MS  $m/z$  359.2 ( $[M + H]^+$ ).  $^1\text{H NMR}$  ( $\text{CD}_3\text{OD}$ )  $\delta$  9.33 (residual NH), 8.03 (d,  $J = 8.3$  Hz, 1H), 7.77 (s, 1H), 7.73 (d,  $J = 8.2$  Hz, 1H), 7.16 (d,  $J = 15.7$  Hz, 1H), 6.34 (d,  $J = 15.7$  Hz, 1H), 4.88 (overlapped with DHO, identified by COSY, 2H), 3.63 (br t like, 2H), 3.32 (d,  $J = 7.9$  Hz, 2H), 3.15 (q,  $J = 7.1$  Hz, 2H), 1.94 (quintet,  $J = 7.1$  Hz, 2H), 1.53 (quintet,  $J = 6.7$  Hz, 2H), 1.42–1.31 (m, 4H), 1.33 (t,  $J = 7.1$  Hz, 3H), 0.88 (t,  $J = 7.0$  Hz, 3H);  $^{13}\text{C NMR}$  ( $\text{CD}_3\text{OD}$ )  $\delta$  163.4, 155.8, 138.1, 133.0, 132.0, 130.3, 125.1, 117.4, 112.8, 112.5, 44.5, 43.2, 41.1, 30.5, 28.0, 25.3, 25.2, 21.6, 12.4, 9.6. Anal. ( $\text{C}_{20}\text{H}_{30}\text{N}_4\text{O}_2 \cdot 2.05\text{HCl} \cdot \text{H}_2\text{O}$ ) C, H, Cl, N: calcd, 12.42; found, 12.92.

**(E)-3-[2-Butyl-1-(2-diethylaminoethyl)-1H-benzimidazol-5-yl]-N-hydroxyacrylamide Dihydrochloride Salt (3).** The freebase of **3** was prepared according to procedure D. The hydroxamic acid moiety was identified by  $^1\text{H}-^{15}\text{N}$  HSQC ( $\text{DMSO}-d_6$ ) with  $\delta_{\text{N}} = 169.0$  ppm (CONHOH). Other nitrogens in **3** were identified by  $^1\text{H}-^{15}\text{N}$  HMBC ( $\text{DMSO}-d_6$ ) with  $\delta_{\text{N}}$  of 241.4 ppm for  $\text{N}^3$  of the benzimidazole ring, 152.3 ppm for  $\text{N}^1$ , and 41.3 ppm for the diethylamino group (reference to nitromethane  $\delta_{\text{N}} = 380.0$  ppm in  $\text{CDCl}_3$ ). The dihydrochloride salt of **3** was prepared according to procedure D as white or off-white solid or powder in  $\sim 60\%$  yield from **9** in two steps. LC–MS  $m/z$  359.2 ( $[M + H]^+$ ).  $^1\text{H NMR}$  ( $\text{DMSO}-d_6$ )  $\delta$  11.79 (brs, 1H, NH or OH), 10.92 (very br s, 1H), 8.18 (d,  $J = 8.6$  Hz, 1H), 7.97 (s, 1H), 7.79 (d,  $J = 8.6$  Hz, 1H), 7.64 (d,  $J = 15.8$  Hz, 1H), 6.65 (d,  $J = 15.8$  Hz, 1H),

5.01 (t-like,  $J = 7.7$  Hz, 2H), 3.48 (m, 2H), 3.30–3.19 (m, 6H), 1.87 (quintet,  $J = 7.8$  Hz, 2H), 1.47 (sextet,  $J = 7.5$  Hz, 2H), 1.29 (t,  $J = 7.2$  Hz, 6H), 0.97 (t,  $J = 7.3$  Hz, 3H);  $^{13}\text{C}$  NMR (DMSO- $d_6$ )  $\delta$  162.3, 156.0, 137.3 (CH), 132.8, 132.3, 132.0 (br, identified by HMBC), 124.7 (CH), 120.2 (CH), 113.1 ( $2 \times$  CH), 48.2, 46.3, 39.0, 28.1, 25.0, 21.7, 13.6, 8.3. Anal. ( $\text{C}_{20}\text{H}_{30}\text{N}_4\text{O}_2 \cdot 2\text{HCl} \cdot 0.265\text{H}_2\text{O}$ ) C, H, N, Cl. Water content = 1.09% (Karl Fisher method). HRMS (ESI)  $m/z$   $[\text{M} + \text{H}]^+$  calcd for  $\text{C}_{20}\text{H}_{31}\text{N}_4\text{O}_2$ , 359.2442; found, 359.2449.

The following compounds (10a–o and 10q–ab) were prepared according to procedures A–D.

**(E)-3-[2-Butyl-1-(3-dimethylamino-2,2-dimethylpropyl)-1H-benzimidazol-5-yl]-N-hydroxyacrylamide (10a).** 10a was prepared according to procedures B and C but using 7a as starting material and was obtained as the bis-TFA salt (74 mg, 25% in two steps). LC–MS  $m/z$  373.2 ( $[\text{M} + \text{H}]^+$ ).  $^1\text{H}$  NMR ( $\text{CD}_3\text{OD}$ )  $\delta$  8.05 (d,  $J = 8.8$  Hz, 1H), 7.90 (s, 1H), 7.78 (d,  $J = 8.7$  Hz, 1H), 7.61 (d,  $J = 15.8$  Hz, 1H), 6.59 (d,  $J = 15.7$  Hz, 1H), 4.61 (s, 2H), 3.49 (s, 2H), 3.30 (overlapped with  $\text{CD}_2\text{HOD}$ , 2H), 3.07 (s, 6H), 1.96 (quintet,  $J = 7.2$  Hz, 2H), 1.55 (sextet,  $J = 7.6$  Hz, 2H), 1.27 (s, 6H), 1.04 (t,  $J = 7.3$  Hz, 3H);  $^{13}\text{C}$  NMR ( $\text{CD}_3\text{OD}$ )  $\delta$  165.5 (br), 158.2, 139.8, 135.3, 135.1, 132.4, 126.4, 120.6 (br), 115.6, 114.3, 68.7, 53.5, 47.8 ( $\text{Me} \times 2$ ), 39.5, 29.9, 27.2, 23.6 ( $\text{Me} \times 2$ ), 23.3, 13.9 (TFA peaks at 162.0, 161.7, 119.0, 116.1).

**(E)-3-[1-(3-Dimethylamino-2,2-dimethylpropyl)-2-isobutyl-1H-benzimidazol-5-yl]-N-hydroxyacrylamide (10b).** 10b was prepared according to procedures B and C but using 7a as starting material and was obtained as the bis-TFA salt (29 mg, 15% in two steps). LC–MS  $m/z$  373.14 ( $[\text{M} + \text{H}]^+$ ).  $^1\text{H}$  NMR (DMSO- $d_6$ )  $\delta$  10.80 (br s, 0.5H), 9.47 (br s, 1H), 7.92 (d,  $J = 7.2$  Hz, 1H), 7.89 (s, 1H), 7.64 (d,  $J = 7.4$  Hz, 1H), 7.62 (d,  $J = 15.5$  Hz, 1H), 6.54 (d,  $J = 15.8$  Hz, 1H), 4.39 (s, 2H), 3.33 (s, 2H), 2.97 (d,  $J = 7.26$  Hz, 2H), 2.92 (s, 6H,  $\text{Me}_2\text{N}$ ), 2.35 (septet,  $J = 6.8$  Hz, 1H,  $\text{Me}_2\text{CH}$ ), 1.09 (s, 6H,  $\text{Me}_2\text{C}$ ), 0.97 (d,  $J = 6.6$  Hz, 6H,  $\text{Me}_2\text{CH}$ );  $^{13}\text{C}$  NMR (DMSO- $d_6$ )  $\delta$  162.7, 156.1, 138.2, 135.2, 131.1, 122.7, 118.9, 118.1, 115.3, 113.5, 66.7, 51.1, 46.7, 38.1, 34.6, 27.6, 22.8, 22.0 (TFA peaks at 158.5, 158.1).

**(E)-3-[1-(2-Diethylaminoethyl)-2-isobutyl-1H-benzimidazol-5-yl]-N-hydroxyacrylamide (10c).** 10c was prepared according to procedures B and C but using 7b as starting material and was obtained as the bis-TFA salt (17 mg, 10% in two steps). LC–MS  $m/z$  359.1 ( $[\text{M} + \text{H}]^+$ ).  $^1\text{H}$  NMR (DMSO- $d_6$ )  $\delta$  10.81 (s, 0.5H), 10.13 (s, 1H), 7.90 (s, 1H), 7.81 (d,  $J = 8.5$  Hz, 1H), 7.66 (d,  $J = 8.6$  Hz, 1H), 7.61 (d,  $J = 15.8$  Hz, 1H), 6.53 (d,  $J = 15.8$  Hz, 1H), 4.72 (t,  $J = 7.8$  Hz, 2H), 3.47 (t, overlapping with solvent, 2H), 3.30 (m, 4H), 2.93 (d,  $J = 7.2$  Hz, 2H), 2.27 (m,  $J = 6.7$  Hz, 1H), 1.25 (t,  $J = 7.2$  Hz, 6H), 1.03 (d,  $J = 6.6$  Hz, 6H);  $^{13}\text{C}$  NMR (DMSO- $d_6$ )  $\delta$  162.7, 155.2, 138.4, 133.9, 131.0, 123.0, 118.6, 116.0, 111.6, 48.8, 46.8, 34.1, 27.1, 22.2, 8.5 (TFA peaks at 158.5, 158.1).

**(E)-3-[2-Butyl-1-(3-isopropylaminopropyl)-1H-benzimidazol-5-yl]-N-hydroxyacrylamide (10d).** 10d was prepared according to procedures B and C but using 7j as starting material and was obtained as the bis-TFA salt (60 mg, 28% in two steps). LC–MS  $m/z$  359.2 ( $[\text{M} + \text{H}]^+$ ).  $^1\text{H}$  NMR (DMSO- $d_6$ )  $\delta$  8.80 (br s, 2H), 8.00 (d,  $J = 8.7$  Hz, 1H), 7.98 (s, 1H), 7.79 (d,  $J = 8.6$  Hz, 1H), 7.65 (d,  $J = 15.8$  Hz, 1H), 6.63 (d,  $J = 15.8$  Hz, 1H), 4.53 (t,  $J = 7.5$  Hz, 2H), 3.29 (septet,  $J = 6.2$  Hz, 1H), 3.16 (t,  $J = 7.8$  Hz, 1H), 3.11 (m, 2H), 2.15 (quintet,  $J = 7.1$  Hz, 2H), 1.83 (quintet,  $J = 7.7$  Hz, 2H), 1.44 (sextet,  $J = 7.6$  Hz, 2H), 1.23 (d,  $J = 6.5$  Hz, 6H), 0.95 (t,  $J = 7.3$  Hz, 3H).

**(E)-3-[2-Butyl-1-(2-isopropylaminoethyl)-1H-benzimidazol-5-yl]-N-hydroxyacrylamide (10e).** 10e was prepared according to procedures B and D but using 7d as starting material and was obtained as an off-white hydrochloride salt (7 g, 22% in three steps). LC–MS  $m/z$  345.2 ( $[\text{M} + \text{H}]^+$ ).  $^1\text{H}$  NMR (DMSO- $d_6$ )  $\delta$  10.37 (br s, 0.33H), 9.92 (br s, 2H,  $-\text{NH}_2^+ - \text{CHMe}_2$ ), 8.16 (d,  $J = 8.6$  Hz, 1H), 7.97 (s, 1H), 7.78 (d,  $J = 8.6$  Hz, 1H), 7.63 (d,  $J = 15.8$  Hz, 1H), 6.67 (d,  $J = 15.8$  Hz, 1H), 4.93 (t,  $J = 6.4$  Hz, 2H), 3.36 (t,  $J = 5.4$  Hz, 2H), 3.31 (m, 1H), 3.30 (t,  $J = 7.8$  Hz, 2H), 1.86 (quintet,  $J = 7.6$  Hz, 2H), 1.47 (sextet,  $J = 7.5$  Hz, 2H), 1.27 (d,  $J = 6.5$  Hz,

6H), 0.96 (t,  $J = 7.3$  Hz, 3H);  $^{13}\text{C}$  NMR (DMSO- $d_6$ )  $\delta$  162.3, 156.1, 137.3, 132.9, 132.3, 131.5, 124.8, 120.3, 113.1, 112.8, 50.0, 42.1, 41.0, 28.2, 25.1, 21.7, 18.4, 13.5. Anal. ( $\text{C}_{19}\text{H}_{28}\text{N}_4\text{O}_2 \cdot 2.2\text{HCl} \cdot 2.5\text{H}_2\text{O}$ ) C, H, N, Cl.

**(E)-3-[1-(3-Dimethylamino-2,2-dimethylpropyl)-2-(2,2-dimethylpropyl)-1H-benzimidazol-5-yl]-N-hydroxyacrylamide Hydrochloride Salt (10f).** 10f was prepared according to procedures B and D but using 7a as starting material and was obtained as the hydrochloride salt, pinkish solid (3.65 g, 19% in three steps). LC–MS  $m/z$  387.2 ( $[\text{M} + \text{H}]^+$ ).  $^1\text{H}$  NMR ( $\text{CD}_3\text{OD}$ )  $\delta$  8.26 (d,  $J = 10.9$  Hz, 1H), 7.99 (s, 1H), 7.89 (d,  $J = 8.8$  Hz, 1H), 7.75 (d,  $J = 15.8$  Hz, 1H), 6.68 (d,  $J = 15.8$  Hz, 1H), 4.79 (s, 2H), 3.57 (s, 2H), 3.05 (s, 6H), 1.23 (s, 6H), 1.15 (s, 9H);  $^{13}\text{C}$  NMR ( $\text{CD}_3\text{OD}$ )  $\delta$  165.5, 155.3, 140.0, 135.6, 135.0, 132.0, 126.4, 120.7, 116.6, 114.5, 68.6, 53.6, 40.1, 39.7, 35.8, 27.9, 23.9. Anal. ( $\text{C}_{22}\text{H}_{34}\text{N}_4\text{O}_2 \cdot 2.4\text{HCl} \cdot 2.3\text{H}_2\text{O}$ ) C, H, N, Cl.

**(E)-3-[1-(2-Diethylaminoethyl)-2-(2,2-dimethylpropyl)-1H-benzimidazol-5-yl]-N-hydroxyacrylamide (10g).** 10g was prepared according to procedures B and C but using 7b as starting material and was obtained as the bis-TFA salt (50 mg, 28% in two steps). LC–MS  $m/z$  373.1 ( $[\text{M} + \text{H}]^+$ ).  $^1\text{H}$  NMR ( $\text{CD}_3\text{OD}$ )  $\delta$  7.95 (m, 2H), 7.86 (d,  $J = 8.8$  Hz, 1H), 7.72 (d,  $J = 15.8$  Hz, 1H), 6.62 (d,  $J = 15.8$  Hz, 1H), 5.03 (m, 2H), 3.64 (t,  $J = 8.1$  Hz, 2H), 3.42 (q,  $J = 7.3$  Hz, 4H), 3.20 (s, 2H), 1.40 (t,  $J = 7.3$  Hz, 6H), 1.16 (s, 9H);  $^{13}\text{C}$  NMR ( $\text{CD}_3\text{OD}$ )  $\delta$  165.7, 155.3, 140.2, 135.1, 134.6, 133.9, 126.5, 120.3, 115.5, 113.8, 50.2, 41.1, 39.4, 34.9, 29.8, 9.0.

**(E)-3-[2-Butyl-1-(2-dimethylaminoethyl)-1H-benzimidazol-5-yl]-N-hydroxyacrylamide (10h).** 10h was prepared according to procedures B and C but using 7f as starting material and was obtained as the bis-TFA salt. LC–MS  $m/z$  331.1 ( $[\text{M} + \text{H}]^+$ ).  $^1\text{H}$  NMR (DMSO- $d_6$ )  $\delta$  10.68 (br s, 2H), 7.97 (s, 1H), 7.93 (d,  $J = 8.6$  Hz, 1H), 7.71 (d,  $J = 8.6$  Hz, 1H), 7.62 (d,  $J = 15.7$  Hz, 1H), 6.57 (d,  $J = 15.7$  Hz, 1H), 4.74 (t,  $J = 7.6$  Hz, 2H), 3.54 (t,  $J = 7.6$  Hz, 2H), 3.09 (t,  $J = 7.72$  Hz, 2H), 1.83 (quintet,  $J = 7.4$  Hz, 2H), 1.46 (sextet,  $J = 7.5$  Hz, 2H), 0.97 (t,  $J = 7.3$  Hz, 3H);  $^{13}\text{C}$  NMR (DMSO- $d_6$ )  $\delta$  162.6, 156.1, 138.0, 133.3, 131.7, 123.4, 119.2, 115.0, 112.1, 53.4, 42.6, 28.2, 25.2, 21.7, 13.6.

**(E)-3-[2-Butyl-1-(3-methylbutyl)-1H-benzimidazol-5-yl]-N-hydroxyacrylamide (10i).** 10i was prepared according to procedures B and C but using 7k as starting material and was obtained as the TFA salt (10 mg, 3.3% in two steps). LC–MS  $m/z$  330.1 ( $[\text{M} + \text{H}]^+$ ).  $^1\text{H}$  NMR (DMSO- $d_6$ )  $\delta$  10.79 (br s, 1H), 7.91 (s, 1H), 7.84 (d,  $J = 8.6$  Hz, 1H), 7.71 (d,  $J = 8.6$  Hz, 1H), 7.65 (d,  $J = 15.8$  Hz, 1H), 6.55 (d,  $J = 15.8$  Hz, 1H), 4.37 (t,  $J = 7.8$  Hz, 2H), 3.10 (t,  $J = 7.7$  Hz, 2H), 1.82 (quintet,  $J = 7.7$  Hz, 2H), 1.72 (septet or m,  $J = 6.5$  Hz, 1H,  $\text{Me}_2\text{CH}$ ), 1.65 (q or dt-like,  $J = 8.0$  Hz, 2H), 1.45 (sextet,  $J = 7.5$  Hz, 2H), 0.98 (d,  $J = 6.4$  Hz, 6H,  $\text{Me}_2\text{CH}$ ), 0.96 (t,  $J = 7.3$  Hz, 3H).

**(E)-3-[1-(3-Dimethylamino-2,2-dimethylpropyl)-2-isopropyl-1H-benzimidazol-5-yl]-N-hydroxyacrylamide (10j).** 10j was prepared according to procedures B and C but using 7a as starting material and was obtained as the bis-TFA salt. LC–MS  $m/z$  359.2 ( $[\text{M} + \text{H}]^+$ ).  $^1\text{H}$  NMR (DMSO- $d_6$ )  $\delta$  10.80 (br s, 1H), 9.71 (br s, 1H), 7.95 (d,  $J = 8.7$  Hz, 1H), 7.90 (s, 1H), 7.66 (d,  $J = 8.7$  Hz, 1H), 7.63 (d,  $J = 15.8$  Hz, 1H), 6.55 (d,  $J = 15.8$  Hz, 1H), 4.44 (s, 2H), 3.58 (septet,  $J = 6.8$  Hz, 1H,  $\text{Me}_2\text{CH}$ ), 3.36 (s, 2H), 2.92 (s, 6H,  $\text{Me}_2\text{N}$ ), 1.40 (d,  $J = 6.4$  Hz, 6H,  $\text{Me}_2\text{CH}$ ), 1.05 (s, 6H,  $\text{Me}_2\text{C}$ ).

**(E)-3-[2-Cyclohexyl-1-(3-dimethylamino-2,2-dimethylpropyl)-1H-benzimidazol-5-yl]-N-hydroxyacrylamide (10k).** 10k was prepared according to procedures B and C but using 7a as starting material and was obtained as the bis-TFA salt. LC–MS  $m/z$  399.1 ( $[\text{M} + \text{H}]^+$ ).  $^1\text{H}$  NMR ( $\text{CD}_3\text{OD}$ )  $\delta$  8.06 (d,  $J = 8.8$  Hz, 1H), 7.91 (s, 1H), 7.80 (d,  $J = 8.8$  Hz, 1H), 7.68 (d,  $J = 15.8$  Hz, 1H), 6.61 (d,  $J = 15.8$  Hz, 1H), 4.64 (s, 2H), 3.50 (s, 2H), 3.39 (m, 1H), 3.07 (s, 6H), 2.12 (d,  $J = 12.0$  Hz, 2H), 1.96 (d,  $J = 13.0$  Hz, 2H), 1.87 (d,  $J = 12.8$  Hz, 1H), 1.79 (q-like,  $J = 10.7$  Hz, 2H), 1.58 (q-like,  $J = 12.9$  Hz, 2H), 1.47 (t-like,  $J = 12.6$  Hz, 1H), 1.26 (s, 6H);  $^{13}\text{C}$  NMR ( $\text{CD}_3\text{OD}$ )  $\delta$  165.7, 161.3, 140.1, 135.4, 134.8, 134.0, 126.1, 120.3, 115.5, 114.9, 68.7, 53.1, 47.9, 39.2, 37.0, 32.4, 26.5, 26.3, 23.6 (TFA peaks at 119.6, 116.7).

(E)-3-[1-(2-Diethylaminoethyl)-2-propyl-1H-benzimidazol-5-yl]-N-hydroxyacrylamide (**10l**). **10l** was prepared according to procedures B and C but using **7b** as starting material and was obtained as the bis-TFA salt (31 mg, 8.2% in two steps). LC–MS  $m/z$  345.1 ( $[M + H]^+$ ).  $^1H$  NMR ( $CD_3OD$ )  $\delta$  8.15 (d,  $J = 8.7$  Hz, 1H), 7.94 (s, 1H), 7.89 (d,  $J = 8.3$  Hz, 1H), 7.68 (d,  $J = 15.8$  Hz, 1H), 6.63 (d,  $J = 15.8$  Hz, 1H), 5.08 (t,  $J = 7.7$  Hz, 2H), 3.70 (t,  $J = 7.7$  Hz, 2H), 3.44 (m, 4H), 3.35 (t,  $J = 6.3$  Hz, 2H), 2.03 (sextet,  $J = 7.9$  Hz, 2H), 1.44 (t,  $J = 7.2$  Hz, 6H), 1.20 (t,  $J = 7.3$  Hz, 3H);  $^{13}C$  NMR ( $CD_3OD$ )  $\delta$  165.5, 157.4, 139.8, 135.5, 133.5, 132.3, 126.8, 120.7, 114.5, 114.3, 50.0, 40.8, 28.5, 21.0, 13.9, 9.1.

(E)-3-[1-(2-Diethylaminoethyl)-2-hexyl-1H-benzimidazol-5-yl]-N-hydroxyacrylamide (**10m**). **10m** was prepared according to procedures B and C but using **7b** as starting material and was obtained as the bis-TFA salt. LC–MS  $m/z$  387.16 ( $[M + H]^+$ ).  $^1H$  NMR ( $DMSO-d_6$ )  $\delta$  10.60 (br s, 2H), 7.94 (s, 1H), 7.93 (d,  $J = 8.8$  Hz, 1H), 7.73 (d,  $J = 8.8$  Hz, 1H), 7.63 (d,  $J = 15.8$  Hz, 1H), 6.59 (d,  $J = 15.8$  Hz, 1H), 4.81 (t,  $J = 7.7$  Hz, 2H), 3.51 (t,  $J = 7.7$  Hz, 2H), 3.31 (m, 4H), 3.12 (t,  $J = 7.7$  Hz, 2H), 1.85 (quintet,  $J = 7.6$  Hz, 2H), 1.44 (m, 2H), 1.37–1.30 (m, 4H), 1.26 (t,  $J = 7.2$  Hz, 6H), 0.88 (t,  $J = 7.0$  Hz, 3H);  $^{13}C$  NMR ( $DMSO-d_6$ )  $\delta$  162.6, 156.2, 137.9, 134.7, 133.1, 131.9, 123.7, 119.4, 114.7, 112.2, 48.6, 46.7, 38.6, 30.8, 28.2, 26.1, 25.4, 21.9, 13.8, 8.5 (TFA peaks at 159.1, 158.8, 158.4, 158.1, 117.8).

(E)-3-[2-Butyl-1-(2-ethylaminoethyl)-1H-benzimidazol-5-yl]-N-hydroxyacrylamide (**10n**). **10n** was prepared according to procedures B and D but using **7c** as starting material and was obtained as the hydrochloride salt, light pinkish solid (0.98 g, 24% in three steps). LC–MS  $m/z$  331.2 ( $[M + H]^+$ ).  $^1H$  NMR ( $DMSO-d_6$ )  $\delta$  10.94 (br s, 0.8H), 9.85 (br s, 2H,  $-NH_2^+ - Et$ ), 8.13 (d,  $J = 8.6$  Hz, 1H), 7.97 (s, 1H), 7.78 (d,  $J = 8.5$  Hz, 1H), 7.64 (d,  $J = 15.8$  Hz, 1H), 6.65 (d,  $J = 15.8$  Hz, 1H), 4.88 (t,  $J = 5.9$  Hz, 2H), 3.37 (m, 2H), 3.29 (t,  $J = 7.7$  Hz, 2H), 2.96 (m, 2H), 1.86 (quintet,  $J = 7.6$  Hz, 2H), 1.47 (sextet,  $J = 7.5$  Hz, 2H), 1.21 (t,  $J = 7.2$  Hz, 3H), 0.95 (t,  $J = 7.0$  Hz, 3H,  $-(CH_2)_3CH_3$ );  $^{13}C$  NMR ( $DMSO-d_6$ )  $\delta$  162.4, 156.1, 137.4, 132.8, 132.7, 131.9 (br), 124.6, 120.3, 113.2, 112.9, 44.5, 42.2, 41.1, 28.2, 25.2, 21.7, 13.6, 10.8. HRMS (ESI)  $m/z$   $[M + H]^+$  calcd for  $C_{18}H_{27}N_4O_2$ , 331.2129; found, 331.2131.

(E)-3-[1-(2-Ethylaminoethyl)-2-pentyl-1H-benzimidazol-5-yl]-N-hydroxyacrylamide (**10o**). **10o** was prepared according to procedures B and C but using **7b** as starting material and was obtained as the bis-TFA salt (30 mg, 5.3% in two steps). LC–MS  $m/z$  345.2 ( $[M + H]^+$ ).  $^1H$  NMR ( $CD_3OD$ )  $\delta$  7.87 (d,  $J = 8.6$  Hz, 1H), 7.81 (s, 1H), 7.75 (d,  $J = 8.6$  Hz, 1H), 7.45 (d,  $J = 15.7$  Hz, 1H), 6.44 (d,  $J = 15.7$  Hz, 1H), 4.79 (t,  $J = 6.5$  Hz, 2H), 3.62 (t,  $J = 6.4$  Hz, 2H), 3.21 (t,  $J = 7.2$  Hz, 2H), 3.18 (q,  $J = 7.2$  Hz, 2H), 1.95 (quintet,  $J = 7.6$  Hz, 2H), 1.55–1.43 (m, 4H), 1.34 (t,  $J = 7.3$  Hz, 3H), 0.98 (t,  $J = 7.1$  Hz, 3H);  $^{13}C$  NMR ( $CD_3OD$ )  $\delta$  165.7, 157.8, 140.5, 135.1, 134.7, 134.3, 126.2, 119.2, 115.8, 113.3, 46.3, 45.0, 42.4, 32.5, 27.3, 27.0, 23.3, 14.2, 11.5.

(E)-3-[2-Hexyl-1-(2-isopropylaminoethyl)-1H-benzimidazol-5-yl]-N-hydroxyacrylamide (**10q**). **10q** was prepared according to procedures B and C but using **7d** as starting material and was obtained as the bis-TFA salt (11.2 mg, 2.5% in two steps). LC–MS  $m/z$  373.1 ( $[M + H]^+$ ).  $^1H$  NMR ( $CD_3OD$ )  $\delta$  7.85 (m, 2H), 7.74 (s, 1H), 7.57 (br d, 1H), 6.52 (br d, 1H), 4.76 (d,  $J = 6.6$  Hz, 2H), 3.58 (d,  $J = 6.6$  Hz, 2H), 3.48 (m,  $J = 6.5$  Hz, 1H), 3.18 (t,  $J = 5.9$  Hz, 2H), 1.94 (m, 2H), 1.55 (m, 2H), 1.47–1.37 (m, 4H), 1.37 (d,  $J = 6.5$  Hz, 6H), 0.84 (d,  $J = 7.0$  Hz, 3H).

(E)-3-[2-Butyl-1-(2-diisopropylaminoethyl)-1H-benzimidazol-5-yl]-N-hydroxyacrylamide (**10r**). **10r** was prepared according to procedures B and C but using **7e** as starting material and was obtained as the bis-TFA salt (30 mg, 9.8% in two steps). LC–MS  $m/z$  387.1 ( $[M + H]^+$ ).  $^1H$  NMR ( $DMSO-d_6$ )  $\delta$  10.73 (s, 1H), 9.08 (s, 1H), 7.84 (s, 1H), 7.62–7.57 (m, 2H), 7.60 (d,  $J = 15.7$  Hz, 1H), 6.47 (d,  $J = 15.7$  Hz, 2H), 4.61 (br t-like, 2H), 3.80 (m, 2H), 3.40 (masked by solvent peak, 2H), 2.96 (t,  $J = 7.2$  Hz, 2H), 1.85 (quintet,  $J = 7.5$  Hz, 2H), 1.47 (sextet,  $J = 7.4$  Hz, 2H), 1.37 (d,  $J = 6.0$  Hz, 6H), 1.34 (d,  $J = 6.2$  Hz, 6H), 0.97 (t,  $J = 7.4$  Hz, 3H).

(E)-3-[1-(2-Dimethylaminoethyl)-2-hexyl-1H-benzimidazol-5-yl]-N-hydroxyacrylamide (**10s**). **10s** was prepared according to procedures B and D but using **7f** as starting material and was obtained as the hydrochloride salt, pinkish solid (3.09 g, 26% in three steps). LC–MS  $m/z$  359.2 ( $[M + H]^+$ ).  $^1H$  NMR ( $CD_3OD$ )  $\delta$  8.09 (d,  $J = 8.7$  Hz, 1H), 7.90 (s, 1H), 7.87 (d,  $J = 8.8$  Hz, 1H), 7.63 (d,  $J = 15.8$  Hz, 1H), 6.58 (d,  $J = 15.8$  Hz, 1H), 4.98 (t,  $J = 7.8$  Hz, 2H), 3.71 (t,  $J = 7.8$  Hz, 2H), 3.34 (t,  $J = 10.0$  Hz, 2H), 3.07 (s, 6H), 1.98 (quintet,  $J = 7.8$  Hz, 2H), 1.59 (quintet,  $J = 7.5$  Hz, 2H), 1.50–1.34 (m, 4H), 0.95 (t,  $J = 7.1$  Hz, 3H);  $^{13}C$  NMR ( $CD_3OD$ )  $\delta$  165.5, 157.7, 140.0, 135.5, 133.7, 132.5, 126.8, 120.6, 114.6, 114.2, 54.9, 44.0, 40.9, 32.5, 30.0, 27.4, 26.9, 23.5, 14.3. Anal. ( $C_{20}H_{30}N_4O_2 \cdot 1.9HCl \cdot H_2O$ ) C, H, N, Cl.

(E)-N-Hydroxy-3-[1-(2-methylaminoethyl)-2-pentyl-1H-benzimidazol-5-yl]acrylamide (**10t**). **10t** was prepared according to procedures B and C but using **7g** as starting material and was obtained as the bis-TFA salt (10 mg, 1.8% in two steps). LC–MS  $m/z$  331.2 ( $[M + H]^+$ ).  $^1H$  NMR ( $DMSO-d_6$ )  $\delta$  9.13 (2H, s,  $-NH_2^+ - CH_3$ ), 7.94 (d,  $J = 8.1$  Hz, 1H), 7.93 (s, 1H), 7.73 (d,  $J = 8.8$  Hz, 1H), 7.64 (d,  $J = 15.8$  Hz, 1H), 6.58 (d,  $J = 15.8$  Hz, 1H), 4.71 (t,  $J = 6.3$  Hz, 2H), 3.38 (t-like, 2H), 3.13 (t,  $J = 7.8$  Hz, 2H), 2.61 (t,  $J = 4.6$  Hz, 3H,  $-NH_2^+ - CH_3$ ), 1.84 (sextet,  $J = 7.7$  Hz, 2H), 1.48–1.35 (m, 4H), 0.92 (t,  $J = 7.1$  Hz, 3H).

(E)-3-[2-Hexyl-1-(2-methylaminoethyl)-1H-benzimidazol-5-yl]-N-hydroxyacrylamide (**10u**). **10u** was prepared according to procedures B and C but using **7g** as starting material and was obtained as the bis-TFA salt (10 mg, yield 3.4% in two steps). LC–MS  $m/z$  345.2 ( $[M + H]^+$ ).  $^1H$  NMR ( $CD_3OD$ )  $\delta$  7.87 (s, 2H), 7.8 (d,  $J = 8.6$  Hz, 1H), 7.60 (d,  $J = 15.7$  Hz, 1H), 6.53 (d,  $J = 15.7$  Hz, 1H), 4.81 (overlapped with solvent, 2H), 3.59 (m, 2H), 3.18 (t,  $J = 7.8$  Hz, 2H), 2.81 (s, 3H), 1.95 (m, 2H), 1.56 (m, 2H), 1.49–1.35 (m, 4H), 0.95 (t,  $J = 7.1$  Hz, 3H);  $^{13}C$  NMR ( $CD_3OD$ )  $\delta$  140.5, 134.7, 126.2, 119.6, 115.7, 113.2, 42.2, 34.2, 32.5, 30.0, 27.6, 27.1, 23.5, 14.3.

(E)-N-Hydroxy-3-[1-(2-methylaminoethyl)-2-octyl-1H-benzimidazol-5-yl]acrylamide (**10v**). **10v** was prepared according to procedures B and C but using **7f** as starting material and was obtained as the bis-TFA salt. LC–MS  $m/z$  373.2 ( $[M + H]^+$ ).  $^1H$  NMR ( $CD_3OD$ )  $\delta$  7.91 (d,  $J = 8.4$  Hz, 1H), 7.80 (s, 1H), 7.76 (d,  $J = 8.6$  Hz, 1H), 7.38 (d,  $J = 15.7$  Hz, 1H), 6.42 (d,  $J = 15.7$  Hz, 1H), 4.84 (overlapped with solvent, 2H), 3.64 (t-like, 2H), 3.24 (t,  $J = 7.8$  Hz, 2H), 2.81 (s, 3H), 1.96 (m, 2H), 1.54 (m, 2H), 1.46–1.32 (m, 8H), 0.91 (t,  $J = 6.6$  Hz, 3H);  $^{13}C$  NMR ( $CD_3OD$ )  $\delta$  165.7, 157.8, 140.4, 134.5, 126.3, 119.2, 115.6, 113.6, 48.3, 42.5, 34.3, 32.9, 30.33, 30.27, 30.23, 27.5, 27.0, 23.7, 14.4 (TFA peaks at 163.0, 162.7).

(E)-N-Hydroxy-3-[1-(2-aminoethyl)-2-octyl-1H-benzimidazol-5-yl]acrylamide (**10w**). Boc protected **9w** was prepared according to procedure B using **7i** as starting material. Then it was deprotected (concentrated HCl in HOAc, 70 °C) to afford **9w1**, which was further converted to the bis-TFA salt of **10w** according to procedure C. LC–MS  $m/z$  359.2 ( $[M + H]^+$ ).  $^1H$  NMR ( $CD_3OD$ )  $\delta$  7.90 (d,  $J = 8.5$  Hz, 1H), 7.85 (s, 1H), 7.78 (d,  $J = 8.6$  Hz, 1H), 7.49 (d,  $J = 15.6$  Hz, 1H), 6.49 (d,  $J = 15.7$  Hz, 1H), 4.78 (t,  $J = 6.3$  Hz, 2H), 3.56 (t,  $J = 6.3$  Hz, 2H), 3.23 (t,  $J = 8.3$  Hz, 2H), 1.95 (m, 2H), 1.55 (m, 2H), 1.47–1.30 (m, 8H), 0.91 (t,  $J = 6.9$  Hz, 3H);  $^{13}C$  NMR ( $CD_3OD$ )  $\delta$  165.7, 157.8, 140.3, 134.6, 134.5, 126.4, 119.6, 115.5, 113.4, 43.2, 39.1, 32.9, 30.34, 30.28, 30.23, 27.6, 27.0, 23.7, 14.4 (TFA peaks at 163.0, 162.6).

(E)-3-[1-(2-Ethylaminoethyl)-2-(Z)-hex-3-enyl]-1H-benzimidazol-5-yl]-N-hydroxyacrylamide (**10x**). **10x** was prepared according to procedures B and D but using **7c** as starting material and was obtained as the hydrochloride salt (82 mg, 1.8% in three steps). LC–MS  $m/z$  357.1 ( $[M + H]^+$ ).  $^1H$  NMR ( $CD_3OD$ )  $\delta$  8.08 (d,  $J = 8.0$  Hz, 1H), 7.87 (s, 1H), 7.83 (d,  $J = 8.1$  Hz, 1H), 7.35 (d,  $J = 15.7$  Hz, 1H), 6.47 (d,  $J = 15.7$  Hz, 1H), 5.57 (dt,  $J = 10.7, 7.1$  Hz, 1H), 5.55 (dt,  $J = 10.7, 7.1$  Hz, 1H), 4.90 (masked peaks, 2H), 3.66 (t-like, 2H), 3.42 (t,  $J = 7.4$  Hz, 2H), 3.20 (q-like,  $J = 7.0$  Hz, 2H), 2.75 (q-like,  $J = 7.0$  Hz, 2H), 2.05 (quintet,  $J = 7.2$  Hz, 2H), 1.38 (t,  $J = 6.9$  Hz, 3H), 0.89 (t,  $J = 7.5$  Hz, 3H);

$^{13}\text{C}$  NMR ( $\text{CD}_3\text{OD}$ )  $\delta$  165.4, 157.1, 140.0, 136.2, 135.2, 133.9, 132.6, 127.0, 125.8, 119.8, 114.9, 114.4, 46.4, 45.1, 42.9, 27.1, 25.3, 21.5, 14.4, 11.6.

**(E)-N-Hydroxy-3-[1-(2-isopropylaminoethyl)-2-pentyl-1H-benzimidazol-5-yl]acrylamide (10y).** 10y was prepared according to procedures B and D but using 7d as starting material and was obtained as the hydrochloride salt, light pinkish solid (1.4 g, 20% in three steps). LC-MS  $m/z$  359.2 ( $[\text{M} + \text{H}]^+$ ).  $^1\text{H}$  NMR ( $\text{CD}_3\text{OD}$ )  $\delta$  9.27 (residual proton after exchange, 0.16 H), 8.09 (d,  $J = 8.4$  Hz, 1H), 7.85 (s, 1H), 7.80 (d,  $J = 8.2$  Hz, 1H), 7.34 (d,  $J = 15.7$  Hz, 1H), 6.46 (d,  $J = 15.8$  Hz, 1H), 4.93 (overlapped with solvent peak, 2H), 3.65 (t-like, 2H), 3.51 (septet,  $J = 6.3$  Hz, 1H), 3.36 (t,  $J = 7.8$  Hz, 2H), 1.99 (quintet,  $J = 7.2$  Hz, 2H), 1.56 (m, 2H), 1.49 (m, 2H), 1.42 (t,  $J = 6.4$  Hz, 6H), 0.98 (t,  $J = 7.2$  Hz, 3H);  $^{13}\text{C}$  NMR ( $\text{CD}_3\text{OD}$ )  $\delta$  165.3, 157.7, 140.0, 135.0, 133.9, 132.5, 127.0, 119.7, 114.8, 114.3, 53.3, 44.0, 42.8, 32.4, 27.1, 27.0, 23.3, 19.2, 14.2.

**(E)-3-[1-(3-Dimethylamino-2,2-dimethylpropyl)-2-(Z)-hex-3-enyl]-1H-benzimidazol-5-yl]-N-hydroxyacrylamide (10z).** 10z was prepared according to procedures B and C but using 7a as starting material and was obtained as the bis-TFA salt. LC-MS  $m/z$  399.1 ( $[\text{M} + \text{H}]^+$ ).  $^1\text{H}$  NMR ( $\text{CD}_3\text{OD}$ )  $\delta$  8.05 (d,  $J = 8.7$  Hz, 1H), 7.93 (s, 1H), 7.79 (d,  $J = 8.63$  Hz, 1H), 7.64 (d,  $J = 15.8$  Hz, 1H), 6.51 (d,  $J = 15.8$  Hz, 1H), 5.53–5.40 (m, 2H), 4.61 (s, 2H), 3.48 (s, 2H), 3.37 (t,  $J = 7.3$  Hz, 2H), 3.06 (s, 6H), 2.74 (q,  $J = 6.8$  Hz, 2H), 2.00 (quintet,  $J = 7.3$  Hz, 2H), 1.26 (s, 6H), 0.84 (t,  $J = 7.5$  Hz, 3H);  $^{13}\text{C}$  NMR ( $\text{CD}_3\text{OD}$ )  $\delta$  165.7, 157.9, 140.2, 135.8, 134.549, 134.458, 126.1, 126.0, 120.0, 115.2, 115.1, 68.7, 53.3, 47.9, 39.6, 27.6, 25.9, 23.7, 21.4, 14.4 (TFA peaks at 163.1, 162.8, 119.6, 116.7).

**(E)-3-[1-(3-Dimethylamino-2,2-dimethylpropyl)-2-(2,4,4-trimethylpentyl)-1H-benzimidazol-5-yl]-N-hydroxyacrylamide (10aa).** 10aa was prepared according to procedures B and C but using 7a as starting material and was obtained as the bis-TFA salt. LC-MS  $m/z$  429.2 ( $[\text{M} + \text{H}]^+$ ).  $^1\text{H}$  NMR ( $\text{CD}_3\text{OD}$ )  $\delta$  8.19 (d,  $J = 8.8$  Hz, 1H), 8.08 (s, 1H), 7.90 (d,  $J = 8.8$  Hz, 1H), 7.76 (d,  $J = 15.7$  Hz, 1H), 6.75 (d,  $J = 15.8$  Hz, 1H), 4.79 (s, 2H), 3.61 (s, 2H), 3.41 (dd,  $J = 10.1$ , 6.5 Hz, 1H), 3.32 (dd,  $J = 15.7$ , 9.0 Hz, 1H), 3.18 (s, 6H,  $\text{Me}_2\text{N}$ ), 2.52 (br s, 1H), 1.50–1.45 (m, 2H), 1.36 (d,  $J = 3.8$  Hz, 6H,  $\text{Me}_2\text{C}$ ), 1.12 (d,  $J = 5.5$  Hz, 3H,  $\text{MeCH}$ ), 1.02 (s, 9H,  $\text{Me}_3\text{C}$ );  $^{13}\text{C}$  NMR ( $\text{CD}_3\text{OD}$ )  $\delta$  165.6, 157.4, 139.9, 135.2, 135.1, 132.9, 126.4, 120.6, 115.7, 114.6, 68.6, 53.3, 51.4, 47.9, 39.7, 36.3, 31.9, 31.3, 30.2, 23.8, 22.3 (TFA peaks at 163.4, 163.0, 162.7, 162.3, 122.4, 119.5, 116.6, and 113.7).

**(E)-3-[1-(2-Ethylaminoethyl)-2-(2,4,4-trimethylpentyl)-1H-benzimidazol-5-yl]-N-hydroxyacrylamide (10ab).** 10ab was prepared according to procedures B and C but using 7c as starting material and was obtained as the bis-TFA salt. LC-MS  $m/z$  387.15 ( $[\text{M} + \text{H}]^+$ ).  $^1\text{H}$  NMR ( $\text{CD}_3\text{OD}$ )  $\delta$  7.96 (d,  $J = 8.6$  Hz, 1H), 7.79 (s, 1H), 7.78–7.75 (d,  $J = 8.7$  Hz, 1H), 7.23 (d,  $J = 15.7$  Hz, 1H), 6.37 (d,  $J = 15.7$  Hz, 1H), 4.92 (masked peaks, 2H), 3.70 (m, 2H), 3.36–3.28 (masked peak, 1H), 3.26–3.14 (m, 3H), 2.31 (m, 1H), 1.44–1.27 (m, 2H), 1.35 (t,  $J = 7.2$  Hz, 3H), 1.07 (d,  $J = 6.6$  Hz, 3H,  $\text{MeCH}$ ), 0.92 (s, 9H,  $\text{Me}_3\text{C}$ );  $^{13}\text{C}$  NMR ( $\text{CD}_3\text{OD}$ )  $\delta$  165.6, 156.9, 140.6, 134.9, 134.5, 134.2, 126.2, 118.7, 116.0, 113.7, 51.6, 46.5, 45.0, 42.7, 35.8, 31.9, 30.8, 30.2, 22.6, 11.4 (TFA peaks at 163.4 and 163.0).

**Representative Procedures for Compounds 11 (Procedure E). Preparation of (E)-3-[3-Amino-4-(2-diethylaminoethylamino)phenyl]acrylic Acid Methyl Ester (11b).** To a prestirred solution of 7b (3.21 g, 10.0 mmol) in MeOH/HOAc (3:1, 50 mL),  $\text{SnCl}_2 \cdot 2\text{H}_2\text{O}$  was added (9.45 g, 41.9 mmol). The resulting solution was heated at 45 °C overnight. Then the solvent was removed under vacuum. The residue was basified and extracted with DCM and purified by flash chromatography (silica, 0–10% MeOH in DCM) to afford 11b (2.30 g, 79%). LC-MS  $m/z$  292.2 ( $[\text{M} + \text{H}]^+$ ).

**Representative Procedures for Synthesis of Compounds 15 (Procedure F). (E)-3-[1-(2-Diethylaminoethyl)-2-(2-phenylcyclopropyl)-1H-benzimidazol-5-yl]-N-hydroxyacrylamide (15b).** To a prestirred solution of *trans*-2-phenylcyclopropanecarboxylic

acid (145 mg, 0.896 mmol) in DCM (7 mL) was added a coupling cocktail solution containing EDCl (0.288 g, 1.50 mmol), HOBT hydrate (0.230 g, 1.50 mmol), DIEA (0.26 mL, 1.50 mmol), and DCM (7 mL). After the mixture was stirred for 0.5 h, aniline 11b (0.200 g, 0.686 mmol) was added and stirred until the reaction was completed. The usual workup afforded crude amide 13b which was added to acetic acid (5 mL) and heated at 90 °C overnight. When the reaction was completed, the mixture was concentrated to dryness, diluted with DCM, washed with  $\text{NaHCO}_3$ , and dried over  $\text{Na}_2\text{SO}_4$ . The mixture was filtered and concentrated, and the resulting crude was purified by flash chromatography (silica, 50–100% EtOAc in hexanes with 1%  $\text{Et}_3\text{N}$ ) to afford methyl ester 14b (120 mg, 42%) which was converted to hydroxamic acid 15b as bis-TFA salt (30 mg, 16%) according to procedure C. LC-MS  $m/z$  419.1 ( $[\text{M} + \text{H}]^+$ ).  $^1\text{H}$  NMR ( $\text{CD}_3\text{OD}$ )  $\delta$  7.89 (d,  $J = 8.7$  Hz, 1H), 7.83 (s, 1H), 7.75 (d,  $J = 8.8$  Hz, 1H), 7.54 (d,  $J = 15.8$  Hz, 1H), 7.40–7.27 (m, 5H), 6.49 (d,  $J = 15.8$  Hz, 1H), 4.97 (overlapped with solvent peak, 2H), 3.71 (m, 1H), 3.63 (m, 1H), 3.49 (m, 1H), 3.22 (m, 4H), 2.90 (m, 1H), 2.84 (m, 1H), 2.16 (m, 1H), 2.05 (m, 1H), 1.18 (t,  $J = 7.2$  Hz, 6H).  $^{13}\text{C}$  NMR ( $\text{CD}_3\text{OD}$ )  $\delta$  165.9, 157.4, 140.8, 140.4, 137.1, 135.5, 133.7, 130.0, 128.3, 127.1, 125.7, 118.9, 116.4, 112.4, 50.4, 48.7, 39.9, 24.5, 19.5, 17.9 ( $\text{CH}_2$ ), 8.8 (TFA peaks at 163.2, 162.9, 162.5, and 162.2).

**(E)-3-[2-(2-Diethylaminoethyl)-1-(3-methylbutyl)-1H-benzimidazol-5-yl]-N-hydroxyacrylamide (15a).** 15a was prepared according to the procedures described for compound 15b but using diamine 11k and 3-diethylaminopropionic acid hydrochloride as starting materials and was obtained as the bis-TFA salt (30 mg, 6.9% from 11k in three steps). LC-MS  $m/z$  373.4 ( $[\text{M} + \text{H}]^+$ ).  $^1\text{H}$  NMR ( $\text{DMSO}-d_6$ )  $\delta$  9.87 (br s, 1H), 7.85 (s, 1H), 7.67 (d,  $J = 8.5$  Hz, 1H), 7.60 (d,  $J = 15.3$  Hz, 1H), 7.57 (d,  $J = 6.7$  Hz, 1H), 6.49 (d,  $J = 15.8$  Hz, 1H), 4.28 (t,  $J = 7.6$  Hz, 2H), 3.68 (t,  $J = 7.5$  Hz, 2H), 3.43 (t,  $J = 7.6$  Hz, 2H), 3.28 (q,  $J = 7.3$  Hz, 4H), 1.69–1.61 (m, 3H), 1.28 (t,  $J = 7.2$  Hz, 6H), 0.98 (d,  $J = 6.4$  Hz, 6H);  $^{13}\text{C}$  NMR ( $\text{DMSO}-d_6$ )  $\delta$  162.9, 151.9, 139.8, 138.9, 135.1, 129.7, 122.1, 117.7, 117.4, 111.1, 48.0, 46.6, 41.9, 37.9, 25.4, 22.3, 21.2, 8.5 (TFA peaks at 158.5, 158.1, 117.4, and 114.5).

**(E)-3-[1-(2-Dimethylaminoethyl)-2-(2-phenylcyclopropyl)-1H-benzimidazol-5-yl]-N-hydroxyacrylamide (15c).** 15c was prepared according to the procedure described for compound 15b but using diamine 11c (37% from 7f) as starting material and was obtained as bis-TFA salt (25 mg, 5.3% in three steps from 11c). LC-MS  $m/z$  391.1 ( $[\text{M} + \text{H}]^+$ ).  $^1\text{H}$  NMR ( $\text{DMSO}-d_6$ )  $\delta$  10.80 (br s, 1H), 10.21 (br s, 1H), 7.84 (s, 1H), 7.77 (d,  $J = 7.5$  Hz, 1H), 7.615 (d,  $J = 10.7$  Hz, 1H), 7.609 (d,  $J = 15.2$  Hz, 1H), 7.37–7.31 (m, 4H), 7.26 (m, 1H), 6.52 (d,  $J = 15.8$  Hz, 1H), 4.77 (m, 2H), 3.55–3.40 (m, 2H), 2.81 (s, 6H), 2.85–2.72 (m, 2H), 1.89 (m, 1H), 1.76 (m, 1H).

**(E)-3-[1-(2-Aminoethyl)-2-(2-phenylcyclopropyl)-1H-benzimidazol-5-yl]-N-hydroxyacrylamide (15d).** 15d was prepared according to the procedure described for compound 15b but using diamine 11i (78% from 7i) as starting material. Amide 13d (126.0 mg, 75% from 7i) was cyclized to 14d, and then the Boc group was removed with HCl to give 14d1 (104 mg, 91% as hydrochloride salt), which was further converted to 15d as the bis-TFA salt (14 mg, 10%) according to procedure C. LC-MS  $m/z$  363.1 ( $[\text{M} + \text{H}]^+$ ).  $^1\text{H}$  NMR ( $\text{CD}_3\text{OD}$ )  $\delta$  7.82 (s, 1H), 7.75 (d,  $J = 8.6$  Hz, 1H), 7.70 (d,  $J = 8.5$  Hz, 1H), 7.60 (d,  $J = 15.8$  Hz, 2H), 7.37–7.30 (m, 4H), 7.28–7.23 (m, 1H), 4.76 (m, 2H), 3.45 (t,  $J = 6.6$  Hz, 2H), 2.89 (m, 1H), 2.67 (m, 1H), 2.03 (m, 1H), 1.95 (m, 1H);  $^{13}\text{C}$  NMR ( $\text{CD}_3\text{OD}$ )  $\delta$  165.9, 157.7, 140.8, 140.2, 137.2, 135.7, 133.6, 129.8 ( $\text{CH} \times 2$ ), 128.1, 127.2 ( $\text{CH} \times 2$ ), 125.6, 118.8, 116.2, 112.2, 42.7, 39.3, 29.3, 19.0, 18.5 (TFA peaks at 162.6, 162.3)

**(E)-3-[2-Bicyclo[2.2.1]hept-2-ylmethyl-1-(2-diethylaminoethyl)-1H-benzimidazol-5-yl]-N-hydroxyacrylamide (15e).** 15e was prepared according to a similar procedure used for 15b and was obtained as the bis-TFA salt (30 mg, 7.2% in three steps from 11b). LC-MS  $m/z$  411.2 ( $[\text{M} + \text{H}]^+$ ).  $^1\text{H}$  NMR ( $\text{DMSO}-d_6$ )  $\delta$  10.36 (br s, 1H), 7.93 (s, 1H), 7.87 (d,  $J = 8.6$  Hz, 1H), 7.71 (d,  $J = 8.5$  Hz, 1H), 7.63

(d,  $J = 15.8$  Hz, 1H), 6.56 (d,  $J = 15.8$  Hz, 1H), 4.77 (t,  $J = 7.8$  Hz, 2H), 3.49 (t,  $J = 7.6$  Hz, 2H), 3.31 (m, 4H), 3.06 (dd,  $J = 16.0$  and  $7.9$  Hz, 1H), 3.06 (dd,  $J = 16.0$  and  $7.6$  Hz, 1H), 2.25 (m, 1H), 2.15–2.05 (m, 2H), 1.57–1.42 (m, 4H), 1.25 (t,  $J = 7.2$  Hz, 6H), 1.27–1.10 (m, 4H).

**(E)-3-{2-Butyl-1-[2-(isopropylmethylamino)ethyl]-1H-benzimidazol-5-yl]-N-hydroxyacrylamide (17c).** A solution of 3-[2-butyl-1-(2-isopropylaminoethyl)-1H-benzimidazol-5-yl]acrylic acid methyl ester **9e** (170 mg, 0.495 mmol), formaldehyde (37%, 0.10 mL, 1.34 mmol), NaBH(OAc)<sub>3</sub> (159 mg, 0.75 mmol), and HOAc (36 mg, 0.60 mmol) in MeOH was stirred at room temperature until depletion of **9e**. After base workup, **16c** (170 mg, 96% from **9e**) was converted to **17c** as the bis-TFA salt (20 mg, 7.2%) according to procedure C. LC–MS  $m/z$  359.2 ( $[M + H]^+$ ). <sup>1</sup>H NMR (CD<sub>3</sub>OD)  $\delta$  7.97 (d,  $J = 8.7$  Hz, 1H), 7.89 (s, 1H), 7.82 (d,  $J = 8.6$  Hz, 1H), 7.63 (d,  $J = 15.8$  Hz, 1H), 6.56 (d,  $J = 15.8$  Hz, 1H), 4.93 (t,  $J = 8.1$  Hz, 2H), 3.80 (septet,  $J = 6.6$  Hz, 1H), 3.64 (t,  $J = 7.9$  Hz, 2H), 3.26 (t,  $J = 7.9$  Hz, 2H), 2.99 (s, 3H), 1.94 (quintet,  $J = 6.3$  Hz, 2H), 1.58 (septet,  $J = 7.6$  Hz, 2H), 1.39 (d,  $J = 6.6$  Hz, 6H), 1.06 (t,  $J = 7.3$  Hz, 3H). <sup>13</sup>C NMR (CD<sub>3</sub>OD)  $\delta$  165.6, 157.7, 140.2, 134.9, 134.1, 126.5, 120.1, 115.2, 113.6, 59.9, 40.7, 35.6 (N–Me), 29.5, 26.6, 23.4, 16.6 (identified by HSQC, isopropyl Me  $\times$  2), 14.0 (TFA peaks at 162.8, 162.4).

**(E)-3-{2-Butyl-1-[2-(ethylmethylamino)ethyl]-1H-benzimidazol-5-yl]-N-hydroxyacrylamide (17a).** **17a** was prepared according to the procedure used for **17c** but using **9p** as starting material and was obtained as the bis-TFA salt (20 mg, 20% in two steps). LC–MS  $m/z$  345.2 ( $[M + H]^+$ ). <sup>1</sup>H NMR (DMSO-*d*<sub>6</sub>)  $\delta$  10.59 (br s, 1H), 7.96 (d,  $J = 8.4$  Hz, 1H), 7.95 (s, 1H), 7.75 (d,  $J = 9.2$  Hz, 1H), 7.63 (d,  $J = 15.8$  Hz, 1H), 6.60 (d,  $J = 15.8$  Hz, 1H), 4.80 (t-like, 2H), 3.54 (m, 2H), 3.28 (br, 2H), 3.14 (t,  $J = 7.8$  Hz, 2H), 2.93 (s, 3H), 1.83 (quintet,  $J = 7.7$  Hz, 2H), 1.46 (sextet,  $J = 7.2$  Hz, 2H), 1.25 (t,  $J = 7.2$  Hz, 3H), 0.96 (t,  $J = 7.3$  Hz, 3H).

**(E)-3-{1-[2-(Ethylmethylamino)ethyl]-2-pentyl-1H-benzimidazol-5-yl]-N-hydroxyacrylamide (17b).** **17b** was prepared according to the procedure used for **17c** but using **9q** as starting material and was obtained as the bis-TFA salt (20 mg, 5.3% in two steps). LC–MS  $m/z$  359.2 ( $[M + H]^+$ ). <sup>1</sup>H NMR (DMSO-*d*<sub>6</sub>)  $\delta$  10.46 (br s, 1H), 7.94 (s, 1H), 7.92 (d,  $J = 9.1$  Hz, 1H), 7.74 (d,  $J = 8.4$  Hz, 1H), 7.63 (d,  $J = 15.8$  Hz, 1H), 6.58 (d,  $J = 15.8$  Hz, 1H), 4.77 (br, 2H), 3.52 (m, 2H), 3.27 (br, 2H), 3.11 (t,  $J = 7.8$  Hz, 2H), 2.93 (s, 3H), 1.85 (quintet,  $J = 7.3$  Hz, 2H), 1.44–1.34 (m, 4H), 1.25 (t,  $J = 7.2$  Hz, 3H), 0.91 (t,  $J = 7.1$  Hz, 3H).

**(E)-3-(2-Butyl-1-(pyrrolidin-3-yl)-1H-benzimidazol-5-yl)-N-hydroxyacrylamide (20a).** 3-[2-Butyl-5-(2-methoxycarbonylviny)benzimidazol-1-yl]pyrrolidine-1-carboxylic acid *tert*-butyl ester (**18a**) was prepared according to procedure C using **7l** as starting material and was obtained as a pale-yellow solid (3.8 g, 44%). LC–MS  $m/z$  428.16 ( $[M + H]^+$ ). **18a** (70 mg, 0.16 mmol) was added to 1.25 M HCl in MeOH (4 mL) and heated at 80 °C for 4 h, then evaporated to dryness under reduced pressure to give compound **19a** as HCl salt, which is pure enough for next step without any purification. LC–MS  $m/z$  328.1 ( $[M + H]^+$ ). The crude **19a** (~0.16 mmol) was converted to hydroxamic acid **20a** as the bis-TFA salt (25 mg, 27% from **19a** in two steps) according to procedure C. LC–MS  $m/z$  329.1 ( $[M + H]^+$ ). <sup>1</sup>H NMR (CD<sub>3</sub>OD)  $\delta$  7.97 (d,  $J = 8.7$  Hz, 1H), 7.94 (s, 1H), 7.75 (d,  $J = 8.0$  Hz, 1H), 7.68 (d,  $J = 16.0$  Hz, 1H), 6.59 (d,  $J = 16.0$  Hz, 1H), 5.65 (m, 1H), 4.00–3.80 (m, 3H), 3.57 (m, 1H), 3.27–3.20 (overlapped with solvent peak, 2H), 2.81 (m, 1H), 2.69 (m, 1H), 1.89 (quintet,  $J = 7.7$  Hz, 2H), 1.56 (sextet,  $J = 7.6$  Hz, 2H), 0.95 (t,  $J = 7.2$  Hz, 3H).

**(E)-3-(2-Butyl-1-(piperidin-4-yl)-1H-benzimidazol-5-yl)-N-hydroxyacrylamide (20b).** Compound **20b** was prepared according to the procedure described for compound **20a** but using **7n** as starting material and was obtained as the bis-TFA salt (12 mg, 8.5% from **7n**). LC–MS  $m/z$  343.2 ( $[M + H]^+$ ). <sup>1</sup>H NMR (CD<sub>3</sub>OD)  $\delta$  8.07 (d,  $J = 8.8$  Hz, 1H), 7.92 (1H, s), 7.76 (1H, d,  $J = 8.0$  Hz), 7.70 (1H, d,  $J = 15.8$  Hz), 6.60 (1H, d,  $J = 15.8$  Hz), 5.05 (1H, m), 3.70 (d,  $J = 12.5$  Hz, 2H),

3.48–3.30 (m, 2H), 3.30–3.27 (m, 2H), 2.84 (m, 2H), 2.30 (d,  $J = 13.0$  Hz, 2H), 1.89 (quintet,  $J = 7.5$  Hz, 2H), 1.56 (sextet,  $J = 7.5$  Hz, 2H), 1.06 (t,  $J = 7.2$  Hz, 3H).

**(E)-3-(2-Butyl-1-(piperidin-3-yl)-1H-benzimidazol-5-yl)-N-hydroxyacrylamide (20c).** **20c** was prepared according to the procedures described for compound **20a** but using **7m** as starting material and was obtained as the bis-TFA salt (25 mg, 8.8% in three steps from **7m**). LC–MS  $m/z$  343.2 ( $[M + H]^+$ ). <sup>1</sup>H NMR (CD<sub>3</sub>OD)  $\delta$  8.12 (d,  $J = 8.8$  Hz, 1H), 7.92 (s, 1H), 7.76 (d,  $J = 9.2$  Hz, 1H), 7.70 (d,  $J = 15.8$  Hz, 1H), 6.60 (d,  $J = 15.8$  Hz, 1H), 5.03 (tt,  $J = 12.3, 4.0$  Hz, 1H), 3.84 (t,  $J = 12.0$  Hz, 1H), 3.71 (dd,  $J = 11.9, 3.1$  Hz, 1H), 3.56 (d,  $J = 12.5$  Hz, 1H), 3.35–3.25 (m, 1H), 3.23 (m, 2H), 2.68 (m, 1H), 2.26 (m, 2H), 2.09 (m, 1H), 1.89 (quintet,  $J = 7.4$  Hz, 2H), 1.56 (sextet,  $J = 7.6$  Hz, 2H), 1.06 (t,  $J = 7.2$  Hz, 3H).

**(E)-3-(2-Hexyl-1-(pyrrolidin-3-yl)-1H-benzimidazol-5-yl)-N-hydroxyacrylamide (20d).** **20d** was prepared according to the procedures described for compound **20a** but using **7l** as starting material and was obtained as the bis-TFA salt (85 mg, 58% from **19d**). LC–MS  $m/z$  357.1 ( $[M + H]^+$ ). <sup>1</sup>H NMR (CD<sub>3</sub>OD)  $\delta$  7.99 (d,  $J = 8.7$  Hz, 1H), 7.94 (s, 1H), 7.76 (d,  $J = 8.7$  Hz, 1H), 7.67 (d,  $J = 15.8$  Hz, 1H), 6.59 (d,  $J = 15.8$  Hz, 1H), 5.67 (quintet,  $J = 9.2$  Hz, 1H), 4.00–3.85 (m, 3H), 3.57 (td,  $J = 11.4, 3.5$  Hz, 1H), 3.26 (d,  $J = 7.9$  Hz, 2H), 2.82 (m, 1H), 2.70 (m, 1H), 1.91 (quintet,  $J = 7.4$  Hz, 2H), 1.54 (m, 2H), 1.46–1.34 (m, 4H), 0.94 (t,  $J = 7.1$  Hz, 3H).

**(E)-3-(2-Hexyl-1-(piperidin-3-yl)-1H-benzimidazol-5-yl)-N-hydroxyacrylamide (20e).** **20e** was prepared according to the procedures described for compound **20a** but using **7m** as starting material and was obtained as the bis-TFA salt (28 mg, 9.3% in three steps from **7m**). LC–MS  $m/z$  371.4 ( $[M + H]^+$ ). <sup>1</sup>H NMR (CD<sub>3</sub>OD)  $\delta$  8.12 (d,  $J = 8.8$  Hz, 1H), 7.92 (s, 1H), 7.76 (d,  $J = 9.2$  Hz, 1H), 7.68 (d,  $J = 15.8$  Hz, 1H), 6.60 (d,  $J = 15.8$  Hz, 1H), 5.05 (tt-like,  $J = 12.2, 4.0$  Hz, 1H), 3.85 (t,  $J = 12.0$  Hz, 1H), 3.72 (dd,  $J = 11.9, 3.0$  Hz, 1H), 3.56 (d,  $J = 12.1$  Hz, 1H), 3.32 (overlapped with solvent peak, 1H), 3.24 (m, 2H), 2.68 (m, 1H), 2.26 (m, 2H), 2.10 (m, 1H), 1.90 (quintet,  $J = 7.4$  Hz, 2H), 1.54 (m, 2H), 1.48–1.32 (m, 4H), 0.94 (t,  $J = 7.2$  Hz, 3H).

**(E)-3-[2-Butyl-1-(1-methylpyrrolidin-3-yl)-1H-benzimidazol-5-yl]-N-hydroxyacrylamide (22a).** Tertiary amine **21a** was prepared by reductive amination of **19a** with formaldehyde and NaBH(OAc)<sub>3</sub> according to similar procedures used for **17c** and then converted to hydroxamic acid according to procedure C to obtain **22a** as the bis-TFA salt (25 mg, 22% in two steps). LC–MS  $m/z$  343.2 ( $[M + H]^+$ ). <sup>1</sup>H NMR (CD<sub>3</sub>OD)  $\delta$  8.05 (d,  $J = 8.8$  Hz, 1H), 7.94 (s, 1H), 7.76 (d,  $J = 8.6$  Hz, 1H), 7.65 (d,  $J = 15.8$  Hz, 1H), 6.58 (d,  $J = 15.8$  Hz, 1H), 5.79 (quintet,  $J = 9.1$  Hz, 1H), 4.20–3.8 (m, 3H), 3.66 (br s, 1H), 3.26 (t,  $J = 7.9$  Hz, 2H), 3.15 (s, 3H), 2.89 (m, 1H), 2.79 (m, 1H), 1.89 (quintet,  $J = 7.8$  Hz, 2H), 1.56 (sextet,  $J = 7.6$  Hz, 2H), 1.05 (t,  $J = 7.4$  Hz, 3H).

**(E)-N-Hydroxy-3-[1-(1-methylpiperidin-3-yl)-2-pentyl-1H-benzimidazol-5-yl]acrylamide (22b).** Tertiary amine **21b** (144.5 mg, 53% in two steps from **18f**) was prepared according to similar procedures used for **17c** and then converted to hydroxamic acid according to procedure C to obtain **22b** as the bis-TFA salt. LC–MS  $m/z$  371.2 ( $[M + H]^+$ ). <sup>1</sup>H NMR (CD<sub>3</sub>OD)  $\delta$  8.18 (d,  $J = 7.9$  Hz, 1H), 7.92 (s, 1H), 7.77 (d,  $J = 8.1$  Hz, 1H), 7.61 (d,  $J = 15.7$  Hz, 1H), 6.58 (d,  $J = 15.7$  Hz, 1H), 5.21 (m, 1H), 4.00–3.80 (m, 2H), 3.75–3.60 (m, 1H), 3.43–3.24 (masked peaks, 3H), 3.03 (s, 3H), 2.64 (m, 1H), 2.36–2.14 (m, 3H), 1.92 (m, 2H), 1.60–1.49 (m, 4H), 0.96 (t,  $J = 7.1$  Hz, 3H); <sup>13</sup>C NMR (CD<sub>3</sub>OD)  $\delta$  165.6, 157.6, 139.9, 134.6, 134.1, 132.5, 126.3, 120.4, 115.5, 115.2, 54.9, 54.4, 53.3, 44.1, 32.4, 27.5, 27.3, 26.8, 23.2, 23.1, 14.2 (TFA peaks at 163.0, 162.7, 119.4, and 116.5).

**HDAC Enzyme Assay.** The recombinant HDAC enzymes, including HDACs 1–11, were produced by the Protein Biochemistry Group in S<sup>3</sup>BIO Pte Ltd. (see supplements of ref 19 for details). All HDACs are purified full-length proteins except HDAC5 (191–1122). The assay protocols have been reported in our early publications.<sup>18</sup> The assay was



performed in a 96-well or 384-well format using the BIOMOL fluorometric-based HDAC activity assay (BIOMOL International, L.P.). Fluor de Lys substrate (KI-104) was used for HDAC1 IC<sub>50</sub> and HDACs 1–11 isoform dissociation constant *K<sub>i</sub>* determination. The reaction mixture was composed of assay buffer, containing 25 mM Tris, pH 7.5, 137 mM NaCl, 2.7 mM KCl, 1 mM MgCl<sub>2</sub>, 1 mg/mL BSA, tested compounds, an appropriate concentration of HDAC1, and 250 μM Fluor de Lys generic substrate. The fluorescence was detected at the excitation wavelength of 360 nm and the emission wavelength of 460 nm using Tecan Ultra microplate detection system (Tecan Group Ltd., Switzerland). The analytical software, Prism 4.0 (GraphPad Software, Inc.), was used to generate IC<sub>50</sub> values from the data. IC<sub>50</sub> values for HDACs 2–11 were obtained by using analogous protocols but with appropriate adjustment of protein and substrate concentrations (20 μM substrate for HDAC6, 100 or 250 μM for HDACs 2–5, 8–11). The *K<sub>i</sub>* was calculated using the Cheng–Prusoff equation:  $K_i = IC_{50} / \{1 + ([\text{substrate}]/K_m)\}$ .

**Cell-Based Proliferation Assay for Determination of IC<sub>50</sub>.** Human colon cancer cell lines were obtained from the American Type Culture Collection (ATCC; VA, U.S.) or the European Collection of Cell Culture (ECACC; Wilshire, U.K.). They were cultivated according to the supplier's instructions. After subconfluent growth, cells were seeded in a 96-well plate at log growth phase. Before treatment, the plates were incubated at 37 °C, 5% CO<sub>2</sub> for 24 h (adherent cells) or 2 h (suspension cells). Treatment with compounds was carried out in triplicate wells for 96 h. Proliferation of adherent cells was monitored using Cyquant cell proliferation assay (Invitrogen Pte Ltd., Singapore), while proliferation of suspension cells was monitored using CellTiter96 Aqueous One solution cell proliferation assay (Promega Pte Ltd., Singapore). Dose response curves were plotted to determine the IC<sub>50</sub> values using XL-fit (ID Business Solution Ltd., U.S.). IC<sub>50</sub> is the concentration needed for inhibition of 50% cell proliferation of tumor cells.

**Histone H3 Acetylation Assay: ELISA Approach and EC<sub>50</sub> Determination.** COLO 205 cells was cultivated in a 96-well plate at  $1 \times 10^5$  cells/well for 24 h. COLO 205 cells were subsequently treated with HDAC inhibitors (10 μM), reference (vorinostat, 10 μM), and negative control (1% DMSO) in triplicate. After treatment for 24 h, cells were lysed according to the instructions from Sigma mammalian cell lysis kit (Sigma no. MCL-1) and the protein concentration was determined. The ELISA plate (Immulon 2HB plate, Bio Laboratories Pte Ltd., Singapore) was coated with 4 μg/mL mouse monoclonal antibody against H3 (Upsate no. 05-499, Upstate Pte Ltd., Singapore) in PBS, pH 7.4, incubated at 37 °C for 1 h and then at 4 °C overnight. Subsequently the plate was washed with washing buffer [PBS containing 0.05% (v/v) Tween-20] and blocked with SuperBlock solution (Pierce no. 37515, Pierce Pte Ltd., Singapore) at 37 °C for 1 h. The SuperBlock solution was removed, and the plate was washed with washing buffer. The ACh3 peptide standards (24 doses, 2-fold serial dilutions starting from 200 μg/mL, Upsate no. 12-360, Upstate Pte Ltd., Singapore) and the protein lysates from COLO 205 cells treated with HDAC inhibitors were applied to the plate (final volume, 50 μL/well) in triplicate and incubated for 1 h at 37 °C. After removal of the samples, the plate was washed with washing buffer. The plate was incubated with secondary antibody [100 μL, 0.5 μg/mL rabbit polyclonal antibody against ACh3 (Lys9/14) (Upsate no. 06-599, Upstate Pte Ltd., Singapore)] at 37 °C for 1 h. Subsequently the plate was washed with washing buffer and incubated with a detection antibody [100 μL, 1:5000 donkey anti-rabbit IgG antibody coupled to HRPO (Pierce no. 31458, Pierce Pte Ltd., Singapore)] that was applied at 37 °C for 30 min. The plate was washed with washing buffer, then incubated with substrate [100 μL, Turbo TMB substrate solution (Pierce no. 34022, Pierce Pte Ltd., Singapore)] at room temperature for 30 min. The reaction was stopped using 1 M H<sub>2</sub>SO<sub>4</sub>. The absorbance was measured at 450 nm on a SpectraMax absorbance microplate reader (Molecular Devices Corporation, Sunnyvale, CA). The standard curve was drawn, and the concentration of ACh3 [(Lys9/14), μg/mL] in a

sample was determined using the SoftMax Pro software in SpectraMax. The content of ACh3 in a sample was normalized by dividing the ACh3 concentration by the protein concentration: ACh3 relative to vorinostat (fold) = ACh3 content (HDAC inhibitor)/ACh3 content (vorinostat).

**EC<sub>50</sub> Determination.** The assays were performed according to the above protocol except that COLO 205 cells were treated with HDAC inhibitors at different doses (in triplicate, nine doses, 4-fold serial dilutions starting from 100 μM). The absorbance at 450 nm for each sample was normalized by the protein concentration, and the dose response curve was plotted (OD<sub>450</sub> vs compound concentration) using XL-fit (ID Business Solution, Emeryville, CA) to determine EC<sub>50</sub> values of HDAC inhibitors.

**Homology Modeling.** HDAC1 homology model was built from HDLP as reported in our earlier report.<sup>18</sup> A similar model was also built from a recent published HDAC2 structure PDB entry 3MAX<sup>24</sup> with 90% sequence identity to HDAC1. The X-ray structure was prepared using the protein preparation wizard in Maestro 9.1 as recommended by Schrodinger (<http://www.schrodinger.com/>). The homology model was built using Prime 2.2 with standard settings. Crystal water was removed from the template. However, water molecule 457 was added to the homology model, as this was in a position to hydrogen-bond with N<sup>3</sup> of the benzimidazole HDAC inhibitors and His178. The identity of binding site residues of HDAC1 and HDAC2 is 100%.

**In Vitro ADME Studies.** Solubility and log *D* were measured using our published methods.<sup>41</sup> Microsomal stability studies and Caco-2 permeability assays were performed according to published methods.<sup>42</sup> Primary screen for inhibition of CYP3A4 and 2D6 was carried by using BD Biosciences' high throughput inhibitor screening kits (catalogue no. 459100 and no. 459200). For CYP3A4 inhibition, to a 96-well plate, each 200 μL well reaction mixture containing 1 pmol (5 nM) of P450 CYP3A4, 8.1 μM NADP<sup>+</sup>, 0.41 mM glucose 6-phosphate, 0.4 U/mL glucose 6-phosphate dehydrogenase, 0.41 mM magnesium chloride, 50 μM BFC in 25 mM potassium phosphate (pH 7.4), and test compound (eight doses, 3-fold serial dilution starting from 20 to 0.00915 μM) or positive control ketoconazole (eight doses, 3-fold serial dilution starting from 5 to 0.0023 μM) was incubated at 37 °C for 30 min. The reaction was stopped by the addition of acetonitrile (75 μL), and the metabolite HFC was detected (403 nm excitation and 535 nm emission) and quantified. Data were analyzed using Prism 4.0 (GraphPad Software, Inc.). IC<sub>50</sub> values for inhibition of CYP1A, CYP3A4, CYP2D6, CYP2C9, and CYP2C19 using HLM system with isozyme specific probe substrates and inhibitors were determined by Cyprotex (U.K.).

**Pharmacokinetic Analysis.** The analysis followed protocols similar to those published for 2<sup>42</sup> and 3.<sup>19</sup>

**Human Tumor Xenograft Studies.** These studies followed protocols similar to those previously published.<sup>18,19,41</sup>

## ■ ASSOCIATED CONTENT

**S Supporting Information.** Figures S1–3 showing additional correlations with potency; Tables S1–10 listing target compounds, IC<sub>50</sub>, clogP, acetylation data, microsomal data, pharmacokinetic parameters, and tissue distribution; Table S11 listing elemental analysis results and HPLC purity data for key and reference compounds; synthesis and analytical data of additional compounds for establishing SARs (10ac–ax, 15f–v, and 17d–x). This material is available free of charge via the Internet at <http://pubs.acs.org>.

## ■ AUTHOR INFORMATION

### Corresponding Author

\*Phone: +65-68275019. Fax: +65-68275005. E-mail: haishan\_wang@sbio.com.

## ACKNOWLEDGMENT

The authors thank Evelyn Goh and Lee Sun New for performing ADME analytical experiments, Tony Ng for support of in vivo experiments, Wai Chung Ong for carrying out HDAC assays, Miah Kiat Goh and Chee Pang Ng for preparation of HDAC proteins, Chang Kai Soh for making the freebase of 3, Noah Tu for HPLC purification system support, Bee Kheng Ng for preparation of compound assay solutions, Drs. Michael Entzeroth and Binhui Ni for their early inputs and administrative work in biology, and Dr. Veronica Novotny-Diermayr for critical reading of this manuscript.

## ABBREVIATIONS USED

A2780, human ovary carcinoma cell line; AcH3, acetyl histone H3; ADME, absorption, distribution, metabolism, and excretion; AUC, area under curve; BEI, binding efficiency index; BFC, 7-benzyl-oxytrifluoromethylcoumarin; Boc, *tert*-butoxycarbonyl; Cl, clearance; COLO 205, human colorectal adenocarcinoma; CR, complete tumor regression, no measurable tumor (less than 3 mm × 3 mm) for three consecutive measurements; CYP, cytochrome P450 super family; DCM, dichloromethane; DIEA, *N,N*-diisopropylethylamine; ELISA, enzyme-linked immunosorbent assay; EDCI, *N*-(3-dimethylaminopropyl)-*N'*-ethylcarbodiimide hydrochloride; EtOAc, ethyl acetate; F, percent oral bioavailability; HCT-116, human colorectal adenocarcinoma cell line; HDAC, histone deacetylase; HFC, 7-hydroxytrifluoromethylcoumarin; HLM, human liver microsomes; HOBt, 1-hydroxybenzotriazole; MCA, 4-methylcoumarin-7-amide; MeOH, methanol; MLM, mouse liver microsomes; MV4-11, human acute monocytic leukemia cell line; PC-3, human prostate cancer cell line; PR, partial tumor regression, reduction to <50% of initial tumor volume for three consecutive measurements; PyBOP, benzotriazole-1-yloxytripyrrolidinophosphonium hexafluorophosphate; Ramos, human Burkitt's lymphoma cell line; qd, quaque die, once a day; SAHA, suberoylanilide hydroxamic acid; SAR, structure–activity relationship; TBME, *tert*-butyl methyl ether; TFA, trifluoroacetic acid; TGI, tumor growth inhibition; TRD, treatment related death; ZBG, zinc binding group

## REFERENCES

- (1) Amato, I. Pulling genes' strings. *Chem. Eng. News* **2006**, *84* (29), 13–20.
- (2) Grunstein, M. Histone acetylation in chromatin structure and transcription. *Nature* **1997**, *389*, 349–352.
- (3) Struhl, K. Histone acetylation and transcriptional regulatory mechanisms. *Genes Dev.* **1998**, *12*, 599–606.
- (4) Wade, P. A. Transcriptional control at regulatory checkpoints by histone deacetylases: molecular connections between cancer and chromatin. *Hum. Mol. Genet.* **2001**, *10*, 693–698.
- (5) de Ruijter, A. J. M.; van Gennip, A. H.; Caron, H. N. P.; Kemp, S.; van Kuilenburg, A. B. P. Histone deacetylases (HDACs): characterization of the classical HDAC family. *Biochem. J.* **2003**, *370*, 737–749.
- (6) Michan, S.; Sinclair, D. Sirtuins in mammals: insights into their biological function. *Biochem. J.* **2007**, *404*, 1–13.
- (7) Ellis, L.; Atadja, P. W.; Johnstone, R. W. Epigenetics in cancer: targeting chromatin modifications. *Mol. Cancer Ther.* **2009**, *8*, 1409–1420.
- (8) Curtin, M.; Glaser, K. Histone deacetylase inhibitors: the Abbott experience. *Curr. Med. Chem.* **2003**, *10*, 2373–2392.
- (9) Glaser, K. B.; Li, J.; Staver, M. J.; Wei, R.-Q.; Albert, D. H.; Davidsen, S. K. Role of class I and class II histone deacetylases in carcinoma cells using siRNA. *Biochem. Biophys. Res. Commun.* **2003**, *310*, 529–536.
- (10) Witt, O.; Deubzer, H. E.; Milde, T.; Oehme, I. HDAC family: What are the cancer relevant targets? *Cancer Lett.* **2009**, *277*, 8–21.
- (11) Glozak, M. A.; Sengupta, N.; Zhang, X.; Seto, E. Acetylation and deacetylation of non-histone proteins. *Gene* **2005**, *363*, 15–23.
- (12) Butler, L. M.; Agus, D. B.; Scher, H. I.; Higgins, B.; Rose, A.; Cordon-Cardo, C.; Thaler, H. T.; Rifkind, R. A.; Marks, P. A.; Richon, V. M. Suberoylanilide hydroxamic acid, an inhibitor of histone deacetylase, suppresses the growth of prostate cancer cells in vitro and in vivo. *Cancer Res.* **2000**, *60*, 5165–5170.
- (13) FDA approval and new drug application (NDA) documents for Zolinza (SAHA, vorinostat): [http://www.accessdata.fda.gov/drugsatfda\\_docs/nda/2006/021991s000\\_ZolinzaTOC.cfm](http://www.accessdata.fda.gov/drugsatfda_docs/nda/2006/021991s000_ZolinzaTOC.cfm).
- (14) FK228: <http://www.fda.gov/NewsEvents/Newsroom/Press-Announcements/2009/ucm189629.htm>.
- (15) Wang, H.; Dymock, B. W. New patented histone deacetylase inhibitors. *Expert Opin. Ther. Pat.* **2009**, *19*, 1727–1757.
- (16) Paris, M.; Porcelloni, M.; Binaschi, M.; Fattori, D. Histone deacetylase inhibitors: from bench to clinic. *J. Med. Chem.* **2008**, *51*, 1505–1529. Correction in *J. Med. Chem.* **2008**, *51*, 3330.
- (17) S\*Bio patent applications on HDAC inhibitors. (a) Chen, D.; Deng, W.; Sangthongpitag, K.; Song, H.; Sun, E. T.; Yu, N.; Zou, Y. Benzimidazole Derivates: Preparation and Pharmaceutical Applications. PCT Int. Appl. WO2005028447, March 31, 2005. (b) Lim, Z.-Y.; Wang, H.; Zhou, Y. Acylurea and Sulfonylurea Connected Hydroxamates. PCT Int. Appl. WO2005040101, May 6, 2005. (c) Stunkel, W.; Wang, H.; Yin, Z. Biaryl Linked Hydroxamates: Preparation and Pharmaceutical Applications. PCT Int. Appl. WO2005040161, May 6, 2005. (d) Deng, W.; Lye, P. L.; Lim, Y. H. Benzothiophene Derivatives: Preparation and Pharmaceutical Applications. PCT Int. Appl. WO2006101454, September 28, 2006. (e) Lee, K. C. L.; Sun, E. T. Imidazo[1,2-*a*]pyridine Derivatives: Preparation and Pharmaceutical Applications. PCT Int. Appl. WO2006101455, September 28, 2006. (f) Deng, W.; Chen, D.; Zhou, Y. Bicyclic Heterocycles Hydroxamate Compounds Useful as Histone Deacetylase (HDAC) Inhibitors. PCT Int. Appl. WO2006101456, September 28, 2006. (g) Chen, D.; Deng, W.; Lee, K. C. L.; Lye, P. L.; Sun, E. T.; Wang, H.; Yu, N. Heterocyclic Compounds. PCT Int. Appl. WO2007030080, March 15, 2007. (h) Lee, K. C. L.; Sun, E. T.; Wang, H. Imidazo[1,2-*a*]pyridine Hydroxamate Compounds That Are Inhibitors of Histone Deacetylase. PCT Int. Appl. WO2008036046, March 27, 2008.
- (18) Wang, H.; Yu, N.; Song, H.; Chen, D.; Zou, Y.; Deng, W.; Lye, P. L.; Chang, J.; Ng, M.; Blanchard, S.; Sun, E. T.; Sangthongpitag, K.; Wang, X.; Goh, K. C.; Wu, X.; Khng, H. H.; Fang, L.; Goh, S. K.; Ong, W. C.; Bonday, Z.; Stunkel, W.; Poulsen, A.; Entzeroth, M. *N*-Hydroxy-1,2-disubstituted-1*H*-benzimidazol-5-yl acrylamides as novel histone deacetylase inhibitors: design, synthesis, SAR studies, and in vivo antitumor activity. *Bioorg. Med. Chem. Lett.* **2009**, *19*, 1403–1408.
- (19) Novotny-Diermayr, V.; Sangthongpitag, K.; Hu, C. Y.; Wu, X.; Sausgruber, N.; Yeo, P.; Greicius, G.; Pettersson, S.; Liang, A. L.; Loh, Y. K.; Bonday, Z.; Goh, K.; Hentze, H.; Hart, S.; Wang, H.; Ethirajulu, K.; Wood, J. M. SB939, a novel potent and orally active histone deacetylase inhibitor with high tumor exposure and efficacy in mouse models of colorectal cancer. *Mol. Cancer Ther.* **2010**, *9*, 642–652.
- (20) Razak, A. R.; Hotte, S. J.; Siu, L. L.; Chen, E. X.; Hirte, H. W.; Powers, J.; Walsh, W.; Stayner, L. A.; Laughlin, A.; Novotny-Diermayr, V.; Zhu, J.; Eisenhauer, E. A. Phase I clinical, pharmacokinetic and pharmacodynamic study of SB939, an oral histone deacetylase (HDAC) inhibitor, in patients with advanced solid tumours. *Br. J. Cancer* **2011**, *104*, 756–762.
- (21) Yong, W. P.; Goh, B. C.; Soo, R. A.; Toh, H. C.; Ethirajulu, K.; Wood, J.; Novotny-Diermayr, V.; Lee, S. C.; Yeo, W. L.; Chan, D.; Lim, D.; Seah, E.; Lim, R.; Zhu, J. Phase I and pharmacodynamic study of an orally administered novel inhibitor of histone deacetylases, SB939, in patients with refractory solid malignancies. *Ann. Oncol.* [Online early access]. DOI: 10.1093/annonc/mdq784. Published Online: Mar 8, 2011.
- (22) Wu, Z.; Rea, P.; Wickham, G. “One-pot” nitro reduction–cyclisation solid phase route to benzimidazoles. *Tetrahedron Lett.* **2000**, *41*, 9871–9874.
- (23) Abad-Zapatero, C. Ligand efficiency indices for effective drug discovery. *Expert Opin. Drug Discovery* **2007**, *2*, 469–488.

- (24) For homology modeling, two human HDAC1 models were built from HDLP X-ray structure 1C3R (see ref 18) and HDAC2 structure 3MAX (see Bressi et al.). Bressi, J. C.; Jennings, A. J.; Skene, R.; Wu, Y.; Melkus, R.; De Jong, R.; O'Connell, S.; Grimshaw, C. E.; Navre, M.; Gangloff, A. R. Exploration of the HDAC2 foot pocket: synthesis and SAR of substituted *N*-(2-aminophenyl)benzamides. *Bioorg. Med. Chem. Lett.* **2010**, *20*, 3142–3145.
- (25) Khan, N.; Jeffers, M.; Kumar, S.; Hackett, C.; Boldog, F.; Khrantsov, N.; Qian, X.; Mills, E.; Berghs, S. C.; Carey, N.; Finn, P. W.; Collins, L. S.; Tumber, A.; Ritchie, J. W.; Jensen, P. B.; Lichenstein, H. S.; Sehested, M. Determination of the class and isoform selectivity of small-molecule histone deacetylase inhibitors. *Biochem. J.* **2008**, *409*, 581–589.
- (26) Arts, J.; King, P.; Mariën, A.; Floren, W.; Beliën, A.; Janssen, L.; Pilatte, I.; Roux, B.; Decrane, L.; Gilissen, R.; Hickson, I.; Vreys, V.; Cox, E.; Bol, K.; Talloen, W.; Goris, L.; Andries, L.; Du Jardin, M.; Janicot, M.; Page, M.; van Emelen, K.; Angibaud, P. JNJ-26481585, a novel "second generation" oral histone deacetylase inhibitor, shows broad-spectrum preclinical antitumor activity. *Clin. Cancer Res.* **2009**, *15*, 6841–6851.
- (27) Hanessian, S.; Auzzas, L.; Larsson, A.; Zhang, J.; Giannini, G.; Gallo, G.; Ciacci, A.; Cabri, W. Vorinostat-like molecules as structural, stereochemical, and pharmacological tools. *ACS Med. Chem. Lett.* **2010**, *1*, 70–74.
- (28) Lahm, A.; Paolini, C.; Pallaoro, M.; Nardi, M. C.; Jones, P.; Neddermann, P.; Sambucini, S.; Bottomley, M. J.; Lo Surdo, P.; Carfi, A.; Koch, U.; De Francesco, R.; Steinkühler, C.; Gallinari, P. Unraveling the hidden catalytic activity of vertebrate class IIa histone deacetylases. *Proc. Natl. Acad. Sci. U.S.A.* **2007**, *104*, 17335–17340.
- (29) Jones, P.; Altamura, S.; De Francesco, R.; Paz, O. G.; Kinzel, O.; Mesiti, G.; Monteagudo, E.; Pescatore, G.; Rowley, M.; Verdirame, M.; Steinkühler, C. A novel series of potent and selective ketone histone deacetylase inhibitors with antitumor activity in vivo. *J. Med. Chem.* **2008**, *51*, 2350–2353.
- (30) Tessier, P.; Smil, D. V.; Wahhab, A.; Leit, S.; Rahil, J.; Li, Z.; Déziel, R.; Besterman, J. M. Diphenylmethane hydroxamic acids as selective class IIa histone deacetylase inhibitors. *Bioorg. Med. Chem. Lett.* **2009**, *19*, 5684–5688.
- (31) Bradner, J. E.; West, N.; Grachan, M. L.; Greenberg, E. F.; Haggarty, S. J.; Warnow, T.; Mazitschek, R. Chemical phylogenetics of histone deacetylases. *Nat. Chem. Biol.* **2010**, *6*, 238–243.
- (32) Ontoria, J. M.; Altamura, S.; Di Marco, A.; Ferrigno, F.; Laufer, R.; Muraglia, E.; Palumbi, M. C.; Rowley, M.; Scarpelli, R.; Schultz-Fademrecht, C.; Serafini, S.; Steinkühler, C.; Jones, P. Identification of novel, selective, and stable inhibitors of class II histone deacetylases. Validation studies of the inhibition of the enzymatic activity of HDAC4 by small molecules as a novel approach for cancer therapy. *J. Med. Chem.* **2009**, *52*, 6782–6789.
- (33) Wilson, A. J.; Byun, D. S.; Popova, N.; Murray, L. B.; L'Italien, K.; Sowa, Y.; Arango, D.; Velcich, A.; Augenlicht, L. H.; Mariadason, J. M. Histone deacetylase 3 (HDAC3) and other class I HDACs regulate colon cell maturation and p21 expression and are deregulated in human colon cancer. *J. Biol. Chem.* **2006**, *281*, 13548–13558.
- (34) Gupta, P.; Ho, P.-C.; Ha, S. G.; Lin, Y.-W.; Wei, L.-N. HDAC3 as a molecular chaperone for shuttling phosphorylated TR2 to PML: a novel deacetylase activity-independent function of HDAC3. *PLoS One* **2009**, *4*, No. e4363. DOI: 10.1371/journal.pone.0004363.
- (35) Jayaraman, R.; Wang, H.; Sangthongpitag, K.; Yeo, P.; Hu, C.; Wu, X.; Liu, X.; Reddy, V. P.; Goh, E.; New, L. S.; Pasha, M. K.; Ethirajulu, K. Preclinical metabolism and disposition of SB939, an orally active histone deacetylase (HDAC) inhibitor, and prediction of human pharmacokinetics. Submitted to *Drug Metab. Dispos.*
- (36) Yeo, P.; Liu, X.; Goh, E.; New, L. S.; Zeng, P.; Wu, X.; Venkatesh, P.; Kantharaj, E. Development and validation of high-performance liquid chromatography–tandem mass spectrometry assay for 6-(3-benzoyl-ureido)-hexanoic acid hydroxyamide, a novel HDAC inhibitor, in mouse plasma for pharmacokinetic studies. *Biomed. Chromatogr.* **2007**, *21*, 184–189.
- (37) Sangthongpitag, K.; Wang, H.; Yeo, P.; Liu, X.; Goh, E.; New, L. S.; Zeng, P.; Venkatesh, P.; Wu, X.; Hu, C.; Ethirajulu, K. ADME and PK/PD Attributes of SB939, Potent Orally Active HDAC Inhibitor. Presented at the 18th EORTC-NCI-AACR Symposium on Molecular Targets and Cancer Therapeutics, Prague, Czech Republic, November 7–10, 2006.
- (38) Plumb, J. A.; Finn, P. W.; Williams, R. J.; Bandara, M. J.; Romero, M. R.; Watkins, C. J.; La Tangué, N. B.; Brown, R. Pharmacodynamic response and inhibition of growth of human tumor xenografts by the novel histone deacetylase inhibitor PXD101. *Mol. Cancer Ther.* **2003**, *2*, 721–728.
- (39) Remiszewski, S. W.; Sambucetti, L. C.; Bair, K. W.; Bontempo, J.; Cesarz, D.; Chandramouli, N.; Chen, R.; Cheung, M.; Cornell-Kennon, S.; Dean, K.; Diamantidis, G.; France, D.; Green, M. A.; Howell, K. L.; Kashi, R.; Kwon, P.; Lassota, P.; Martin, M. S.; Mou, Y.; Perez, L. B.; Sharma, S.; Smith, T.; Sorensen, E.; Taplin, F.; Trogani, N.; Versace, R.; Walker, H.; Weltchek-Engler, S.; Wood, A.; Wu, A.; Atadja, P. *N*-Hydroxy-3-phenyl-2-propenamides as novel inhibitors of human histone deacetylase with in vivo antitumor activity: discovery of (2*E*)-*N*-hydroxy-3-[4-[(2-hydroxyethyl)-[2-(1*H*-indol-3-yl)ethyl]amino]methyl]phenyl]-2-propenamide (NVP-LAQ824). *J. Med. Chem.* **2003**, *46*, 4609–4624.
- (40) Atadja, P.; Shao, W.; Wang, Y.; Growney, J.; Feng, Y.; Yao, Y.-M.; Wallace, A.; Crisanti, C.; Fawell, S.; Albelda, S. Efficacy of Panobinostat (LBH589) in Lung Cancer: Potent Anticancer Activity in Both in Vitro and in Vivo Tumor Models. Presented at the 20th EORTC-NCI-AACR Symposium on Molecular Targets and Cancer Therapeutics, Geneva, Switzerland, Oct 21–24, 2008; Abstract No. 151.
- (41) Wang, H.; Lim, Z.-Y.; Zhou, Y.; Ng, M.; Lu, T.; Lee, K.; Sangthongpitag, K.; Goh, K. C.; Wang, X.; Wu, X.; Khng, H. H.; Goh, S. K.; Ong, W. C.; Bonday, Z.; Sun, E. T. Acylurea connected straight chain hydroxamates as novel histone deacetylase inhibitors: synthesis, SAR, and in vivo antitumor activity. *Bioorg. Med. Chem. Lett.* **2010**, *20*, 3314–3321.
- (42) Venkatesh, P. R.; Goh, E.; Zeng, P.; New, L. S.; Xin, L.; Pasha, M. K.; Sangthongpitag, K.; Yeo, P.; Kantharaj, E. In vitro phase I cytochrome P450 metabolism, permeability and pharmacokinetics of SB639, a novel histone deacetylase inhibitor in preclinical species. *Biol. Pharm. Bull.* **2007**, *30*, 1021–1024.